THE EFFECT OF HYDRODYNAMIC STRESS ON PLANT EMBRYO DEVELOPMENT

A Dissertation
Presented to
The Academic Faculty

by

Hong Sun

In Partial Fulfillment
of the Requirements for the Degree
Doctor of Philosophy in the
George W. Woodruff School of Mechanical Engineering

Georgia Institute of Technology
May 2010

THE EFFECT OF HYDRODYNAMIC STRESS ON PLANT EMBRYO DEVELOPMENT

Approved by:

Dr. Cyrus K. Aidun, Advisor
Committee Chair
George W. Woodruff School of
Mechanical Engineering
Georgia Institute of Technology

Dr. Ulrika Egertsdotter, Co-Advisor
Committee Co-Chair
School of Biology,
Georgia Institute of Technology

Dr. Janet K. Allen
George W. Woodruff School of
Mechanical Engineering (Professor
Emeritus)
Georgia Institute of Technology
John and Mary Moore Chair
and Professor of Industrial Engineering
University of Oklahoma

Dr. Jeannette Yen
School of Biology
Georgia Institute of Technology

Dr. Evan Zamir
George W. Woodruff School of
Mechanical Engineering
Georgia Institute of Technology

Date Approved: [March 29, 2010]

ACKNOWLEDGEMENTS

The research involved in this thesis would not have been possible without the help and support of many people. Foremost, I would like to express my sincere gratitude to my advisors, Professors Cyrus Aidun and Ulrika Egertsdotter, for their constant encouragement, trust and invaluable suggestions over all of these years. I am sincerely grateful to my reading committee members: Professor Janet Allen, Professor Jeannette Yen and Professor Evan Zamir for their effort in reviewing this work and their advices and clarifying remarks.

I would like to thank my colleagues in the research group. I learned different aspects of study and life through the discussions and cooperation with them. I would like to thank my family, especially my husband, for the support and encouragement during this long journey. I would not be me today without them.

TABLE OF CONTENTS

LIST OF TABLES

LIST OF FIGURES

LIST OF SYMBOLS AND ABBREVIATIONS

A_α	Image matrix
$\overline{A}_\alpha$	Mean value of A_α
$A'_{\alpha+1}$	Shifted $A_{\alpha+1}$ image
a	Significance level
$1 - a$	Confidence level
C_N	Mass concentration
c_α	Correlation value
i_{os}	Dimensionless van 't Hoff factor
k	Index of experiment time
M	Number of clusters recorded in one experiment
M_W	Molecular weight
m	Molarity
N	Number of clusters processed in one experiment
P	Probability
$R_\alpha(\theta)$	Radial length of cluster along θ direction
R_{gas}	Gas constant
s	Standard deviation
T	Thermodynamic (absolute) temperature
t	t-test statistic
t_α	Time step

α	Time index
β	Two times of angle division
ΔR	Raw data/mean growth rate of one cell cluster
$\overline{\Delta R}$	Mean value of raw data/mean growth rate of clusters in one experiment
μ	Population mean
μm	Microns
Π	Osmotic pressure

BSA	Bovine serum albumin
DHR123	Dihydrorhodamine 123
EC	Endothelial cell
EM	Emitter
EX	Exciter
LDA	Laser doppler anemometer
MAPK	Mitogen-activated protein kinase
Mechanical stress	Hydrodynamically-induced mechanical stress
min	Minute
ml	Milliliter
nm	Nanometer
PEMs	Pro embryogenic masses
PBS	Phosphate-buffered saline
PIV	Particle image velocimetry
rpm	Round per minute
TRITC	Tetramethylrhodamine isothiocyanate

SUMMARY

Somatic embryogenesis is a clonal propagation method that encompasses many advantages for large-scale propagation of plants. Application of somatic embryogenesis is however limited due to unresolved problems in culture techniques. One major obstacle is the inhibition from culture of embryos in liquid culture medium, i.e. in a bioreactor environment, on subsequent plant development. To overcome this obstacle, it is important to gain insight into the effects of flow on somatic embryo development. Specifically, preliminary data points to the importance of the effect from hydrodynamically-induced mechanical stress, on the development of a polarized somatic embryo in the proliferation phase. This doctoral research program intends to establish the correlation between shear stress in liquid culture conditions and somatic embryo development.

The effect of steady shear stress on somatic embryos were investigated in a flow chamber and evaluated at different time intervals using microscopy technique. The development of meristematic cell clusters, i.e. the immature embryos, into a polarized somatic embryo, and the effect on the localization of the suspensor cells that form during development of the immature embryos, were studied as a function of shear stresses. With the distribution and growth rate of the meristematic and suspensor cells, the effect of stress on the embryo development was established. Furthermore, the effect of shear stress on the cells at molecular level, the reaction of integrin-like proteins, the production

of reactive oxygen species and the pore size of the cell walls involved in the shear stress responses, were investigated with molecular techniques.

In general, shear stress inhibits meristematic cells growth. Meristematic cells grow fastest at shear rate of 86 s^{-1} among all the tested shear stress conditions. By combining the results of meristematic cells growth and suspensor cells formation, it suggests that there is a critical shear rate between 86 and 140 s^{-1}, at which no suspensor cells form. The unidirectional flow with different shear stresses helps the polarized growth and the unidirectional alignment of suspensor cells. Reactive oxygen species and integrin-like protein are detected in the stressed cells as cellular responses to shear stresses. By monitoring the pore size and uptake time of cells to macromolecules with solute-exclusive experiments, it suggests that the stressed cells expedite the response to plasmolyzing components that are used to induce maturation treatment thus affect the response to maturation stimuli. The results from this research program will contribute to the knowledge of somatic embryo development in liquid condition under different shear stresses.

CHAPTER 1

INTRODUCTION

Plants play a vital role in human lives and have important functions in ecosystems (Forest Trees, Committee on Managing Global Genetic Resources: Agricultural Imperatives, National Research Council 1991). Plants provide not only renewable sources such as food, fibers, wood and chemicals for human societies, but also habitats for numerous organisms. Forest trees draw special attentions among all the plants due to their broad coverage area and the influence to ecosystems. They provide essential ecological functions as land preservation, water purification and carbon storage. Nearly 4 billion hectares of forest cover the earth's surface that is roughly 30% of the total land area on earth. However, the world's forests have shrunk by nearly 30% in the last two centuries as land was cleared to make way for farms and to meet demand for wood (Mygatt 2006).

Forests are cleared to grow food and energy crops and meet demand for wood products. As the global population increases, there is a high demand for food, energy and chemicals according to the resources on the website of United Nations Food & Agriculture Organization (data from Food and Agriculture Organizations of United Nations, 2008-2009). The global wood harvest totaled 3.4 billion cubic meters in 2004, up from 2.3 billion cubic meters in 1961. Fifty-two percent of this is used as fuel, though this varies regionally. Fuel wood accounts for 89 percent of Africa's wood harvest, where it is often the only accessible and affordable source of energy for heating and

cooking, but only 17 percent in North and Central America, where other energy sources are more readily available (Global Forest Resources Assessment 2005, United Nations Food and Agriculture Organization). For North America, conifers are the most widespread forest trees. Plant materials have also been used to produce Biofuel which, as a green energy source, lessens the toxic pollutant emissions produced by burning gasoline, and cuts down on the dumping of used oil. Although large scale production of this renewable energy is still under debate mainly because of the high production energy consumption, Biofuel technology has gained rapid development over the past few years and Biofuel supplied 1.5% of the world's transportation fuel in 2008 (Bringezu et al 2009).

The increasing global need for food and bio products demands a steady supply of a large amount of plant materials (e.g., potato, corn, etc.). One possibility to meet the increased need for wood products is to naturally grow highly productive plants (von Arnold et al 2005). This approach, however, is limited by the scarce natural resources, unpredictable climate conditions and the long life cycle. The world suffered a net loss of some 37 million hectares of forest over the last five years, according to data from FOA. This number reflects the felling of 64.4 million hectares of trees and the planting or natural regeneration of 27.8 million hectares of new forest. Each year the world loses around 7.3 million hectares of forest, an area the size of Panama. Due to extensive reforestation, this net forest shrinkage has slowed slightly from the 8.9 million hectares lost annually in the 1990s. While this is encouraging, it obscures the fact that gross deforestation has not declined significantly since 2000. Another possibility is to grow modified cells in a bioreactor to produce certain compounds in a more controlled

environment to increase productivity and save the forest trees. This relatively new approach warranties further research to ensure it is safe and sustainable.

With the rapid advance of technology, bioreactors can now be used to culture cells and eventually will produce plants in a much faster pace (Ingram & Mavituna 2000; Preil 1991; Tautorus & Dunstan 1995; Ziv et al 1994). For example, some of the chemical compounds that play an important role in the pharmaceutical and health but only exist in small amount in naturally-grown plants, can be produced in bioreactors with cell culture technique. Such as shikonin (Fujii et al 1992; Inouye et al 1979; Papageorgiou et al 1999; Sankawa et al 1977), ginseng (Ang-Lee et al 2001; Attele et al 1999; Fugh-Berman 2000) and paclitaxel (Herbst et al 2004; McGuire et al 1996; Rowinsky & Donehower 1995; Sandler et al 2006) are now commercially available. Angelica (*Angelica archangelica*) plantlets cultured in an air-sparged bioreactor has been successfully transferred to soil and grow to maturity after two seasons (Eeva et al 2003).

Years of studies have shown that propagating trees vegetatively creates significant advantages both for deployment of selected genotypes through mass-propagation and for capturing and enhancing the genetic gain in the breeding program (Egertsdotter 1999; Harry & Thorpe 1999). The methods of clonal propagation and especially somatic embryogenesis provide powerful options for breeding and management. Somatic embryogenesis is the only clonal propagation technique with the potential for practical application in large scale propagation of softwood trees. The technique has thus the potential to enable mass propagation of selected genotypes and can be used as part of breeding programs(Egertsdotter 1999; Harry & Thorpe 1999). Before the technique can be effectively implemented on a larger scale, however, it is necessary to eliminate the

costly and time consuming manual processing of somatic embryos. Furthermore, to automate the laboratory procedure for handling somatic embryos in bioreactors, it is essential to establish an efficient system for propagation and plant formation in a liquid culture medium (Gupta and Timmis 2005; Moorhouse et al. 1996; Tautorus et al. 1992).

1.1 Motivation, hypotheses and objectives

The progress in application of somatic embryogenesis to large-scale clonal propagation of plants and agricultural goods is partially halted because the majority of the embryos growing in liquid do not mature to produce a plant. Past studies by Egertsdotter (1996) and others (Krishna & Singh 2007; Stadler et al 2005) have shown that the underlying problem is the lack of polarity in suspensor cell growth on the surface of the early embryo. To overcome this obstacle, it is important to gain insight into how flow affects somatic embryo development and distribution and orientation of suspensor cells on the embryo. The most important effect is the hydrodynamically-induced mechanical stress (hereafter referred to as "mechanical stress" only) on the development of suspensor cells.

Somatic embryos of gymnosperm species develop into plants in vitro by passing through three culture phases of proliferation, maturation and germination, in response to a sequence of different compositions of culture media (Von Arnold & Clapham 2007). During proliferation phase, embryos at several stages of development are present at the same time, ranging from pro embryogenic masses (PEMs) to extended, polarized embryos comprised of a bundle of unidirectional suspensor cells attached to a meristematic region (Bozhkov et al 2002; Filonova et al 2000). The composition of

embryos at different stages relating to the physical culture conditions is either proliferating on the surface of a solidified culture medium, or within a liquid culture medium under rotation (Egertsdotter & von Arnold 1998). Liquid culture conditions have shown to be able to support growth of predominantly earlier stage embryos and PEMs that are at a too early developmental stage to respond to the maturation stimuli. However, it rarely occurs that somatic embryos fully mature in liquid culture condition (Gorbatenko & Hakman 2001). In contrast, the solid culture conditions can support growth of PEMs, and produce embryos successfully responding to maturation stimuli. Currently, it remains unclear why embryos develop differently in liquid and solid culture conditions.

The motivation of this thesis is to understand the inhibition of development of somatic embryos in liquid culture bioreactor. Especially, this thesis will focus on the effect of flow-induced shear stress on the embryo development. This research is based on the following two hypotheses that during proliferation phase, (1) somatic embryos need to be polarized to develop into mature embryos and (2) shear stress generated under liquid culture conditions has an effect on polarized growth of somatic embryos. The objectives of this thesis are to:

1) Investigate how shear stress affects immature somatic embryo growth;

2) Investigate the directional growth of suspensor cell in response to shear stress;

3) Investigate possible mechanisms of stress signal transduction.

1.2 Plant clonal propagation techniques

1.2.1 Advantages of plant clonal propagation techniques

The natural way of plant propagation is through seeds. Matured plants produce seeds, and seeds either undergo a period of hibernation or develop and grow into new plants under proper conditions, such as light, temperature, water, etc. However, some plants do not produce seeds at all and this makes the propagation of such species more difficult, if not impossible. For these species, clonal propagation techniques can be a good option for reproduction without the present of seeds. Clonal propagation techniques also make large scale production of certain wood products possible.

Large scale production of high value plants for forest plants, agricultural applications, biofuel production, ornamental purposes, or molecular pharming within the pharmaceutical sector, relies on production of clonal propagules from selected superior genotypes. To make this process more efficient, the concept of automated production of clonal plant propgaules for plantation growth has been introduced. Clonal propagation gives an opportunity for transgenic modification and further improvements of the quality of the raw material (Merkle & Dean 2000), which is also the pre requisite for production of plants that have been genetically improved by traditional breeding strategies, or direct genetic transformation. Optimal growth and yield from plantations can only be achieved when genetically identical (clonal) plants are utilized.

There are many advantages from clonal plantations. Most importantly, it is overall a more cost effective approach when dealing with a uniform crop throughout the processes from planting to harvesting. A uniform planting stock for which the growth

requirements are previously known, and where the genotype has been optimally matched to the environment, is more cost effective to maintain and results in higher gain. Uniform crop makes harvesting easier and the final processing of the raw material better tailored to fit the quality characteristics.

1.2.2 Application of different plant clonal propagation techniques

Different clonal propagation techniques have been developed for producing clonal plant propagules depending on the plant species of interest and the ultimate use for the propagule. For example, traditionally, clonal propagation of plants has been through grafting and rooting of cuttings. Propagation of many important species of ornamental plants (Rout et al 2006) and medicinal plants (Rout et al 2000) requires meristem culture or axillary bud/shoot culture. However, application of these techniques is limited. Most woody plant species (e.g. coffee, cotton, mango and all trees) are highly recalcitrant to propagation through cuttings, which frequently cause the resulting plants to display plagiotropic (un-naturally directed) growth. For many plant species, vital normal looking clonal plants can not be obtained from meristems or bud/shoot explants either. Furthermore, the number of cuttings that can be obtained from the same plant is limited, preventing large scale propagation efforts. For large scale production of woody plants, somatic embryogenesis is currently the only clonal propagation method suitable (Thorpe et al 2006). This technique is discussed further next.

For many agricultural plant species, vital normal looking clonal plants can only be obtained from embryos through the process of somatic embryogenesis. This process has been demonstrated to be essential scalable clonal propagation technology for sugarcane

(Lakshmanan et al 2006), mango (Krishna & Singh 2007), maize (Che et al 2006), oil palm (Morcillo et al 2006), coffee (Barry-Etienne et al 2002), cotton (Rathore et al 2006) and all soft wood trees (e.g., Loblolly pine, Radiata pine, White spruces and Douglas fir (Thorpe et al 2006)). Somatic embryogenesis technique has also shown great potential for important hard wood trees like Eucalyptus (Pinto et al 2004). The somatic embryos can be stored for many years under liquid nitrogen. In cryogenic storage, combination of somatic embryogenesis with cryopreservation allows testing of the clonal plants in field trials before multiplying and deploying a certain genotype on a large scale. Somatic embryogenesis can produce unlimited numbers of clonal plants with a good connection between root and shoot, which is often a problem in cuttings. The somatic embryogenesis process is suitable for automation even considering the obstacles the process has to overcome, as discussed below.

Sufficient numbers of genetically identical plants suitable for industrial scale operations requires a clonal propagation system that allows for scaleable propagation in liquid medium. Different types of bioreactors have been developed for automation of the somatic embryogenesis procedures, as reviewed by Moorhouse et al. (1996). However, for most current clonal propagation technologies, one or more developmental stages have to be conducted in air. This greatly complicates the handling of propagules and makes the technology inefficient and more expensive. For somatic embryogenesis in particular, the development of polarized somatic embryos is rare in liquid culture conditions. Therefore, large scale propagation of plants through somatic embryogenesis in bioreactors has thus not been realized due to a lack of understanding how flow-induced

mechanical stress/shear stress affects the development of somatic embryos in liquid culture.

1.2.3 Somatic embryogenesis technique

Somatic embryogenesis is a clonal propagation technology (Fowke et al 1995; Hakman & von Arnold 1985) based on the multiplication of the earliest organized structures in plants, the embryos (Figure 1). Somatic embryos are induced from somatic cells (seed embryos) of the initial explants from the donor plant, followed by a developmental process starting with multiplication of the initiated somatic embryo in response to growth regulators, in which immature embryos undergo continuous divisions and thereby multiply indefinitely. The immature embryos then transit into the next step of development, maturation, by the influence of plant growth regulators and other growth medium components. At this stage, the embryos have ceased to divide and start to accumulate storage products that enable them to go through the final step of the process *in vitro*, germination.

The process of somatic embryogenesis in softwood trees was first established for a conifer species, Norway spruce (*Picea abies*) in 1985 (Hakman & von Arnold 1985). Embryogenic cell lines of Norway spruce are established from zygotic embryos. An embryogenic cell line established from one seed can generate a large number of somatic embryos. Therefore, it is possible to produce genetically identical plants within a short period of time in a large scale. Since then, most conifer species for which somatic embryogenesis has been applied responded to the cultural treatments but at varying degrees of success (Merkle & Dean 2000). Significant efforts have thus globally been

directed towards improving the somatic embryogenesis technology for critical species like loblolly pine (*Pinus taeda*) in the U.S. and Norway spruce (*Picea abies*) in Europe (Thorpe et al 2006).

To date, Norway spruce is the best described somatic embryogenesis system in a woody species. Due to the robustness of the plant regeneration process and relative amenability to genetic transformation, Norway spruce has been the preferred model system for studying fundamental processes during somatic embryogenesis and the regulation of embryo development. In this thesis, somatic embryo cells of Norway spruce are used as the model system.

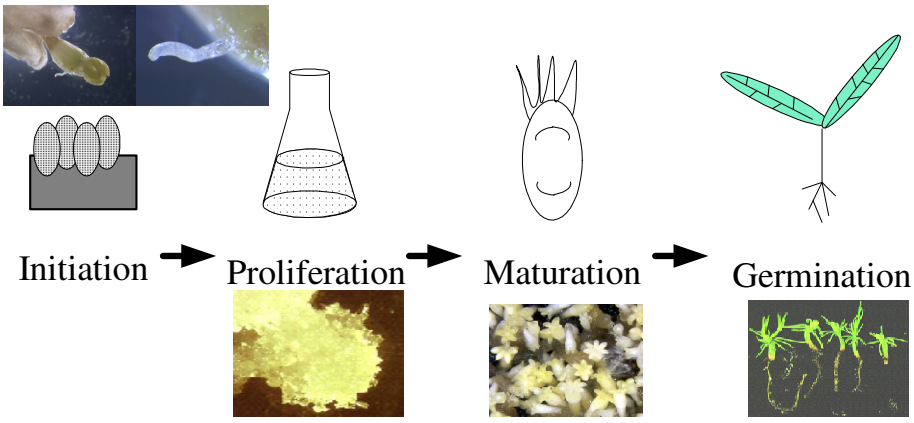

Figure 1. Somatic embryogenesis process for clonal propagation of plants. Somatic embryos are initiated from an initial explant from the donor plant. The embryos multiply during the proliferation phase. Maturation of somatic embryos prepares individual embryos for germination into the final plant structure.

1.2.3.1 Laboratory protocol for somatic embryogenesis

Current laboratory protocol for small scale production includes in order, proliferation, maturation, and germination. Proliferation is the multiplication of somatic embryos in culture that occurs through repeated cycles of divisions of existing embryos and formation of new somatic embryos from small cell aggregates (Figure 2A). This process is successful both on solid medium and in liquid medium and thus allows for efficient production of unlimited numbers of immature somatic embryos of different developmental stages.

Maturation is the next stage of development, which takes place in conjunction with ceased multiplication of immature embryos and further development of the most developed immature somatic embryos presenting amongst the population of proliferating embryos in culture (Figures 2B and C). Embryo maturation involves the expansion of polarized immature embryos containing an embryo "head" region composed of meristematic cells and the suspensor region composed of highly vacuolated tubular cells. In current laboratory protocol, the maturation phase takes place in air on a solid medium. The mature embryos have to be manually separated from a flocculated cluster of embryos on the solid medium and the process is very tedious (Figure 2E).

Germination is a stage that a polarized maturing embryo develops into a fully mature embryo from the expanded "head" region, whereby the suspensor region will be reduced and eventually disappear. The mature embryo contains two meristematic regions that will give rise to the shoot and root of the resulting plant (Figure 2D). It is a prerequisite for normal development of the embryos into plants that the meristematic

regions develop correctly and are positioned in the correct locations. If the embryo develops appropriately in the maturation stage, the same success rate can be achieved no matter if the germination occurs in air or liquid. It should be noted that keeping the process in liquid will be much more efficient and lends itself to automation and large-scale production.

In summary, the current methods to grow plants from somatic embryos are quite labor-intensive and therefore costly. The underlying reason is due to the tedious laboratory procedure for manually selecting, separating and sorting the embryos during the maturation and germination processes. The current laboratory protocol for somatic embryogenesis is therefore only suitable for small scale production. For large scale production, an automated liquid handling protocol is desired.

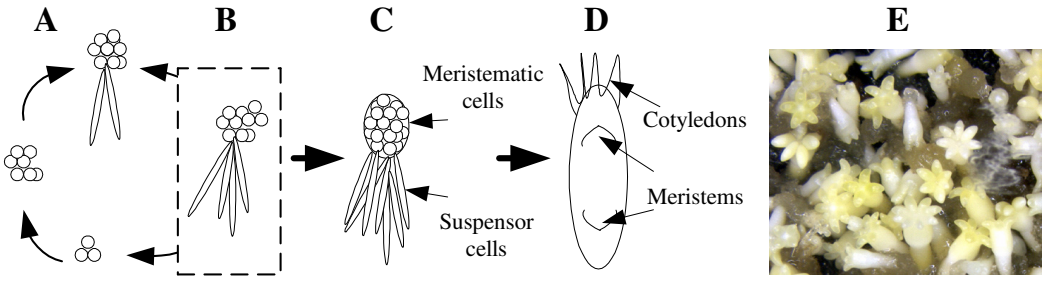

Figure 2. Somatic embryo developmental stages in soft wood trees. (A) Different cellular structures corresponding to different stages of immature embryo development are present during the proliferation phase. (B) Only the more differentiated, polarized structures, i.e. more developed immature embryos, will proceed into the maturation phase. (C) The maturing somatic embryo is a polarized structure composed of a "head" region of meristematic cells, and a suspensor region of oblong vacuolated cells. (D) A mature embryo shows the initial cotyledons in one end of the embryo. A proper mature embryo has distinctive meristems that will give rise to shoot and root, respectively. (E) Cluster of mature embryos combined with partially mature embryos.

1.2.3.2 Desired protocols for large scale production

The desired liquid-based protocol for automated mass production, has the same proliferation as the current laboratory protocol except the maturation and germination stages. The proliferation stage requires continuous agitation of the culture medium to keep a sufficient supply of oxygen to the embryos and to prevent the embryos from flocculating into a clump that is difficult to handle. Agitation also mixes the medium components and increases the nutrient accessibility for the embryos. Since medium nutrient access is already sufficient in the situation when embryos are cultured on solid medium without direct contact with the liquid culture medium, this aspect of the agitation is not considered here. However, the majority of embryos cultured in liquid medium grow in a non-polar form with the suspensor cells growing in all directions. The desired embryos should have a polarized structure which is composed of a "head" region of meristematic cells and a suspensor region of oblong vacuolated cells that will later successfully germinate in liquid.

1.2.3.3 Prerequisite for proper embryo development

A prerequisite for proper embryo development from proliferation to maturation is polarization, which is also one of the hypotheses of this research. This is a generally known effect for somatic embryogenesis of Norway spruce, but not published yet. The transition from proliferation to maturation only occurs in the more developed immature somatic embryos displaying a differentiated, polarized structure (Egertsdotter & von Arnold 1998). Embryos showing polarized structures are common when the proliferation occurs on a solid culture medium and exposed to air (Figure 3A). Polarized embryos,

however, rarely form in liquid medium. Instead, a few suspensor cells form in random directions (Figure 3B). Size fractionation of a liquid culture of somatic embryos, collecting and culturing the smallest clusters of cells and embryos (less than 200 µm; Figure 3C), shows that the early stages of immature embryos develop into polarized structures when being cultured in liquid medium without agitation (Figure 3D), although with a large level of aggregation and cluster formation. The clusters of cells and embryos less than 200 µm are the main study objects for this thesis.

Due to the difficulties in obtaining polarized and developed embryos in liquid medium, maturation of somatic embryos in liquid medium has rarely been reported for any soft wood species, for example, Norway spruce (Gorbatenko & Hakman 2001). Currently, the standard procedure for obtaining mature somatic embryos from a soft wood species involves transferring the proliferating immature embryos from the liquid proliferation medium onto a solid culture medium of the same composition, which allows large, polarized embryos to form (Figure 4A). Somatic embryos cultured in liquid medium are subjected to mechanical stresses incurred by agitation of the culture vessel containing the liquid culture medium. As discussed earlier, this motion is necessary to supply the embryos with sufficient oxygen and to avoid flocculation of the embryos. The early stages of immature embryos respond to this motion by forming immature embryos with multidirectional development of suspensor cells surrounding the embryo "head" region in later stage (Figure 4B).

The advantages of using liquid culture medium in the early stages are to keep the embryos dispersed in liquid and to maximize the growth rate, which greatly affect the

probability of successful germination and plant formation during later stages. It should be noted, however, complete isolation of embryos may not necessarily facilitate growth. It has long been known that cultured cells release conditioning factors into the surrounding medium and that the conditioned medium has a positive feed back effect on newly started cultures. Several studies have been conducted on the nature and mechanism of the conditioning factors using Norway spruce (Egertsdotter et al 1993; Egertsdotter & von Arnold 1995; Egertsdotter & von Arnold 1998). These studies revealed correlations between the amount of stress-related proteins that are released into the culture medium and the morphology of the somatic embryos and the number of suspensor cells produced. It is likely that such conditioning factors also affect the further development of the somatic embryos from proliferation to maturation. The studies reported in this thesis focus on the effects of the mechanical stresses on the embryo development. The effects from any conditioning factors will be normalized by keeping the concentration of embryos constant in all experiments.

The possible mechanism of shear stress signal transduction will be studied separately.

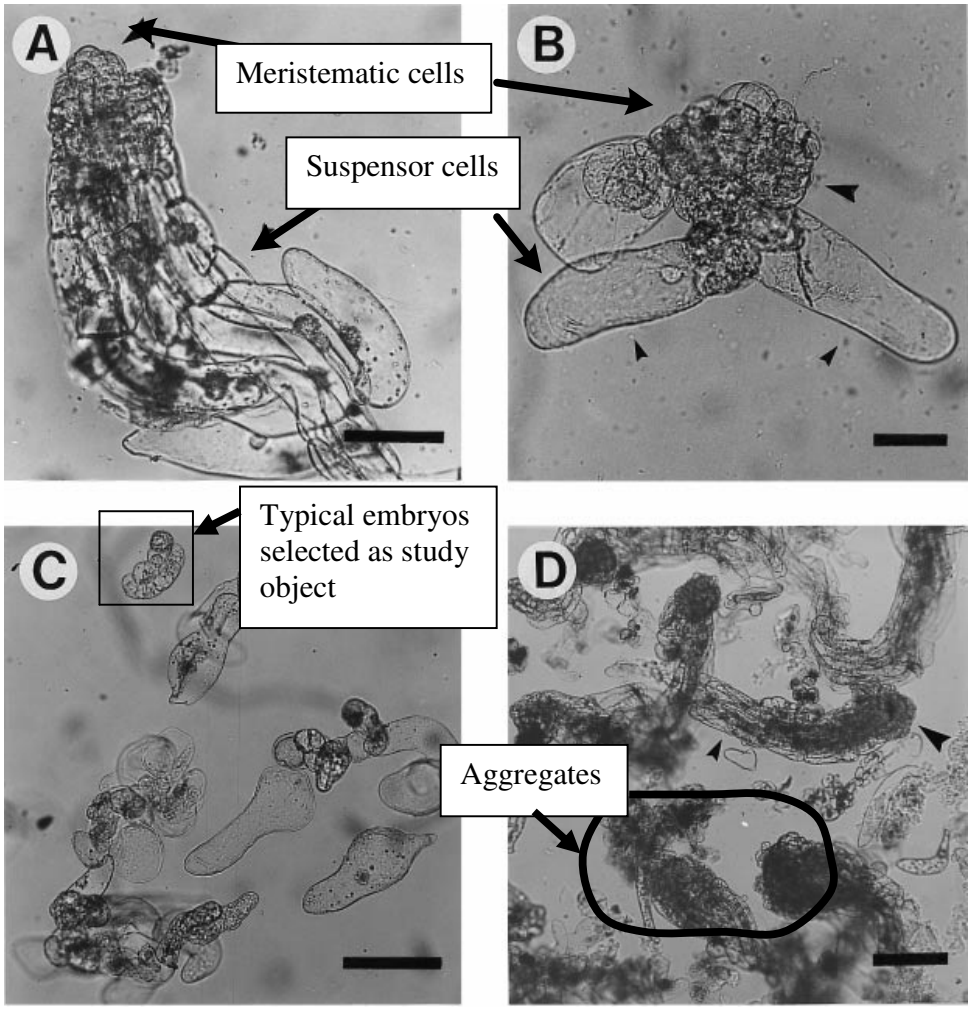

Figure 3. Immature somatic embryos in the proliferation phase. (A) Early stage immature somatic embryo cultured on solid medium. (B) Early stage immature somatic embryo cultured in liquid medium. (C) The fraction of cells and somatic embryos smaller than 200 μm in a liquid culture of somatic embryos at proliferation. (D) The same fraction cultured in liquid medium after 4 weeks in culture without agitation. The big aggregations of polarized immature somatic embryos are shown in the black circle. Scale bars in A-D represent 150, 100, 100 and 300 μm. (Egertsdotter & von Arnold 1998)

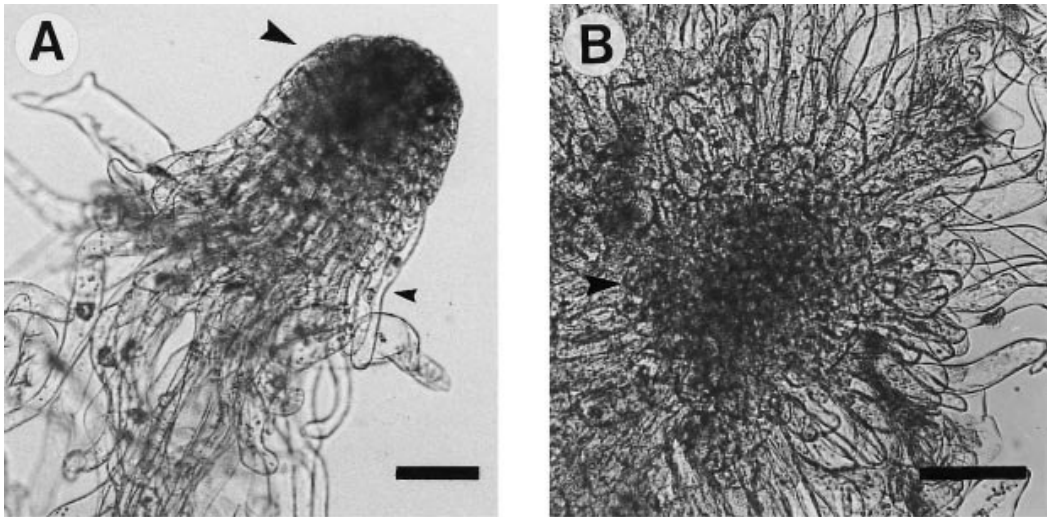

Figure 4. Morphology of somatic embryos of Norway spruce (*Picea abies*) (A) cultured on solid medium, and (B) in liquid medium. Scale bars represent 200 µm. (Egertsdotter & von Arnold 1998)

1.3 Usage of bioreactors for plant cells

1.3.1 Bioreactor for large-scale production in plant cell culture

Plants make an important contribution to the industry, such as the plant secondary metabolites used in pharmaceutical preparations, food additives, as process aids, and in cosmetic and perfumes. Higher plants synthesis a tremendous array of chemical structures, probably greater than any other group of living organisms, like microbial cells (Kieran et al 1997; Sajc et al 2000; Tautorus & Dunstan 1995). In commercial terms, the group of structures which come under the secondary metabolites is the most important. Secondary metabolites are substances whose structure and metabolic interactions appear to be functionally distinct from those involved with primary metabolism. Quite a number of secondary metabolites have properties which are of social and commercial benefits to humans. There are currently three major approaches to produce such fine chemicals,

through extraction of whole plants, synthetic organic chemistry and cell culture. Cell culture is a promising and the cheapest and eco-friendly way among the three approaches (Brodelius & Rosevear 1985; Harry & Thorpe 1999; Holden et al 1987; Kieran et al 1997; Scragg & Fowler 1985; Scragg et al 1987; Street 1977).

It has long been hoped that the unique biosynthetic capacity of plants could be exploited *in vitro* using culture systems analogous to microbial fermentations. The use of mass cultivation of plant cells to produce a continuous supply of material independent of disease, climate, or seasons has obvious attractions to industrial applications. Since the first successful plant-cell culture process was announced in 1983 (Curtin 1983), a large number of bioreactors have been designed and applied to grow plant cells. It should be noted, however, the characteristics of both the growth and metabolism of plant cells *in vitro* differ considerably from those of microbial cells (Brodelius & Rosevear 1985; Harry & Thorpe 1999; Kieran et al 1997; Sajc et al 2000; Scragg & Fowler 1985; Scragg et al 1987). Great efforts have been invested by various researchers to optimize the plant-cell culture process. For example, Tanaka (1981) investigated how to enhance product yield (Tanaka 1981); McDonald et al. (1996), Mo et al. (1996) and Ziv et al. (1994) focused their research on developing growth media and production media that better support plant cell growth and secondary metabolites productions (McDonald et al 1996; Mo et al 1996; Ziv et al 1994); Pinto et al. (2004) studied how product synthesis and growth affect stability and variability of cell lines (Pinto et al 2004); and many groups have investigated the secondary metabolite biosynthesis process, which provides an additional production option to natural product synthesis (Aoyagi et al 1992; Archambault et al 1994; Brodelius & Rosevear 1985; Cervantes et al 2006; Chi et al

1994; Egertsdotter 1999; Fleischer et al 1998; Ingram & Mavituna 2000; Kieran et al 1997; Mehrotra et al 2007; Moorhouse et al 1996; Morris & Fowler 1981; Scragg et al 1987; Serra et al 2009; Shi et al 2003; Street 1977; von Arnold et al 2005; Zhang et al 2008; Ziv et al 1994). Plant-cell culture can be used as an alterative route to whole plant or established product synthesis, a means of synthesizing novel products, and a source of enzymes as process aids for biotransformation systems and natural products where the source plant is difficult to grow.

Its large-scale production capability makes bioreactors more appealing in the cell and tissue culture industry. Bioreactors provide a well-controlled cultivation environment. The physical and chemical conditions inside of bioreactors can be controlled for optimum growth. The increased working volume coupled with the potential for automation of culture is ideal for reducing labor-intensive manual tasks and production costs. Most bioreactors are designed with either a mechanical or gas agitation mechanism to provide mixing and maintain the homogeneity of the culture media by dispersing the cells to avoid aggregation.

Somatic embryogenesis technique has the potential for large scale clonal propagation of plants in a short period of time. The ability to grow somatic embryos in liquid medium would make the production more efficient. For cultivation of cells at laboratory scale, a simple mechanically shaking flask can be used and normally very effective; however, for large scale or industrial scale production, bioreactors provide many advantages for the growth of plant cell and organ cultures. Various types of bioreactors have been developed to automatically and continuously monitor and control the culture conditions for somatic embryogenesis.

1.3.2 Bioreactor types

Over the past two decades, many reviews have been done on bioreactors that were designed and configured for culturing plant cell suspensions, plant tissue and organs (Kargi & Rosenberg 1987). Bioreactors for plant cell culture can be classified according to the type of agitation used (Mehrotra et al. 2007; Sajc et al. 2000): mechanically agitated bioreactors, including aeration agitation bioreactors, rotating drum and spin-filter bioreactors; air-driven bioreactors, including bubble column, concentric tube airlift reactors, external loop airlift bioreactors, propeller loop reactors and jet loop reactors; non-agitated bioreactors, including packed bed, fluidized bed and membrane reactors with immobilized cells. Among all types of bioreactors, the aeration-agitation bioreactors are the most popularly used, which are often referred as stirred tank with impellers as turbines, screws, paddles and helical ribbons (Gupta & Timmis 2005).

1.3.3 Limitations of bioreactors

At the early stages of growing plant cells in a bioreactor, the relatively low growth rate and rich media requirement make the culturing process prone to microbial contamination. In addition, the large size (20-200 μm) and aggregated nature of plant cells in suspensions cause difficulties in mixing within bioreactors. A further constraint is added to these systems due to the fact that many plant cells are sensitive to shear stress induced during mixing (Chen & Huang 2000; Cunningham & Gotlieb 2005; Shi et al 2003; Sowana et al 2001; Sun & Linden 1999; Tanaka 1981). Since most bioreactors are designed for culturing microbial and plant cells, it is necessary to better understand the requirements imposed on differentiated cells by large-scale culture of clusters, embryos

or buds. As shown by Preil, many factors could affect proliferation, such as, the rate of aeration and circulation, cluster or organ size, O_2 and CO_2 levels and the damaging effects of shearing forces due to rapid mixing and circulation (Preil 1991). It is also necessary to reduce the undesirable conditions encountered in plants that are cultured in liquid media, for example, morphological aberration and hyperhydration (Ziv 1991; Ziv et al 1994). Tautorus and Dunstan (1995) reviewed the suitability of various types of bioreactors for the culture of somatic embryos. However, direct comparisons of different bioreactor configurations for somatic embryo growth and development are rare.

Bioreactors are normally designed and configured for specific purposes with their unique advantages and disadvantages based on their applications. Stirred tank bioreactors typically use bubble aeration to provide oxygen supply. This design is of high power consumption and the cells experience high shear. Many researchers have studied the shear stress effects on the suspension cultured cells in order to improve the reactor design for scale-up production (Ingram & Mavituna 2000; Kieran et al 1995; Sowana et al 2001; Takeda et al 1998). Different blade types, blade numbers, internal positions of blades, and the ratios of stirrer diameter to that of vessel were tried to optimize the reactor for shear-sensitive cells (Paek et al 2001). Another type of reactors, airlift bioreactors, has generally lower relative velocity between liquid and air bubbles, therefore lower shear rate. For this reason, airlift bioreactors have been favorable for culturing cells that are sensitive to shear (Debnath 2007; Ingram and Mavituna 2000; Sajc et al. 1995a; Sajc et al. 1995b). In addition, the design of the airlift reactors is simple and the energy consumption is low. However, air induced foaming makes the cultured cells tend to be thrown out of culture medium and grow on the foam head and the wall of

culture vessel. This leads to big aggregation of cells. Non-agitated bioreactors are mostly used for immobilized cells. Membrane reactors and packed bed reactors are advantageous for the case wherein a large number of cells are immobilized or densely "packed". The disadvantage of these reactors is the inefficient mass transfer that affects transport of nutrient and gas supply (Prenosil & Pedersen 1983).

The approach of immobilizing cells has been successfully applied to culture shear-sensitive cells. In an immobilized system, growth and production phases can be decoupled and controlled by chemical and physical stress conditions. Since most of the plant cells have low tolerance to sustained shear, immobilization offers the cells a microenvironment with well-defined shear field and protects the cells from being exposed to excessively high shear. Mavituna et al. reported that *Capsicum frutescens* Mill. cv. a*nnuum* (chili pepper) cells were entrapped in polyurethane foam matrices to successfully produce the pungent flavor, capsaicin (Mavituna et al 1987). Later, more studies using immobilized cells focused on valuable products of secondary metabolism (Adris et al. 1994; Lopez and Matson 1997; Molina-Munoz et al. 2010; Rosenberger et al. 2000; White and Broadley 2000).

Further improving the bioreactor designs requires knowledge on various media components and the mechanism of signal transduction of plant cell. Researchers have identified different media components for culturing different species, such as the most popularly used half-strength Quoirin and Lepoivre's (½ LP) medium, and Murashige and Skoog (MS) medium (Declerck and Korban 1994; Egertsdotter 1999; Kim et al. 2009). The nutrient requirement for the induction of somatic embryos is quite different from that for the normal development and conversion of somatic embryos into plantlets. Thus, a

majority of studies that use bioreactors were conducted in batch cultures while few studies can be found for micropropagation of plants via tissue cultures, such as meristem tips and shoot propagules (Debnath 2007; Debnath 2009; Jo et al 2008; Sharma et al 2009). So far, only a small number of plant species, several ornamental, vegetable and fruit crop plants are successfully propagated through organogenic or embryogenic pathway using bioreactors (Mehrotra et al 2007).

1.4 Shear stress effects on cells

Cells can sense and respond to a broad range of chemical and mechanical stimuli. Mechanical forces can also influence cell structure, growth and function (Gloe et al. 2002; Li et al. 2005; Lynch and Lintilhac 1997; Wang et al. 1993). Cells *in situ* are subjected to various mechanical stresses, such as gravitational force, mechanical stretch and shear stress. For example, Endothelial cells lining blood vessels as a cellular monolayer experience all those mechanical forces and in particular are exposed to a relatively elevating shear stresses associated with blood flow (Fisher et al 2001; Gloe et al 2002; Li et al 2005; Metallo et al 2008; Nerem et al 1998; Yu et al 2002); Bending and twisting in wind introduce mechanical stress (Carpita et al 1979); Drought and salinization in nature can be manifested by osmotic stress in plant cells, which can cause cell damage or death (Menke et al 2000; Pei & Kuchitsu 2005; Spiteller 2003); Appropriate turgor pressure keeps the plant cells shape (javis 09) (Jarvis 2009; Lynch & Lintilhac 1997; Malinowski & Filipecki 2002). It is of great interest to study how cells sense and respond to changes in shear stress.

1.4.1 Shear stress on cells cultured in bioreactors

A well-designed culture vessel provides a controlled environment inside which the shear stress can be adjusted. This provides controlled test conditions to study how the cells are affected by flow-induced shear stress (e.g., blood flow for endothelial cells or liquid culture media flow for plant cells). The study is expected to help researchers to understand the molecular mechanism and signal transduction.

Studies of shear stress effects on cells can be broadly divided into two categories. Cell suspensions are either exposed to shear stress under permissive growth condition for the duration of cultivation, or cells are exposed to well-defined laminar or turbulent flow for a short time period and under non-permissable growth condition (Kieran et al 1997). In studies done in both categories, scaled-down experiments are typically conducted, which serve as predictions for scaled-up applications. In the first category, the hydrodynamic environment is generally regulated by changing the rate or method of agitation. The level of shear can be estimated from the impeller speed or power input to the agitator. It is, however, rather difficult to accurately quantify the shear rate that the cells are exposed to. The experimental exposure time is limited by the kinetics of the system and the ability of the cells to survive the experimental conditions. In the second category, cells are exposed to well-defined laminar or turbulent flow in a Couette (Kargi & Rosenberg 1987; Paul et al 2003), capillary (Kieran et al 1995; Shin et al 2004), or submerged jet flow (MacLoughlin et al 1998) for short periods of time. Typically, the viability loss is used to describe the resultant death of cells due to exposure to the shearing conditions.

Shear in these experiments mentioned above is experienced by the whole suspension as a presumption and the results are concluded based on an average/statistics. In suspension cultures, the morphology of plant cell clusters exhibits a great variety. For studies that apply shear to the whole suspension and obtain results based on averaging, the shear effects on a single cell or cell cluster cannot be quantified since the averaging process shields the changes of cells in one particular size group. Thus, no single mechanism for cell responding to shear has been conclusively identified.

In 1997, Lynch and Lintilhac (Lynch & Lintilhac 1997) studied the response of embedded protoplasts of tobacco root cells in agarose blocks to mechanical loads by directly applying controlled mechanical load to agarose blocks. The orientation of primary division plane of the embedded protoplasts was used as an indication of the cells' response to the mechanical load. Since the mechanical load was applied on agarose blocks, the stress experienced by individual protoplasts could not be accurately determined. Lynch and coworkers combined two ideas in their experimental design, embedded cells of which are easy to keep a track and controlled mechanical load which is accurately set for each experiment.

In order to track the change or development of a single cell or cells group, immobilization of the cells is necessary. Plant cells can be immobilized by attaching them on carrier beads, net or foam surface; and entrapping into porous gel made of natural or synthetic polymers and membranes in flat sheet and hollow fiber. Immobilization of cells with these methods has been extensively studied with respect to cell viability and function, and physical and mass transfer properties of the immobilization support (Birnbaum & Mosbach 1991; Curtis et al 1995; Gontier et al

1994; Kurata & Furusaki 1993). Pati et al. immobilized protoplast cells on an extra thin alginate film and observed the development of those cells (Pati et al 2005). This extra thin alginate film provides an efficient culture environment for protoplasts and makes it easy to keep track of the development of each single protoplast.

1.4.2 Cell morphology studies

Plant cells undergo various morphological changes during whole culture period. Norway spruce somatic cells even have more varieties of cell shapes at proliferation stage (Figure 2). Since only the most differentiated cells can successfully respond to maturation stimuli and further develop and mature, morphology of cells at proliferation stage is an important factor to study.

1.4.2.1 Different experimental setups

Different setups have been used to study the morphology of cells, for example, agarose or alginate film/block embedded with protoplasts (Golds et al 1992; Lynch & Lintilhac 1997; Pati et al 2005), cytometry combined with motorized microscope stage for automatic image analysis of specimens (Lockett & Herman 1994), fermenters for microorganisms (Thomas 1992), flow chambers culture (Metallo et al 2008; Ye et al 2008). All these setups were designed for specific needs. Agorose or alginate film/block have cells embedded which provide culture environment for cells and make it easy to trace the development of individual cell. Cytometry guides cells flow through the system in order to sample and observe on single cell. Fermenter for microorganism is for scale-up industrial production. Flow chamber provides a well-controlled flow environment inside of which shear stress can be estimated.

Flow cell chambers have been extensively used to study shear stress effects on morphology of mammalian cells in culture (Metallo et al 2008; Ye et al 2008). Different configurations of flow cell offer various flow patterns, such as laminar steady flow, step disturbing flow, turbulent flow, jet flow and capillary flow (Kargi & Rosenberg 1987; Kieran et al 1995; MacLoughlin et al 1998; Paul et al 2003; Shin et al 2004), thus various shear stresses can be studied. Shear stress effects on gene expression and morphology on human endothelial embryonic cells cultured in a flow cell chamber have been described also (Metallo et al 2008).

Combination of alginate film embedded with cells and well-defined fluid field inside of a flow chamber will provide a desirable setup to follow the development and morphological changes of individual cell clusters of Norway spruce.

1.4.2.2 Image analysis methods

To observe the morphology changes of cells, a powerful tool is a microscope. In the past, microscope is used to record the morphology and differentiation of cells. Through analyzing the recorded images, either qualitative information or quantitative information is obtained (Chi et al 1996; Ibaraki & Kenji 2001; Kristensen et al 2008; Petřek et al 2007; Petřek et al 2005; Thomas 1992). Traditional analysis of the recorded images was based on human observations. This makes the measurements subjective and inconsistent. Image analysis, however, is a well established complement to optical microscopy and makes measurements accurate and reproducible, and usually quicker. It also makes repetitive measurements semi-automation/automation possible. The use of image analysis has been widely applied in mammalian cells, filamentous organisms and

plant cells in suspension culture (Chi et al 1996; Petřek et al 2007; Petřek et al 2005; Thomas 1992; Thomas & Paul 1996; Zhang et al 1996).

To extract information from an image, image analysis starts with the capturing of images, the storage of the images and followed by the processing of the images. The algorithms used to process the images are normally based on the feature of the images and the desired application of the extracted data. For example, cross-correlation techniques have been used to reveal the spatial similarity of groups of particles between groups of neurons (Reid & Alonso 1995; Tanaka 1985), in surface patterns detection (Ono et al 2001), and in particle image velocimetry (PIV) technique (Adrian 1991). Spectral analysis through discrete and fast Fourier transformations has been applied to acquire quantitative information on different embryo shapes (Cazzulino et al 1987; Chi et al 1996; Chi et al 1994; Vits et al 1994). The features converted from the segments of an embryo contour by discretizing the entire contour with an equal angle increment, resulted in a non-uniform contour sampling and could not consistently define the cotyledonary embryos (Chi et al 1994). To address this issue, a different Fourier descriptor was employed with the contour of embryos discretized by an equal arc-length increment (Vits et al. 1994). The same algorithm was further applied to liquid cultured carrot embryos to categorize embryos into different groups based on the distinguishable developmental stages for the purpose of rapid evaluation of the overall yield of embryos in a bioreactor, and the robustness of the method tested (Chi et al 1996; Chi et al 1994; Zhang et al 1996). These features have been useful to describe the developmental stages of plant somatic embryos in typical angiosperm species, e.g. carrot, showing distinctive shapes at

different developmental stages. These two methods are especially useful to identify the shape of an embryo and hence sort the picked embryo into one specific category.

1.4.2.3 Parameters used to quantify shear stress effects

To quantify the response of cells to a given hydrodynamic environment, many parameters are used. For example, a critical shear stress of 50 N/m^2 was reported (Kargi & Rosenberg 1987) for suspensions of *Daucus carota* using regrowth potential as an indicator of system response; Another parameter, energy dissipation, was used as a measure for shear stress effects on cells (Dunlop et al 1994; Jeffers et al 2007; Kargi & Rosenberg 1987; Kieran et al 1995; MacLoughlin et al 1998; Sowana et al 2001). Although the energy dissipation rate is a useful parameter for studying the flow inside of bioreactors, it is difficult to accurately predict the shear inside of bioreactors. It is hard to get the exact value of shear stress in shaken flasks and airlift bioreactors but can be estimated based on the reported data (Sajc et al 1995a; Sajc et al 1995b; Stathopoulos & Hellums 1985). For example, Stathopoulos et al. (1985) conducted their experiments using human embryonic kidney cells in vitro and reported that forces of 0.65 N/m^2 had significant effects on cell morphology and forces higher than 2.6 N/m^2 caused marked reduction in cell viability.

In these experiments mentioned above, either study organism under conditions that are either permissive or impermissible to grow. The parameters to quantify the shear stress were selected based on the selection of experimental setups. For example, experimental exposure time was picked for experiments that most of the organism could not survive under the test conditions; in the counterpart, the viability loss and well-

defined shear stress were generally used to describe the resultant death of cells due to exposure to the shearing conditions where most of the organism could survive.

Evidence of sensitivity to hydrodynamic shear in conventional stirred tank and air-lift reactors has been attributed to the physical characteristics of the cells, namely their size, the presence of a rigid cell wall, the existence of a large vacuole, and their tendency to aggregate (Kieran et al 1995; Moorhouse et al 1996; Sowana et al 2001; Sun & Linden 1999). In terms of morphological changes in response to shear stress, different developmental stages of carrot somatic embryos have been characterized by parameters describing the shape of the embryo in terms of axial length, diameter, cotyledon length and cotyledon arc (Schiavone & Cooke 1985).

Other parameters used to describe the response of cells to stress are growth rate by measuring dry weight (Sun & Linden 1999), sugar consumption (Chen & Huang 2000), the first response to environment changes such as the increase of Ca^{2+} or the change of pH and secretion of second messengers, such as stress proteins (Chen & Huang 2000).

1.4.3 Shear stress responses and signal transduction mechanisms

1.4.3.1 Mammalian cell response to shear stress and signal pathways

Mammalian cell response to shear stress has been extensively studied, especially endothelial cells (Cervantes et al 2006; Cheng et al 2008; Cunningham & Gotlieb 2005; Fisher et al 2001; Gloe et al 2002; Li et al 2005; Metallo et al 2008; Nerem et al 1998; Prentice et al 2007; Reneman et al 2006; Ye et al 2008; Yu et al 2002; Zhang et al 2008).

Shear stress is believed to play an important role on endothelial cells (ECs) in vascular development, remodeling and lesion formation. Shear stress also has been recognized as an important modulator of endothelial phenotype, morphology, gene expression and differentiation (Gloe et al 2002). ECs use multiple sensing mechanisms to detect changes in mechanical forces which lead to the activation of signaling networks. Li et al. (Li et al 2005) reported in their work that ECs respond differently to different modes of shear forces, such as laminar, disturbed and oscillatory flows. ECs that are subjected to steady laminar flows tend to elongate along flow direction and the steady flow causes a transient induction of reactive oxygen species (ROS), so called oxidative burst. Pulsatile flows with different levels of mean and oscillatory components make ECs exhibit similar elongation and alignment as steady flows. ECs that are exposed to pure oscillatory flows keep their polygonal shapes that are common to ECs in static culture or at vessel bifurcations. The study also shows that when the shear stress patterns vary, ECs respond differently in the signaling, gene expression and functions (see Fisher et al. 2001 for a review).

There are many mechano-sensors for shear stress in ECs, for example, integrins, ion channels and adhesion molecule-1 (PECAM-1), etc. Past studies have shown that atherosclerotic plaques occur preferentially at arterial locations that experience turbulent flow or shear stress lower than 5 dyne/cm^2 (Reneman et al 2006). In such regions, endothelial cell (EC) repair is reduced, coupled with increasing in ROS, endothelial permeability to lipoproteins, smooth muscle cell proliferation and collagen deposition, etc (Cunningham & Gotlieb 2005). Low shear stress activates IL-8 gene expression (Yu et al 2002) and mitogen-activated protein kinase (MAPK) along ERK1/2 and JNK1/2 regulate

this expression (Cheng et al 2008). Integrins as a family of more than 20 transmembrane heterodimers composed of α and β subunits, mediate both "inside-out" and "outside-in" signaling in mammalian cells. The extracellular domains of integrins bind to extracellular matrix (ECM) ligands for "inside-out" signaling and extracellular stimuli induce the intracellular signaling cascade via integrin activation for "outside-in" signaling (Li et al 2005; Schwartz et al 1995 for a detail describsion of integrin pathway in mammalian cells). Those results suggest shear stress not only change the morphology of mammalian cells, but also activate different signal pathways. ROS have been shown to related to shear stress, activation of some stress proteins, regulation of transporters and ion channels, cell adhesion and spreading, cell proliferation and wound healing, etc. (for a recent review, Bartosz 2009)

The importance of shear stress in determining cell fate has recently received attention in mammalian cell systems through the potential positive effects of shear stress on stem cell development (Stolberg & McCloskey 2009). The recent findings from mammalian cell research may help shed light on plant meristematic cell development, and further suggest signaling pathways involved in the plant meristematic cell response to shear stress. Integrin proteins are conserved in vertebrates, invertebrates, and fungi, according to past studies (Hynes 1992; Schwartz et al. 1995; Swatzell et al. 1999). Evidence from previous research using monoclonal and polyclonal antibodies to localize β1 integrin-like proteins in plants suggests that integrin-like proteins may be present in plants as well, and these proteins may function in signal transduction (Gao et al. 2007; Lü et al. 2007; Sun et al. 2000; Sun and Sun 2001; Swatzell et al. 1999).

1.4.3.2 Plant cell response to shear stress and signal transduction

Integrin-like protein detection in plant cells

The mechanism of plant cell signal transduction is not known as clear as mammalian cell; however, studies on mammalian cells will shine lights on the research of plant cells. There is some evidence suggesting that in some plant species the plant cell wall may interact with extrinsic and intrinsic proteins, for example integrin-like proteins, on the plasma membrane, which are similar to the transmembrane integrin(s) in mammalian cells (Hynes 2002; Luo & Springer 2006).

Integrin proteins in mammalian cells sever as receptors that mediate attachment and signal transductions between cell and ECM. In plant cells, however, the structure of integrin proteins is not fully discovered. A tripeptide sequence Arg-Gly-Asp (RGD) motif which is conserved in each of the adhesive proteins (like integrins) has been recognized in Taxus cells (Gao et al 2007) and *Zea may* cells (Lü et al 2007), and proved to play a role in shear stress signal transduction. Western blot tests of the extracellular proteins proved that these RGD-related proteins have the similiar molecular weight as integrins. This RGD-related protein is so called integrin-like protein in plant cells.(Gao et al 2007)

Integrin-like proteins have been detected in many plant species, for example, soybean root which was the first cell reported to have integrin-like proteins (Schindler et al 1989), onion epidermal cells (Gens et al 1996), pollen tube of *Lilium davidii* and *Nicotiana tabacum* (Sun et al 2000) and root tip cells in *Zea mays* (Lü et al 2007). Integrin-like proteins transmit both outside-in and inside-out signaling and are involved

in development, wound healing and other stressed processes (Brownlee 2002; Hynes 2002; Lü et al 2007; Lynch et al 1998; Sun et al 2000; Sun & Sun 2001; Swatzell et al 1999).

Reactive oxygen species detection in plant cells

Reactive oxygen species (ROS), including hydrogen peroxide (H_2O_2), superoxide ($O_2^{\bullet -}$) and hydroxyl radical (OH-), are natural byproducts of normal metabolism of oxygen. Production of ROS is believed to generally occur by direct transfer of excitation energy from chlorophyll to produce singlet oxygen, or by univalent oxygen reduction at photosystem (Allen 1995; Foyer et al 1994). Past studies suggest that ROS may play a central role in many signaling pathways during stress perception, regulation of photosynthesis, pathogen response and plant growth and development (Apel & Hirt 2004; Dat et al 2000; Foreman et al 2003; Neill et al 2002).

Production of ROS has been studied as a parameter of shear stress on the plant cells (Gao et al 2007; Gens et al 1996; Swatzell et al 1999). The transient generation of ROS, also known as oxidative burst, has been thought to be a hallmark of plant defense response to both biotic and abiotic stresses. Studies with Arabidopsis (*Arabidopsis thaliana*) and rice (*Oryza sativa*) have shown that ROS are associated with aging. ROS are connected with cellular and molecular alteration in animal and plant cells, and are essential to induce disease resistance and mediate resistance to multiple stresses in plant (for a review, Kotchoni & Gachomo 2006).

The role of cell wall in signal transduction

The mechanical strength and contiguous nature of plant cell walls provide mechanical protection for the cell against a wide variety of stresses, such as mechanical and microbial stresses. Cell walls respond to the internal stress of turgor pressure, sense damage or loss of integrity and help the signal pass to cytoplasm (Hematy et al 2007; Turner 2007). Plant cell walls not only play a role in signaling as the cells sense their environment through this large porous network but also represent the first line of defense against pathogens.

Since some substances of smaller size, such as salts, sugars and amino acids, can move freely in the plant, the pore size must be bigger than those molecules in order to provide them a free passage. Signaling molecules also need to pass the cell wall and reach the cell membrane in order to have an effect. It has been argued that size exclusion at this level controls development (Jarvis 2009). Study of loblolly pine (*Pinus taeda*) has shown that osmotic pressure changes during the zygotic embryo development inside of the ovule (Pullman & Johnson 2009). In the maturation culture medium, macromolecules are added into the culture medium to stimulate the maturation process (von Arnold & Eriksson 1981). The osmotic pressure is changed by adding the macromolecules. The medium components have an impact on the growth and development of somatic embryos (Pullman et al 2005a; Pullman et al 2005b). Based on the past studies, pore size is found to play a role in a variety of host-pathogen interactions, such as recognition phenomena involving lectins and integrins (Carpita et al 1979; Gao et al 2007; Jarvis 2009; Sequeira 1978). Jarvis (2009) reviewed, in details, the structure of primary cell wall in nongraminaceous plants and discussed the role of cell wall in providing mechanical support, sensing and signaling, etc.

The past pore size tests with solute exclusion technique are based on the plasmolysis and cytorrhysis responses of cells to macromolecules of known sizes. Based on the phenomena of either plasmolysis or cytorrhysis, one can have an idea of how big the pore size of the cell wall is in comparison with the solute size.

Plasmolysis is a process in plant cells where the plasma membrane pulls away from the cell wall due to the loss of water through osmosis. Molecule concentration outside of the plasma membrane is higher than the inside. In another word, the solute concentration inside of cell is lower than the outside. Since cell wall is a semi-permeable membrane and water can move freely through it but large molecules do not have free passage. The solution outside of plasma membrane is a hypertonic solution having more solutes per unit volume when compared to the solution on the opposite side of the semi-permeable membrane. Water moves outside of the membrane to reach a balanced concentration on both sides of the membrane.

When water loss is severe, cytorrhysis will follow plasmolysis. Cytorrhysis is the complete collapse of a plant cell's cell wall within plants due to the loss of water through osmosis. Cytorrhysis occurs when the size of the molecules constituting the osmoticum exceeds that of the pores of the cell wall matrix. It is formed by the inward bending of the outer wall of a single cell as water goes out and the cell volume decreases. The wall bends until touches in the cell center. Although the cell wall is not actually destroyed, the vacuole, which is a membrane enclosed compartment and contains water in plant cells, seems to increase in size and finally collapses, releasing its components into the cytosol. The plasma membrane seems to be pressed to the cell wall. The collapse will cause a much greater loss of shape and structure comparing with plasmolysis. The cells might be

extremely damaged and possibly dead. This process is reversible and increases the plants resistance of loss to drought.

Shear stress studies on cultured plant cells

Shear stress effects on *undifferentiated* plant cells, not somatic embryos, have been studied in different bioreactor types (Kieran et al 2000). Various approaches of measuring the effect of shear stress on cell growth have been used, notably the viability of cells (Hooker et al 1989; Zhong et al 1994), and the production of secondary metabolites (Takeda et al 1998; Zhong et al 1994). More recent studies have focused on the cellular and molecular responses of plant cells to shear stress, such as RGD peptide, MAPK cascade and ROS being signaling molecules. In particular, the shear stress responses of *Taxus cuspidata* cells have been extensively characterized using a Couette-type shear reactor; where at a shear rate of 95 s^{-1} an oxidative burst similar to the pathogen defense response was recorded (Han & Yuan 2004); at 190 s^{-1} there was a detectable response to RGD peptides by reduced level of phosphorylation of MAPK-like cascades, a reduced alkalinization response, production of ROS and accumulation of phenolics, thus suggesting a cellular response to shear stress resembling the MAPK-like cascades present in mammalian cells (Gao et al 2007). The oxidative response was further investigated by analyzing the proteins released to the culture medium (Cheng & Yuan 2009). Shear rates below 458 s^{-1} enhanced the primary metabolism and shear rates over 719 s^{-1} initiated an oxidative stress response in the *Taxus chinensis* var. *mairei* cells (Shi et al 2003). The hydrodynamic stresses on *Taxus* cells at the gas-liquid interphase in a bubble column studied using a 3D Laser Doppler Anemometer (LDA) system showed an initial damaging effect from the bubble column conditions and a long term

improvement in growth over suspension culture flasks (Zhong & Yuan 2009). Previous studies have shown that the profile of extracellular proteins derived from Norway spruce somatic embryos and presented in culture medium are related to the developmental stage of the proliferating embryos (Egertsdotter et al 1993; Mo et al 1996), and more developed embryos specially relate to presence of extracellular chitinase and zeamatin (Mo et al 1996). These findings suggest that specific proteins may affect the development of somatic embryos at some developmental stage.

It should be noted that undifferentiated plant cells do not have a defined morphology, and also do not progress through stages of development. Thus, the discussion of shear stress in plant cell suspensions has limited applicability to the present study where the focus is specifically on shear stress effects on morphology and development of somatic embryos. However, these responses might shine light on the study of cellular response of Norway spruce somatic cell clusters under shear stress. Studies about shear stress effect on individual somatic embryo development are blank and warranty further research. Next the details of designed experiments in this thesis to study the shear stress effect on individual immature somatic embryo development and the possible mechanisms of stress signal transduction will be presented in Chapter 2.

CHAPTER 2

MATERIALS AND METHODS

This chapter describes the materials used for each experiment, along with methods and detail procedures. Both steady shear stress experiments and signal transduction experiments are introduced. Section 2.1 describes the working materials used in this thesis. The method used for cell immobilization in steady shear experiments is introduced in Section 2.2, followed by steady shear experiments details in Section 2.3. The experimental setup for imaging the cells is described in Section 2.4. Section 2.5 introduces the image processing method and quantification analysis. Section 2.6 details the validation of image processing method with artificial images. Finally, Section 2.7 describes the signal transduction experiments which cover integrin-like proteins and reactive oxygen species (ROS) detections and pore size monitoring with solute-exclusion experiments.

2.1 Plant material

Norway spruce somatic cells in the proliferation phase were primarily used in current studies. Somatic embryos are cultured from open pollinated seeds of Norway spruce following the procedures introduced by (von Arnold 1987). In brief, the somatic embryos are initiated on a solid medium and then proliferated for multiplication in a medium with identical composition. For faster multiplication, the cultures are transferred to liquid medium of the same composition and sub-cultured with fresh medium every seventh day.

Successful proliferation can be achieved using either solid or liquid culture medium. Cells grow on solid medium in callus which is a lump composed of cultured cells and form relatively bigger aggregates compared with liquid cultured cells. This difference is essentially due to the shear stress introduced by agitation that keeps cells well dispersed in the liquid. The size difference makes liquid cultured cells more suitable for shear stress studies since cells in smaller aggregates can be more easily and more evenly exposed to shear stress compared with cells in bigger aggregates.

The somatic embryos of ten different cell lines, cell line #1, #2, #3, #4, #5, #6, #7, #8, #9 and #10, at proliferation stage are treated to produce mature embryos that will subsequently be treated to induce germination and eventually grow into plants (Högberg 2003). Briefly, 2 to 3 callus of immature somatic embryos are transferred from solid medium to 15 ml liquid medium in a 250 ml Erlenmeyer flask rotating on a shaker table. Cells are sub-cultured once a week until well dispersed suspension cells established. Three cell lines that readily produce plants are then selected from the initial ten, to be used for the experiments. Among these three cell lines, cell line #3 has most ideal cell clusters in the range of 100 to 200 μm that are composed of meristematic cells with only few or without suspensor cells. Cell line #3 was picked as the working material for the shear experiments. Proliferating liquid suspension cultures from cell line #3 are cultured in 250 ml Erlenmeyer flasks on an orbital shaker (Lab-line, Model 3520) with a rotation speed of 100 rpm in a dark room at 25 °C. The culture medium is ½ LP (von Arnold & Eriksson 1981) for proliferation stage. Each flask of suspension culture is sub-cultured every two weeks (Egertsdotter 1999). For ROS and integrin-like protein detection experiments, same suspension cultured cells from cell line #3 was used.

For the pore size study in signal transduction experiments, cells cultured on solid medium, which has the same components as liquid medium but solidified with agar, at proliferation stage were used instead of liquid suspension cultured cells in order to eliminate the effect of shear stress experienced by the cells in the liquid medium. For a well established liquid culture, cells can divide and multiply infinitely thus we assume these cells having been acclimated to the shear stress introduced by the liquid condition. However, cells cultured on solid medium do not experience shear stress at all. By using cells cultured on solid medium, cells affected by later introduced shear stress in liquid medium would better stimulate the effects from liquid culture conditions.

2.2 Cell immobilization

Immobilized plant cells show a great potential for production of some enzymes and secondary metabolites (Aoyagi et al 1998; Curtis et al 1995; Lindsey & Yeoman 1984; Lindsey et al 1983; Mavituna et al 1987; Thu et al 1996). In an immobilized system, growth and production phases can be decoupled and controlled by chemical and physical stress conditions. Since most of the plant cells have low tolerance to sustained shear, immobilization also offers a microenvironment with well defined shear field or protection from shear. For cell immobilization and encapsulation, alginate is widely used due to its biocompatibility and simple gelation with a divalent cations such as Ca^{2+}. Thu et al. (1996) described in detail the structure function of alginate gels relevant to their use as immobilization matrix for cells. Their work provided broad background information of understanding the basic structure-function correlations.

To find the shear stress effect on individual cells, the growth of each cell needs to be tracked and recorded. This can not happen in suspension cultures but can in an

immobilized cell system. Since the growth and production of plant cells can be decoupled and controlled in an immobilized system, immobilization offers plant cells a microenvironment exposed to a defined shear field. Once the cells were immobilized on alginate films, culture medium streamed over the cells, as designed in experimental setup, provided nutrients to cells and introduced direct hydrodynamic stresses. Following detail description of how Pati et al. (2005) immobilized protoplast cells on an alginate film and observed the development of those cells, a modified procedure of immobilization of the somatic embryos with alginate is developed in this thesis.

2.2.1 Cell collection procedure

Before immobilization, cell clusters for the steady shear stress experiments were collected in sterile conditions following the procedure:

(1) All the tools, flasks and beakers which are autoclavable were autoclaved; non-autoclavable tools and containers were wiped with 75% alcohol and surface sterilized by exposing to UV light overnight.

(2) 25 ml of dense suspension culture at day 5 after each subculture, when the culture proliferation rate is at peak (Egertsdotter & von Arnold 1992), was passed through 500 μm and 200 μm nylon mesh (Small Parts Inc.) with 1000 μl micropipettor, respectively, in a bio-hood.

(3) The cells were settled for 30 minutes and collected for immobilization in alginate. This fraction of the embryo culture contains small aggregates of

meristematic cells (as highlighted in Figure 3C), without suspensor cells or with just one or a few suspensor cells.

2.2.2 Immobilization procedure

A procedure for immobilizing the cell clusters in alginate suitable for our system was developed under sterile conditions. In brief,

(1) Sodium alginate was dissolved in nanopure water based on concentration of 2.8% (w/v). The solution was then autoclaved at 120 °C in liquid cycle for 20 minutes. After the solution was cool down to room temperature 25 °C, 300 µl of sodium alginate solution was evenly dispersed on a 40 mm diameter bottom glass slide and settled for a few seconds to get a more uniform alginate film.

(2) 100 µl of settled cell clusters was gently placed on top of the alginate film using a 1000 µl micropipettor. Another 40 mm diameter glass slide rinsed with 20 mM $CaCl_2$ solution was put on top of the bottom slide with the rinsed side touching the cell clusters in alginate solution to construct a sandwich-like layered structure.

(3) A 25mm x 60mm glass slide was used as weight on the top of the sandwich and 300 µl of $CaCl_2$ solution was added from the edges of the glass slides to help solidify the film.

(4) After 20 minutes, the top glass slide was gradually pushed to one side and removed with the help of forceps. Another 300 µl of $CaCl_2$ was dripped on the top surface of film to reinforce the film solidification and to rinse off the

loose cells. The film was then washed with culture medium to remove the excess $CaCl_2$.

(5) The film with the immobilized cell clusters on the bottom glass slide was mounted into a flow cell chamber (FCS2, Bioptechs) for shear stress experiments (Figure 6A), or into a Petri plate as the control described below.

(6) A second alginate film with immobilized cell clusters on the top surface made at the same time was used as a stationary control for the shear stress experiments. The glass slide with immobilized cell clusters was cultured in a Petri plate and covered with a thin layer of the same culture medium that was used in the steady shear stress experiment.

2.3 Steady shear stress experiments

The focus of this thesis is to find out the correlation of cell cluster development and shear stress effect. Agitation in the culture flask/bioreactor causes shear flow around cell clusters. A rough estimation of shear rates inside of a shaking flask can be carried out based on the rotation speed of shaker table (100 rpm), rotation radius (15 mm) and radius of culture Erlenmeyer flasks (45 mm). It is determined that the shear rate at the flask wall is in the range of 5 to 50 s^{-1}. In order to get a better estimation or more accurate value of shear stress, a channel with well defined Poiseuille flow profile was picked to conduct the shear stress experiments. Furthermore, immobilized cells with top part exposed to liquid were selected as recording objects. The detail experimental setups and procedure are described in the following section.

2.3.1 Flow cell chamber construction and experimental procedure

The laminar flow channel inside of FCS2 (Bioptech Inc.) was constructed by layers (as shown in the close-up in Figure 5A) under sterile conditions. The average thickness of an alginate film was 100 μm based on measurement of six films made with the same procedure as immobilization of cell clusters. The variance of the film thickness was within 20 μm. The length scale of the roughness due to the embedded cells was within 4% of the channel height (h_1 in Figure 5A). Therefore we assumed the roughness of the film, or the variance of the film thickness, has no significant effect on the laminar flow region. To seal the constructed channel and compensate for the thickness of the film, a 100 μm thick gasket (h_2) was added around the film to secure the film position, and then a gasket with rectangular cutting (22 mm × 14 mm) and thickness of 500 μm (h_1) was put on top to construct the shape of the channel.

Another glass slide was added on top of the film and gaskets to assemble the channel. It was then connected to a reservoir of culture medium, a peristaltic pump (Peristaltic 77, Harvard Apparatus) and a dampener (a flask half-filled with culture medium, Fisher Sci.) with Tygon tubing (ID = 1.6 mm, Harvard) to complete a flow loop (Figure 5B). An air tube with an air filter as stopper in one end was through the plug of reservoir to provide oxygen to the system. This filter was used to make sure the whole system was sterile and had approximated the same air to liquid ratio as in suspension culture. A flow of ½ LP culture medium was streamed across the flow cell, horizontally from left to right. The cell clusters then experienced shear generated by the working fluid

in the laminar flow cell chamber FCS2. The experiments were run under sterile conditions.

The FCS2 was then positioned on the stage of the microscope. The cell clusters immobilized in the alginate film then experienced shear stresses on the surface of the film generated by the flow of liquid medium. Vital cells on the film surface were selected based on appearance of cytoplasm and imaged on the first day. Cells in both FCS2 and control Petri plate were located by recording the relative microscope x-y stage position. Each cell cluster was imaged through a magnification of 10× and 15× lens every 24 hours for 14 days with CCD camera. The raw images were 1024 × 768 by pixels and stored in the computer for later processing.

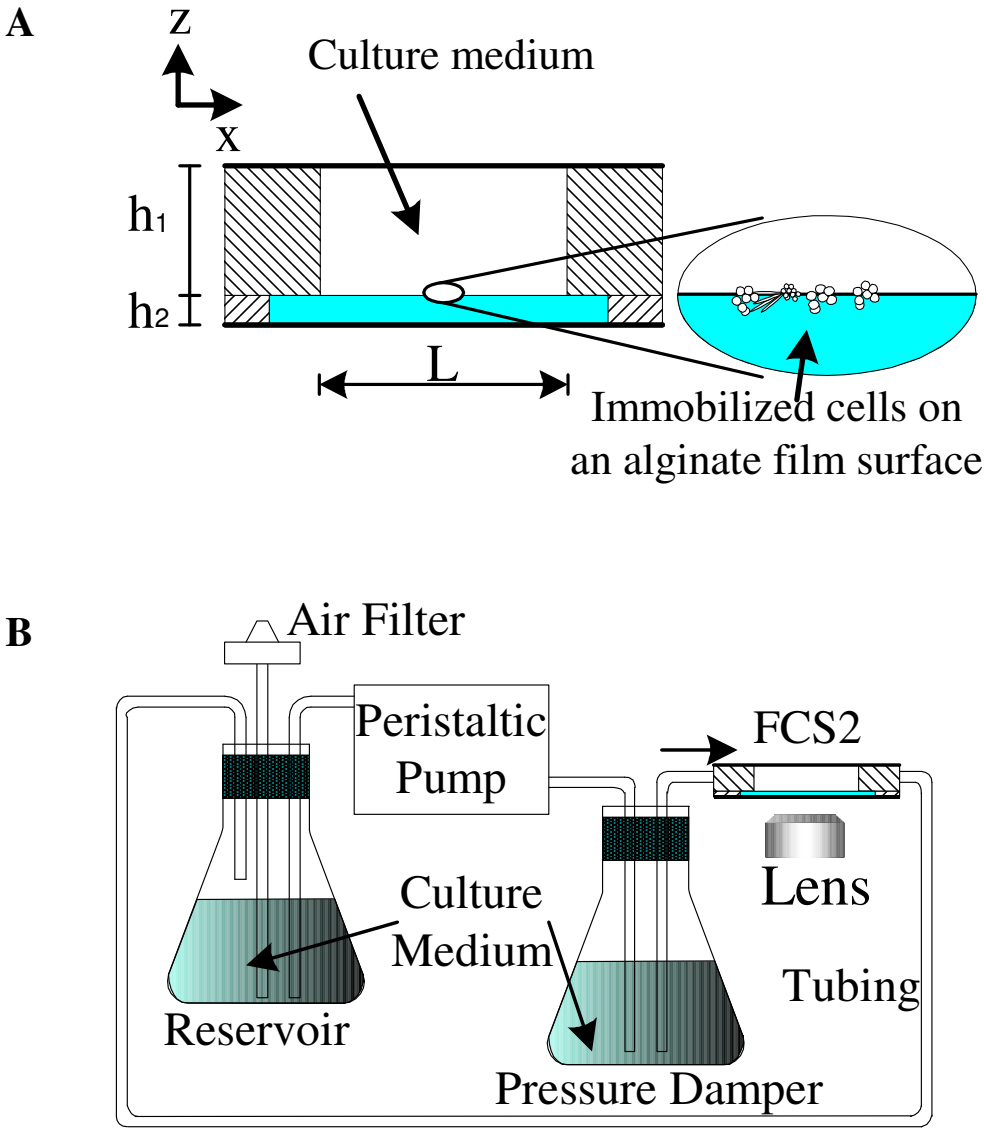

Figure 5. Schematic drawing of the experimental setup used to study shear stress effects on cell clusters of Norway spruce at room temperature 25 °C. (A) Cross section of the flow cell chamber (FCS2), with a close-up look on the top surface of the alginate film with immobilized cell clusters each about 100 - 150 µm across. h_1 = height of the fluid channel; h_2 = thickness of the alginate film; L = length of the alginate film; x = horizontal axis direction; z = vertical axis direction. (B) The flow loop setup with the flow cell chamber FCS2 sitting on the stage of an inverted microscope, a peristaltic pump to drive the flow, a 250 ml Erlenmeyer flask as the reservoir for culture medium that are pumped through the system, and a pressure dampener, connected with Tygon tubing.

2.3.2 Experimental parameters

The shear stress at the bottom wall of FCS2 which is also the top surface of the alginate film affixed on the bottom of the chamber, τ, is estimated based on laminar flow with parabolic velocity profile in a channel, to be given by $\tau = 6\mu Q/\mathrm{wh}^2$, where μ = 0.001 Pa·s is the dynamic viscosity of the culture medium, estimated based on 1% (w/v) concentration of sucrose at 20 °C (Schneider 1979) whose density and viscosity are very close to water; Q is the flow rate that can be controlled by the peristaltic pump; w is the width of the channel which equals 14 mm in this case; h is the height of the channel which equals h_1 (in Figure 6A). The shear rate $\dot{\gamma}$ can be calculated by dividing the shear stress by dynamic viscosity, that is $\dot{\gamma} = 6Q/\mathrm{wh}^2$.

The dimensions of the examined area and the culture medium properties were listed in Table 1. Reynolds number $\mathrm{Re} = \rho U\mathrm{h}/\mu$ based on the height of the chamber and the mean inlet velocity ($U = Q/A$) was in the order of 10^0 to 10^1 thus the flow was in laminar range; entrance length, Le, based on the hydraulic diameter of the chamber (d_{hydro}= 4Lw/(2L+w) for rectangular cross-section) and the Reynolds number. Le = 0.058 $\mathrm{Re}_{hydro}\ d_{hydro}$ was in the order of 10^1 to 10^2 μm that means the flow inside of channel becoming fully developed quickly, in 5×10^{-5} second, and the observation location inside of the chamber needs to avoid such length (Le) on both ends of the channel; Reynolds number based on the size of cells exposed to the flow, Re_d (~30 μm), was greatly less than one which means the roughness of the alginate film due to the cell clusters can be

neglected. The flow parameters with shear rate in the range of 9 to 140s^{-1} cover the most interesting range as studying the shear stress effect on plant cells.

Table 1. Channel dimension and fluid properties

h_1 (m)	h_2 (m)	w (m)	L (m)	A (m^2)	ρ (kg/m^3)	μ (Pa·s)
0.0005	0.0001	0.014	0.022	7.0×10^{-6}	1000	0.001

Table 2. Flow parameters for each steady shear stress experiment. The Reynolds number Re is based on the mean inlet velocity and the height of the channel, h_1; Re_d is based on the size of meristematic cells (30 μm).

Q(ml/min)	U (mm/s)	Re	Le(μm)	τ (N/m^2)	$\dot{\gamma}$ (s^{-1})	Re_d
0.3	0.71	0.36	38.6	0.009	9	0.007
0.5	1.19	0.6	64.4	0.014	14	0.012
1	2.38	1.19	128.7	0.029	29	0.024
3	7.14	3.57	386.2	0.086	86	0.071
5	11.9	5.95	643.7	0.14	140	0.119

2.3.3 Flow field velocity profile check

To further test the uniform of velocity profile in the span-wise direction (y direction) and the small effect of side walls to the fluid field, the velocity profile inside of the flow field of FCS2 chamber is checked with visualization technique—micro-particle imaging velocimety (micro-PIV). Micro-PIV is the most common technique for measuring flows inside of micro-sized channels. Since there is a body of research literatures about micro-PIV technique (Adrian 1991; Adrian 2004; Meinhart et al 2000; Meinhart & Zhang 2000; Santiago et al 1998), the detail of micro-PIV will not be

presented here. Briefly, in this particle-based flow velocimetry, the motion of the bulk fluid in a plane inside of the fluid is inferred from the observed velocity of tracer particles that are seeded in the fluid, and the two in-plane velocity components can be obtained by dividing the displacement of matched tracer particles by the time interval between image pairs. Due to the small length scale and the optical access associated with micro-sized channels, volume illumination is used for micro-PIV. The test region of the channel is then illuminated by a volume of light. The fluorescent particles seeded in the fluid within this region are excited and emit light with appropriate wavelengths. But not all these excited particles look bright and sharp under the objective lens or on the images. Only these ones within the depth of focal plane of lens are sharp and contributed to the velocity measurement. This imaging difference makes optical slicing possible, and the velocity along the direction of illumination can be measured. Thus, not only the velocities in horizontal plane are obtained, but also the velocities along the optical axis directions.

In the shear stress experiments mentioned in this thesis, the FCS2 chamber is placed on the stage of an inverted epi-fluorescent microscope (Leica, DMIRM), as shown in Figure 6. Illumination light from a metal Halid lamp (X-Cite, EXFO Inc.), with wavelength of 450 to 490 nm after passing an I3 filter cube (Leica), shines on the seeded particles with 500 nm in diameter (DUKE) inside of the flow chamber (with a seeding density in term of number of particles in a volume of 2.5×10^{13}/liter), and the fluorescent signal or light of wavelength 515 nm emitted from the particles is imaged on the sensor of charged couple device (CCD, Hamamatsu 1394 ORCA-ERA) camera after passing the filter cube. The images are processed for displacement of particles and the velocity information is obtained when applying the time interval between each image pairs. The

shear rate is obtained by applying the distance along optical axis (z) direction between two imaging sequences. Uniform velocity profiles are obtained after processing images along optical axis and span-wise (y) directions, which mean the side wall effect to the flow field can be neglected.

Velocity profile at the center of the chamber along the optical axis direction is shown on Figure 7, with flow rate set at 0.05 ml/min on the peristaltic pump. Due to the symmetry of the profile, along with our interests only on the velocity profile near the bottom surface, only half of the profile along optical axis is drawn here. The error bars show the standard deviation that is less than 5% of the mean. The experimental data varies with the theoretical solution based on two-dimensional assumption within 15%. Since the Reynolds number for the highest flow rate, 5 ml/min, tested in the controlled shear stress experiments is not greater than 1, flow inside of FCS2 is still in the laminar region and have similar pattern as the one of 0.05 ml/min.

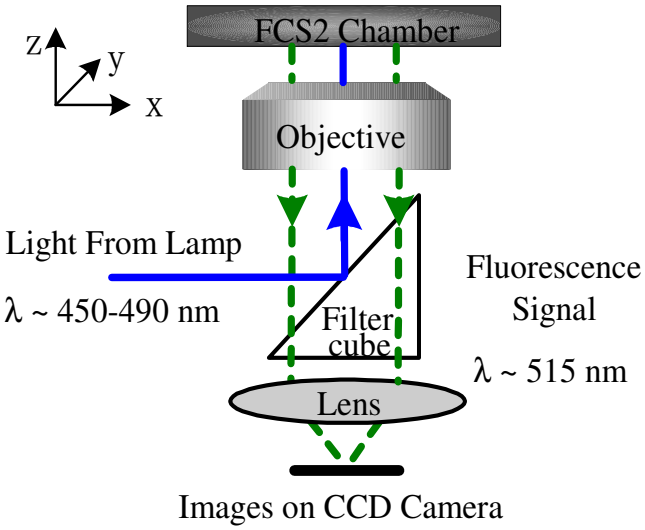

Figure 6. Illustration of micro-PIV setup. Flow chamber FCS2 sits on the stage of microscope; reflective light is used to excite fluorescent particles; fluorescent signals are collected with CCD camera after passing the I3 cube.

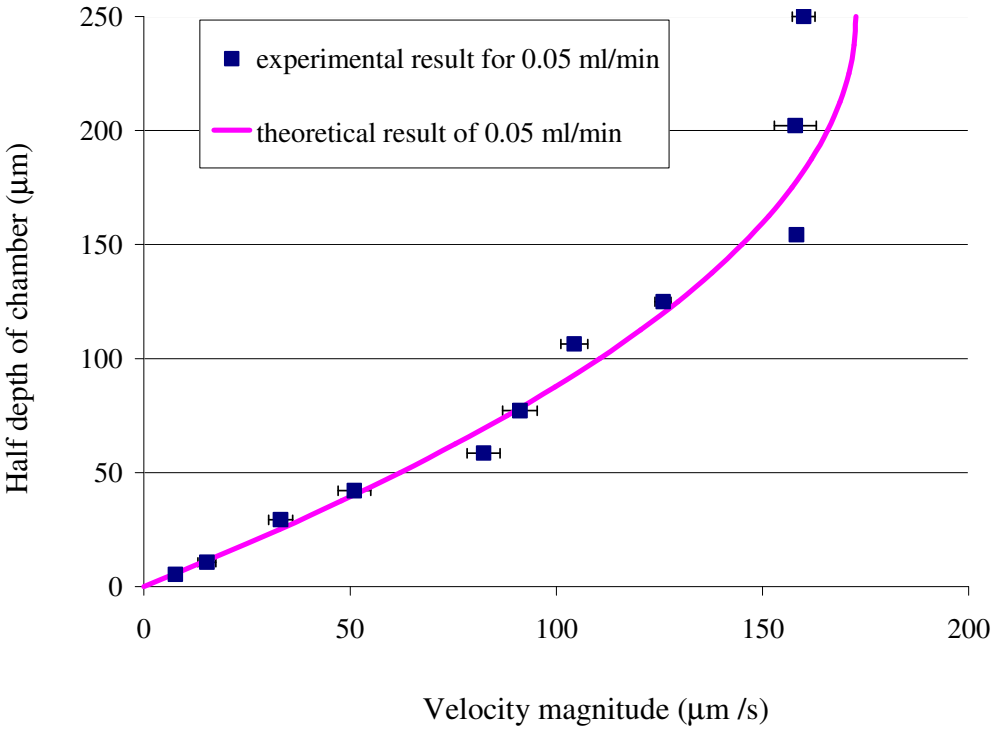

Figure 7. Comparison of velocity profiles at the center of FCS2 chamber along optical axis (z) direction, measured with micro-PIV (■) and theoretical result based on two-dimensional assumption (—), with flow rate of 0.05 ml/min.

2.4 Imaging system

Most plant cells tend to exist in aggregates since the secondary metabolites require cell-to-cell contact due to the transfer of materials from one cell to another through the plasmodesmata (Hall et al 1981; Street 1977). The cells are "glued" together by producing pectin which is a sticky gel-like sugar component. The average size of a meristematic cell in the proliferation stage of Norway spruce somatic embryo ranges between 20 to 30 µm. The cell clusters that are suitable for shear stress studies are 100 to 200 µm in length and these clusters are mainly composed of meristematic cells with few

or no suspensor cells, according to previous sizing study (Egertsdotter & von Arnold 1998).

2.4.1 Imaging system configuration

An inverted fluorescent microscope (Leica DMIRM) connected with a charged couple device (CCD camera; Hamamatsu 1394 ORCA-ERA) and a personal computer (DELL DIMENSION 8250) was used to observe and record the growth of cell clusters. Those are the same setup as for micro-PIV measurement of flow profile inside of FCS2 (Figure 6). Lens with a magnification of 10× and a numerical aperture (NA) of 0.25 was used to fit a cluster in an image area of 1024×768 pixels (which covers the physical dimension of 1052×789 μm^2). The detail of the cluster can be recorded with an extra magnification module of 1.5× (which gives a total magnification of 15×). In order to observe the light transmitted by the cells, transmitted light from an arc metal Halid lamp (X-Cite, EXFO Inc.) was used as illumination. For integrin-like protein and ROS detection, different fluorescent dyes, TRITC and dihydrorhodamine 123, were used. A TRITC filter cube (with excitation: 535/50 nm and emission: 610/75 nm from Chroma) and an I3 filter cube from Leica, with excitation filter of 450-490 nm and suppression long pass filter of 515 nm, was equipped with the microscope to detect the desired fluorescent signals, respectively.

2.4.2 Fine tune drum reading calibration

The size of immobilized cells along the optical axis direction on an alginate film is estimated based on the focal plane of the microscope lens. Essentially, the focal plane of the microscope lens can be moved along the optical axis by adjusting the fine tune

drum on the microscope, which allows different sections of the cell located at different depths to be observed. The cell size along the optical axis can therefore be estimated from the difference in the relative positions of the focal plane when it is aligned with the very top and bottom sections of the cell. The location of the focal plane can be correlated to the scale on the fine tune drum. Calibration experiments are therefore carried out with slides of known thicknesses. The procedure is discussed below.

The thicknesses of microscope slides (VWR) were measured with a micrometer on three different locations. These locations were then marked by different color markers on both top and bottom of the slide for later observation with the microscope. The slides were set rest for five minutes to allow the marker ink to dry completely. Each of the slides was then put on the stage of microscope to measure their thicknesses at the marked locations. At each marked location, the focal plane was adjusted to focus on the top and bottom surfaces of the slide by dialing the fine tune drum. When the top and bottom surfaces of the slide were in focus, the readings on the fine tune drum were recorded. The relative change in the readings can then be translated to actual linear dimension based on the thickness of the slide measured above.

In Figure 8, the relative change in the fine tune drum reading is plotted as a function of the actual slide thickness. For each thickness, three repeated tests are conducted. The four data points represent the mean value and the error bars are standard deviations. For the experiments concerned in this thesis, thicknesses less than 200 μm are of the most interest. More calibrations were therefore conducted in this range, as shown in the inset of Figure 8.

As shown in Figure 8, the drum reading varies linearly with the thickness of the slide, which gives a scaling factor of 2.87 μm/reading. This factor was later used to measure the thickness of alginate films and the relative depth of immobilized cells in the optical axis direction.

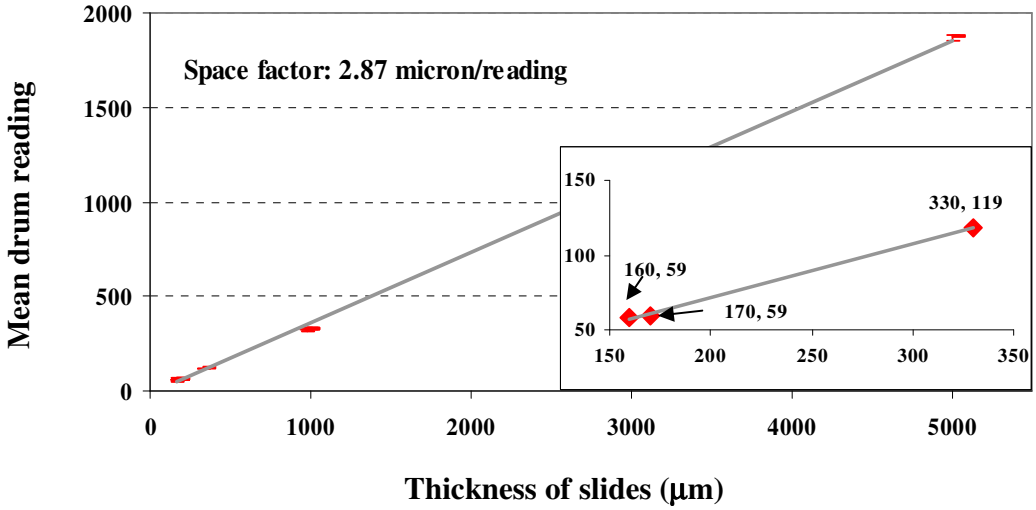

Figure 8. Calibration of drum reading versus known thickness of slides for 10× lens

2.5 Image processing with normalized cross-correlation method

In this thesis, the focus is on the development of gymnosperm somatic embryos in the proliferation phase, during which embryos at several stages of development are present at the same time (Bozhkov et al 2002). In order to measure the effect of shear stress in terms of morphological changes in embryos at different developmental stages, it is necessary to apply direct and quantitative measures of individual somatic embryo development.

The growth of the cell cluster was monitored by taking sequential images in time over a period of several days. By visual inspection one can easily see the growth qualitatively. However, to quantitatively measure the growth rate as a function of the polar angle in the plane of visualization (radial growth rate), one has to establish a systematic method. The method selected in this thesis was based on comparison of each image through cross-correlation of the image at day k to the image taken at the previous day, k-1. Cross-correlation of image pattern is useful when the image pattern moves or deforms slightly relative to the reference image pattern (Ono et al 2001). The mathematical formulation of this cross-correlation is outlined below.

In physical terms, the method consists of "shifting" the image pattern relative to the reference image to identify the "shifted" location that the overlapping between the images is maximized. If the image pattern, in this case the image of the cell cluster, has not changed but only shifted by a small amount, then at the location of the best overlap, the cross-correlation will be perfect (i.e., 1.0). Here, however, the cluster also grows slightly over the period of one time interval (in this case one day). The aim is to measure the growth in each radial direction by finding the best overlap between the cluster image and the reference image from the previous time period (in this case, previous day). Then by directly comparing the cluster image with the reference image, one can quantitatively measure the growth rate in each direction over the time interval (i.e., one day in this study).

In the application here, cell clusters were fixed on an alginate film. Therefore, several cell clusters could be selected, tagged and imaged each time by noting the location of each cluster. This way, in each experiment the growth of several clusters

could be examined simultaneously. The time interval for imaging was selected such that the shape of the cell clusters did not change significantly. In these experiments, a time period of 24 hours was picked based on observations and experiences. Since the brightness of the images varies due to lighting and exposure conditions, the gray scale of each image was normalized to eliminate variations in exposure. This is done by using normalized cross-correlation method by subtracting the mean grayscale value from the images and dividing the correlation value by the standard deviation, a standard method in image analysis.

2.5.1 Image processing procedure

Time-lapsed images of one cell cluster were recorded over a period of time. In this case, the time lapse $\Delta t \equiv t_{\alpha+1} - t_{\alpha} = 24$ hours, where $\alpha = 1, 2, \ldots, k$. The maximum duration of one experiment (i.e., k) was 14 days; thus the maximum number of images per cluster was $k + 1 = 15$. The gray scale values of each image taken in sequence were stored in a 1344×1024 matrix. To reduce the processing time, the images were then cropped to a rectangular region ($I \times J$, row by column) which contains the cell cluster of interest, as shown in Figure 9A. The cropped images were binarized by defining a threshold value to maximize the contrast between the cell cluster and the background (Figure 9B). The background noise, generated during image acquisition, was removed by a thinning algorithm to identify the cluster boundary (Figure 9C). The locations that the cell cluster occupied was then filled in with white color along the boundary of the cluster to get a binary image of a white object on black background (Figure 9D). The last three steps were to enhance the contrast of the image, increase the signal-to-noise ratio, and improve the accuracy of processing results. The images were then stored in a series of

matrices $A_\alpha(i, j)$ where i = 1, 2, …, I, and j = 1, 2, …, J . The normalized cross-correlation of two consecutive images, A_α and $A_{\alpha+1}$, is given by

$$c_\alpha(m,n) = \frac{\sum_{i=1}^{I}\sum_{j=1}^{J}\left\{\left[A_{\alpha+1}(i,j)-\overline{A}_{\alpha+1}\right]\left[A_\alpha(i+m,j+n)-\overline{A}_\alpha\right]\right\}}{\left\{\sum_{i=1}^{I}\sum_{j=1}^{J}\left[A_{\alpha+1}(i,j)-\overline{A}_{\alpha+1}\right]^2\sum_{i=1}^{I}\sum_{j=1}^{J}\left[A_\alpha(i+m,j+n)-\overline{A}_\alpha\right]^2\right\}^{0.5}} \quad (1)$$

where $\overline{A}_\alpha$ is the mean gray scale value of the imaged region A_α; m and n are the pixel row and column locations of the correlation values, c_α, residing in the range of $-2I \le m \le 2I$ and $-2J \le n \le 2J$. The image A_α taken at time t_α serves as the reference or template when correlating with the image $A_{\alpha+1}$ taken at time $t_{\alpha+1}$. Cross-correlation is first used to identify the (m, n) location of the maximum value of $c_\alpha(m,n)$ which indicates the offset corresponding to the best match or overlap between the two cluster images A_α and $A_{\alpha+1}$. The image $A_{\alpha+1}$ was then shifted with respect to the template A_α by m rows and n columns, resulting a new image $A'_{\alpha+1}$. As discussed in Section 2.6, this shift compensates for the slight change in physical location of the cell cluster and inconsistency in locating the cluster when imaging it at different time. Next step was to detect the edge of the cell cluster on each image using the Prewitt approximation (Parker 1997) to get the boundary contours, as shown in Figure 9E. Each contour was individually labeled and the coordinates were recorded.

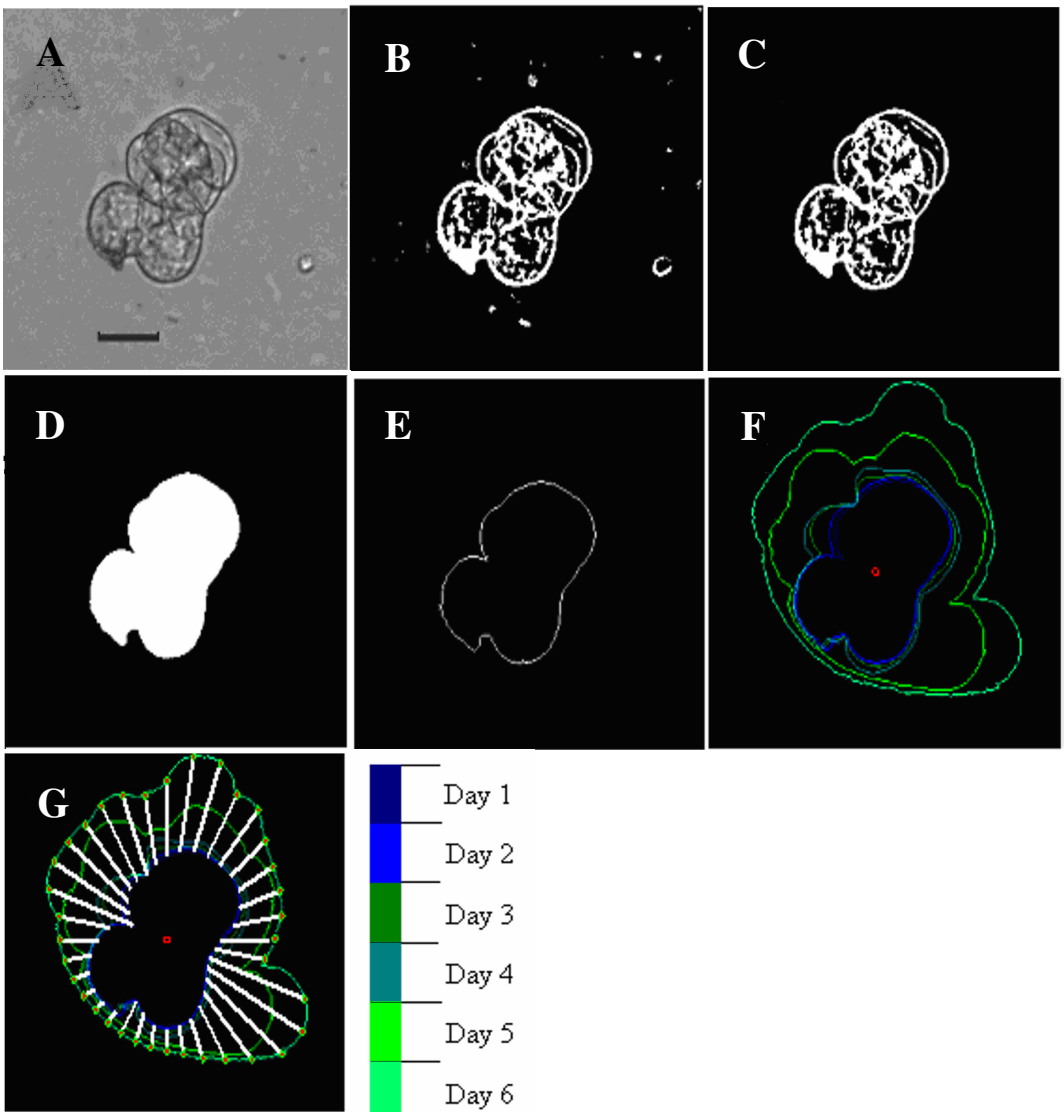

Figure 9. Outline of the step-wise procedure for processing images of the cell clusters monitored in the experiments to estimate growth and development. (A) Cropped image with cell cluster of interest; scale bar = 50 µm. (B) Binarized image; (C) Background and noise removed from binarized image; (D) Filled the inside of the cell cluster followed by normalized cross-correlation; (E) Edge-detection of the cell cluster; (F) Contours superimposed; one reference point was picked in the center of the small red circle. (G) Evaluation of growth by dividing the superimposed contours into 36 sections, and calculating the radii from the reference point to the points on the edge of contours along the same direction. The white rays indicate the directions of the radii; the white arrow indicates the counter-clock-wise rotation of angles. The color bar represents the day of experiment.

2.5.2 Quantification analysis of cell growth

2.5.2.1 Radial growth as a quantification parameter

In the past studies, different developmental stages of carrot somatic embryos have been characterized by parameters that describe the shape of the embryo in terms of axial length/radial growth, diameter, cotyledon length and cotyledon arc, to quantify the individual shape of cells (Schiavone & Cooke 1985). To show how shear stress affects cell growth, monitoring and quantifying the growth and development of individual cell cluster/somatic embryo under shear stress is the focus in this thesis.

In current studies, radial growth of embryos was chosen as the quantity to reflect the morphology change. To quantify the rate and direction of the cell cluster growth, the origin of a polar coordinate on the superimposed contour image (the center of the small red circle as shown in Figure 7F) was selected at the center of mass of the cell cluster at the beginning of an experiment. The directional growth of the cell cluster, which can be characterized by polar angle θ and radius length $R_\alpha(\theta)$ for each point on the contour image, was computed in each direction as demonstrated in Figure 7G.

In each experiment, there was a total of M ($20 \le M \le 60$) clusters recorded. Among those M clusters, typically N ($10 \le N \le M$) clusters that survived the whole duration of experiment were processed with the normalized cross-correlation method. The final growth of cell cluster l ($1 \le l \le$ N) along each direction was calculated as

$$R_{k+1,l}(\theta) - R_{1,l}(\theta).$$

This was further averaged by the number of time intervals during the experiment to get the mean growth rate

$$\Delta R_l(\theta) = \frac{R_{k+1,l}(\theta) - R_{1,l}(\theta)}{k}. \tag{2}$$

The mean growth rate along each direction θ for the total of N clusters in each experiment was calculated as

$$\overline{\Delta R}(\theta) = \frac{1}{N}\sum_{l=1}^{N} \Delta R_l(\theta), \tag{3}$$

thus the standard deviation of this averaged growth is given by

$$s = \sqrt{\frac{1}{N-1}\sum_{l=1}^{N}\left[\Delta R_l(\theta) - \overline{\Delta R}(\theta)\right]^2} = \sqrt{\frac{1}{N-1}\sum_{l=1}^{N}\left[\Delta R_l(\theta)^2 - \overline{\Delta R}(\theta)^2\right]}. \tag{4}$$

The mean growth rate and standard deviation along each direction for the clusters in all three experimental repetitions under each test condition were calculated the same way, by combining all the data from three repetitions.

2.5.2.2 Statistical significance analysis—t-test

Most of the past studies were research on the suspension cells, and the results were concluded based on the average/statistics of individuals. Statistical methods are commonly applied to interpret data in the biological related studies to extract objective conclusions (Davenport et al 2000; Ewing et al 1999; Nyberg et al 1999; Pendzich et al 1997). In order to find out if there is significance among all the directions the cell clusters grow, statistical significance test is applied.

Significance test is an analytical procedure which concentrates on assessing the reasonableness of regarding two (or more) populations as the same in some respect. This particular hypothesis of equality studied by the significance test is called the null hypothesis. In this thesis, it is assumed that cell clusters grow at the same rate along all directions, which can be also claimed that the cell growth rate is isotropic. To decide whether this hypothesis is compatible with the actual mean growth rate data, the probability, P, is obtained as the mean of the actual growth rate is the same as the mean of the total population growth rate. Before making decision of the null hypothesis being either accepted or rejected, a confidence level, $(1 - a)$, is preset, where a is called the significance level that is also preset with the confidence level. If P value is bigger than the preset significance level ($P > a$), then the null hypothesis is accepted. If P value is smaller than the preset significance level ($P < a$), then the null hypothesis is rejected. The rejected result is informally referred as statistically significant. Normally, a probability greater than 5% is regarded as reasonable, and the null hypothesis is accepted under such a probability. Stricter probabilities, such as 0.1%, are used for very sensitive tests.

For the cases that the mean and standard deviation of the total population are not known, only the mean and standard deviation (or so called standard error) of a set of sample data are known, the significance test of such sample data is with t-test. For data ΔR ($\Delta R_1, \Delta R_2, ..., \Delta R_N$) of sample size N (with N-1 degrees of freedom), the null hypothesis is that the sample mean

$$\overline{\Delta R} = \frac{1}{N} \sum_{l=1}^{N} \Delta R_l \qquad (5)$$

is equal to a hypothesized population mean μ. In testing the null hypothesis, one uses t-test statistic, which is defined as

$$t = \frac{\overline{\Delta R} - \mu}{s/\sqrt{N}}, \tag{6}$$

Where $s = \sqrt{\frac{1}{N-1}\sum_{l=1}^{N}\left(\Delta R_l^{\,2} - \overline{\Delta R}^{\,2}\right)}$ is the standard deviation of the sample data. When there is no way to know beforehand that how two or more sample data will perform, two-sided test under a preset significance level *a* is applied first. Based on the two-sided tests, one gains the knowledge of how the sample mean varies to the hypothesized population mean. Then one-sided test with significance level *a*/2 can be used to predict the probability of the null hypothesis being accepted or rejected.

For example, for a set of 11 data of radial growth in an experiment of shear rate of 140 s^{-1} along 45 degree direction, 1.24, -0.59, 1.50, 16.50, 18.38, 6.36, 6.89, 0.24, 5.91, 1.41, 6.60, the sample mean is 5.86 with standard deviation of 6.37, while the hypothesized population mean is 5.88 which is calculated based on all the data along all directions in this experiment. The t-test statistic is equal to (5.86 – 5.88)/(6.37/3.32) = -0.011. The two-sided probability $P(t < -0.011) = P(t > 0.011)$ can be found by the t distribution with 10 degrees of freedom in the Table E in Moore and McCabe (Moore & McCabe 1999), where $P(t > 0.011) = 0.9914$ is great greater than $a = 0.05$. This result is insignificant at the 0.05 significance level, indicating that the null hypotheses can be accepted with the 0.95 confidence level.

Another example of rejecting the null hypothesis will be with 11 data in the same

experiment of shear rate of 140 s^{-1} along 0 degree direction, 3.88, 7.17, 0.88, 24.67, 28.33, 6.00, 1.50, 8.17, 17.00, 10.25, 19.67. The sample mean is 11.60 with standard deviation of 9.41, while the hypothesized population mean is still 5.88 as the last example. The t-test statistic is equal to (11.60 – 5.88)/(9.41/3.32) = 2.016. The two-sided probability $P(t > 2.016)$ can be found by the t distribution with 10 degrees of freedom in the Table E in Moore and McCabe (Moore & McCabe 1999) also, which is $P(t < -2.016) = P(t > 2.016) = 0.0715$ slightly greater than 0.05. This result is insignificant at the 0.05 significant level, indicating that the null hypotheses can be accepted with the 0.95 confidence level on two-sided test. But this result is significant at the 0.1 significant level, indicating that the null hypotheses can be rejected with the 0.90 confidence level on two-sided test; or for the one-sided test, the probability is $1/2\ P = 0.0357 < 0.05$, the result is significant at the 0.05 significant level indicating that the null hypotheses can be rejected with 0.95 confidence level on one-sided test.

All sampled experiments data in this thesis are processed with two-sided tests first, after getting the significant directions under 90 % confidence level, one-sided tests results with confidence level of 95 % are presented in the tables.

2.6 Validation of normalized cross-correlation image processing method

Fluorescent microscope and digital image analysis provide the platform for investigation of cell development. The studies rely on the analysis of digital images, and the validation of image processing methods becomes an important topic especially in the high-throughput measurement technologies involving vast amount of information

(Lehmussola et al 2007; Lehmussola et al 2008; Pepperkok & Ellenberg 2006; Starkuviene & Pepperkok 2007).

In the steady shear stress experiments, somatic embryo cell clusters were affixed with alginate film. Cells grew by enlarging and dividing at the beginning of each experiment. The changes of shape or contour of cell clusters are not significant in a 24 hours period, which makes the observation and record of the cell clusters at different time steps possible. When capturing the first images of clusters, the locations of the clusters were recorded as the positions of the x-y stage of the microscope. During the experiments, the lighting and exposure conditions may vary; the location of clusters may change due to manually relocating; the background of the clusters may not be clean enough to identify the clusters of interest; and it is desire to match the contour of a cluster at different time steps during an experiment.

The image processing method applied here needs to solve all the challenges mentioned above. A normalized cross-correlation Matlab code was developed to meet such requirements. This image processing, as described in section 2.3, was semi-automated, involving manual processes of picking cell clusters of interest out and a threshold value as distinguishing cells out of background if the default value did not work well. Before drawing any meaningful conclusions from the extracted data by the image processing method, the accuracy of the method needs to be ensured. In order to test the robustness and reliability of this method, a series of artificial images were generated to validate this method.

2.6.1 Generation of artificial images

Images obtained from a microscope were preprocessed with an in-house code in order to eliminate the errors originated from the measurement system, such as different lighting and exposure times, detector noise and undesired information from cells not of interest. Then the cell cluster of interest was extracted from the image by cropping the original image. Finally different features were quantified from the correlation of the extracted cluster and stored for further analysis. To better understand the impact of various factors (for example, background noise and threshold value for binarization etc.) and to test the accuracy of the processing method, a series of artificial images were used. With the artificial images, one can effectively control the desired features of the images, such as the location of the cell clusters, the growth of cells, the grayscale of images and the background noise.

The generated artificial images of cell clusters should follow the physical conditions of the testing materials, in order to reflect the real cases of experiments. In liquid suspension culture during the proliferation phase, cells normally grow in small clusters with a few cells together. The individual cell is around 20 μm in diameter. Cell clusters with length in the range of 100 - 200 μm were selected for immobilization and exposed to shear stresses. The representative artificial images are constructed from the superposition of several ellipses with major axis of 20 μm (as shown in Figure 10A). The image size is 253 × 192 pixels in horizontal x direction and vertical y direction, respectively. This sample cluster represents a cluster of 100 μm length.

2.6.2 Translation motion of cells between image pairs

The sample cluster is then shifted in the (x, y) plane by (26, -31) in pixel size along horizontal and vertical directions, as shown in Figure 10B. The red arrow indicates the shifting of cluster positions. These two images are used to test the validity of the cross-correlation method for computing the translation of two objects on a two-dimensional (2D) plane. As shown in Figure 10C, the contours of two clusters match each other perfectly after correlation since two contour lines are overlapped. The contour line of first color in the color bar from cluster A is overlaid by the line of second color in the color bar from cluster B. The plot in Figure 10D shows zero displacement ($R_n(\theta) - R_1(\theta)$) along 36 directions ($\theta$) around the cluster contour between these two correlated images, where R_n, n = 1, 2, is the radial length measured from the reference point (the center of the red circle which is the center of mass of the 2D cell cluster A as shown in Figure 10 C). This supports the accuracy of correlation due to displacement.

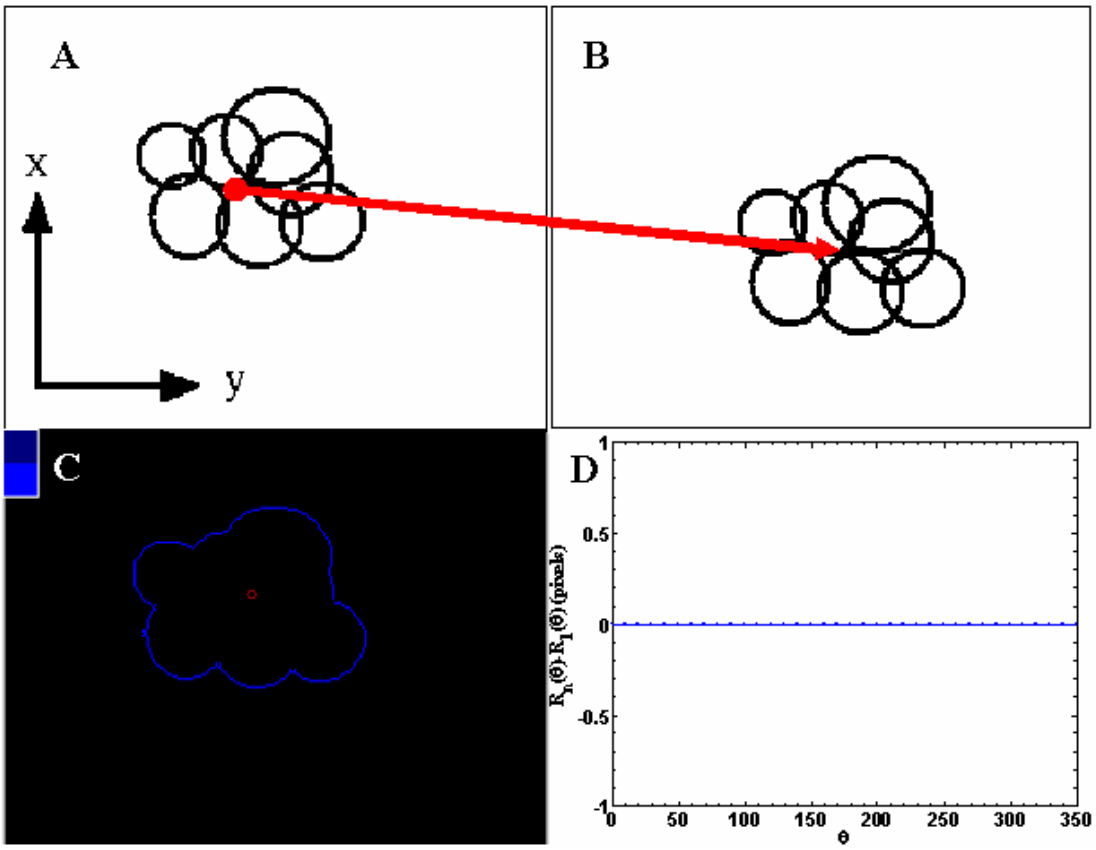

Figure 10. Test accuracy of correlation due to translation. (A) Original cell cluster. (B) Shifted original cluster by moving (26, -31) pixels in the x-y plane. The red arrow indicates the translation motion of cell cluster. (C) Superimposed two clusters in A and B after correlation, with the center of the small red circle representing the reference point and the color bar representing the colors used for two clusters, respectively. (D) Distance between the contours of correlated two clusters along different angle.

2.6.3 Contour changes due to growth between image pairs

As clusters grow, new cells appear in the x-y plane. A new cluster was constructed by adding one additional cell along the original contour of cluster in Figure 11A to test the matching of clusters before and after growth. Newly added cell was labeled in red color to distinguish from the original cluster (as shown in Figure 11B). The correlated image show the partially overlaid contours of two clusters. The overlaid area is the location without new cell. The area not overlaid displays the growth of the new cell (as shown in Figure 11C). The white bars in Figure 11D represent the distance between the contours of two clusters along each direction, which also represent the change or growth of the new cell; the red diamonds along the contour represent the direction of the growth with the origin being the center of the red circle (which is the mass center of the cluster at the beginning of one experiment) that are also the end points of the white bar on the second cluster. A qualitative growth along each direction can be easily identified by the white bars.

2.6.4 Image noise control

To test the computation effectiveness of background noise removal and the effect of background noise on the accuracy of cluster matching and quantification, random noise is added on images (as shown in Figures 12 and B, which are modified from the constructed artificial clusters without noise as in Figures 10A and B). These noises do not blur the edge of the cell cluster and are easy to remove (as shown in Figures 12C and D). The cleaned images of two cell clusters match each other perfectly with zero displacement between the two contours.

In some cases, the noise may make it difficult to distinguish the cells from the background. A threshold value needs to be manually chosen based on the contrast between the object and the background, to binarize the images before removing noise. Such case is represented in Figure 13A compared with image without noise in Figure 13B. Cleaned image in Figure 13C used the mean grayscale value as a threshold to detect the edge of the cluster and remove the background noise, while the cleaned image in Figure 13D used a manually picked higher than mean grayscale value as threshold through a few trials. With the cost of a few more (three in this case) minutes of computation time involving the manually handling, the cluster edge in Figure 13D is sharper than the one in Figure 13C and the measurement error due to the blur edge is within one pixel, as shown in Figure 13E.

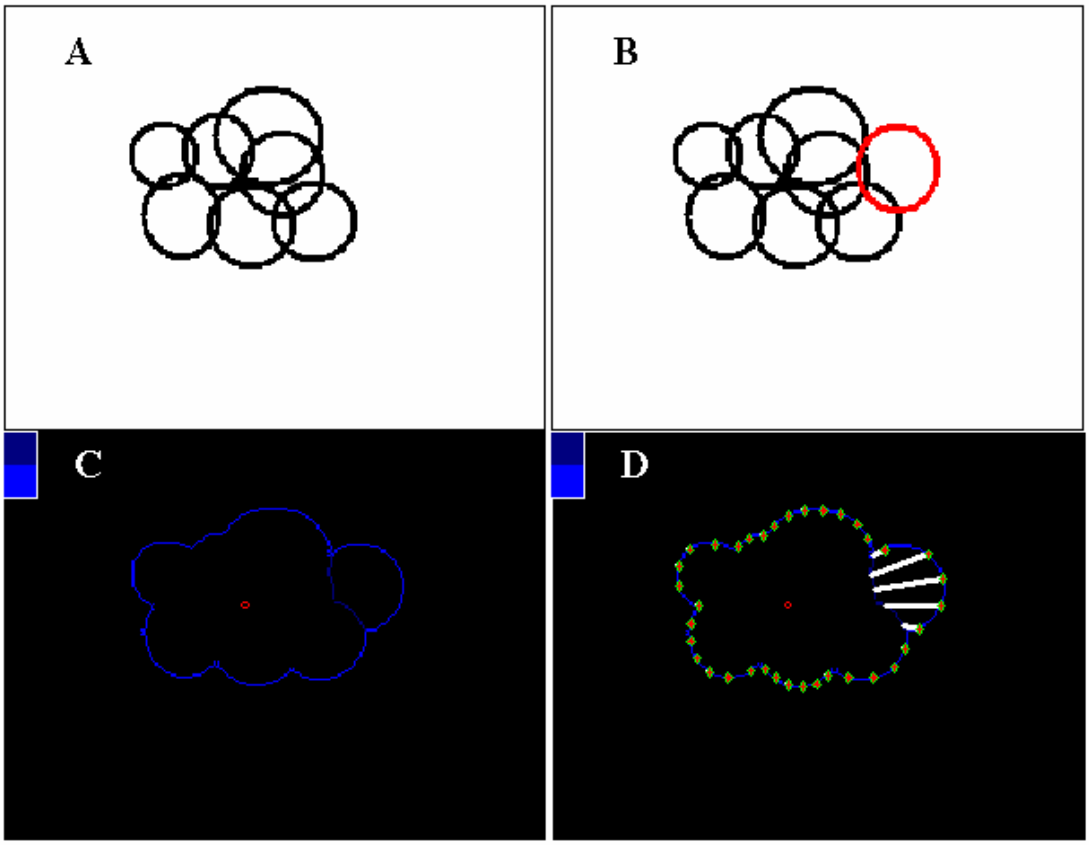

Figure 11. Test accuracy of correlation due to growth introduced deformation. (A) Original cluster. (B) Cluster with a new cell labeled with red color. (C) Superimposed two clusters in A and B after correlation, with the center of the small red circle representing the reference point and the color bar representing the colors used for two clusters, respectively. (D) Distance between the contours of correlated two clusters along different angle.

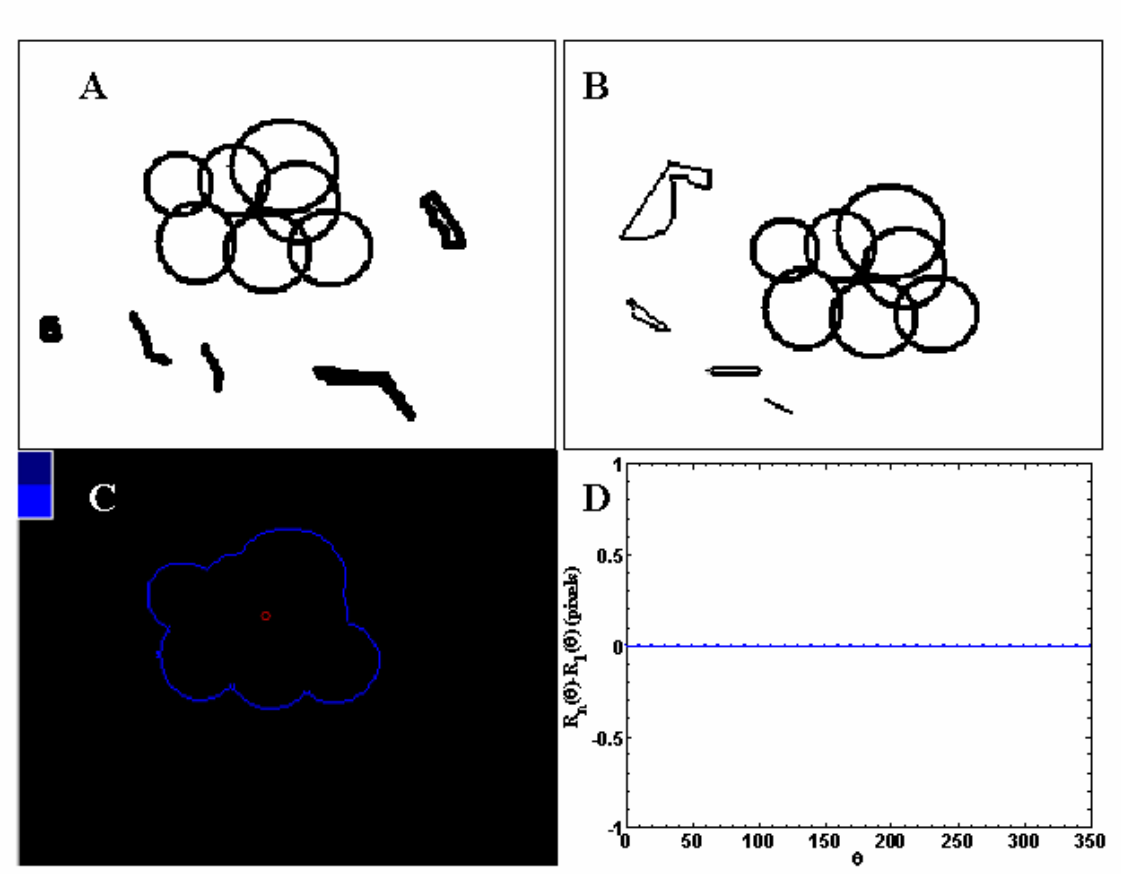

Figure 12. Test accuracy of correlation due to background noise. (A) First cell cluster with background noise. (B) Second cell cluster by moving the first (26, -31) pixels in the x-y plane. (C) Superimposed two clusters in A and B after background noise removal and correlation, with the center of the small red circle representing the reference point and the color bar representing the colors used for two clusters, respectively. (D) Distance between the contours of correlated two clusters along different angle.

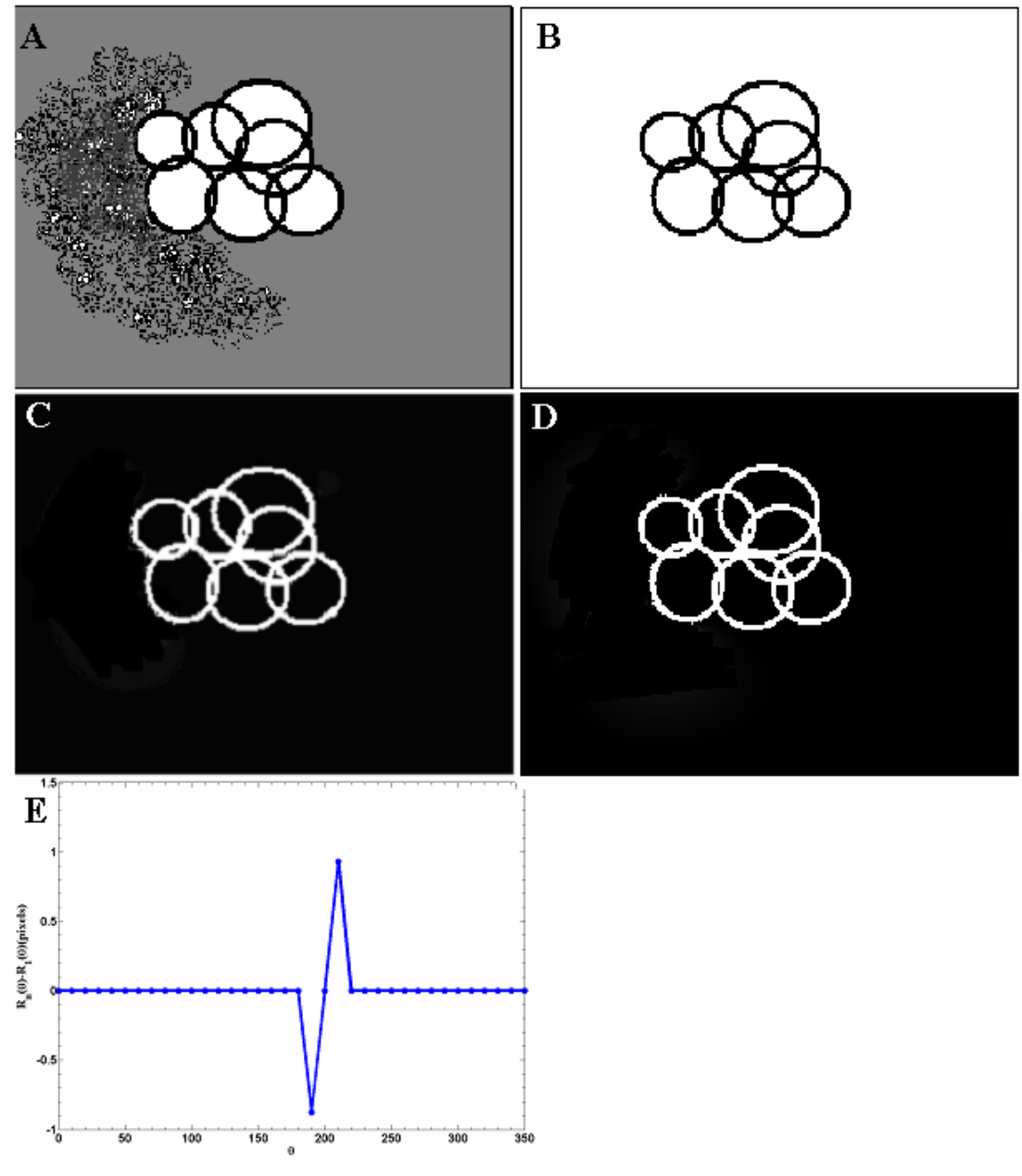

Figure 13. Test accuracy of edge detection by defining threshold values. (A) Cell cluster with blurred edge between cells and background. (B) Cell cluster only as a comparison to A. (C) Edge detection with the mean value of the grayscale as a threshold. (D) Edge detection with a higher than mean grayscale value as threshold, with the cost of manually processing time increasing about three minutes. (E) Displacement between the contours of two clusters along different directions. Measurement error due to the blur edge is within ± 1 pixel with the extra three minutes as processing time.

2.6.5 Small rotation of cell cluster between image pairs

The experimental system is designed to have cell clusters affixed with alginate film. The rotation of film (thus cells) during one experiment can be neglected. To test if the image processing method can resolve the small rotation of the cell clusters, the cluster in Figure 14A is rotated clock-wise for 5° (as shown in Figure 14B). Figure 14C shows the correlated results of original image with the rotated image. The perfect match of two images implicates the method can detect and correct small rotations between image pairs. Past studies about the normalized cross-correlation method also show that cross-correlation method can detect rotation between image pairs, up to a rotation of 5 to 10 degrees (Petrosyan 2009). There is further confirmation with real image processing of all the images taken during experiments.

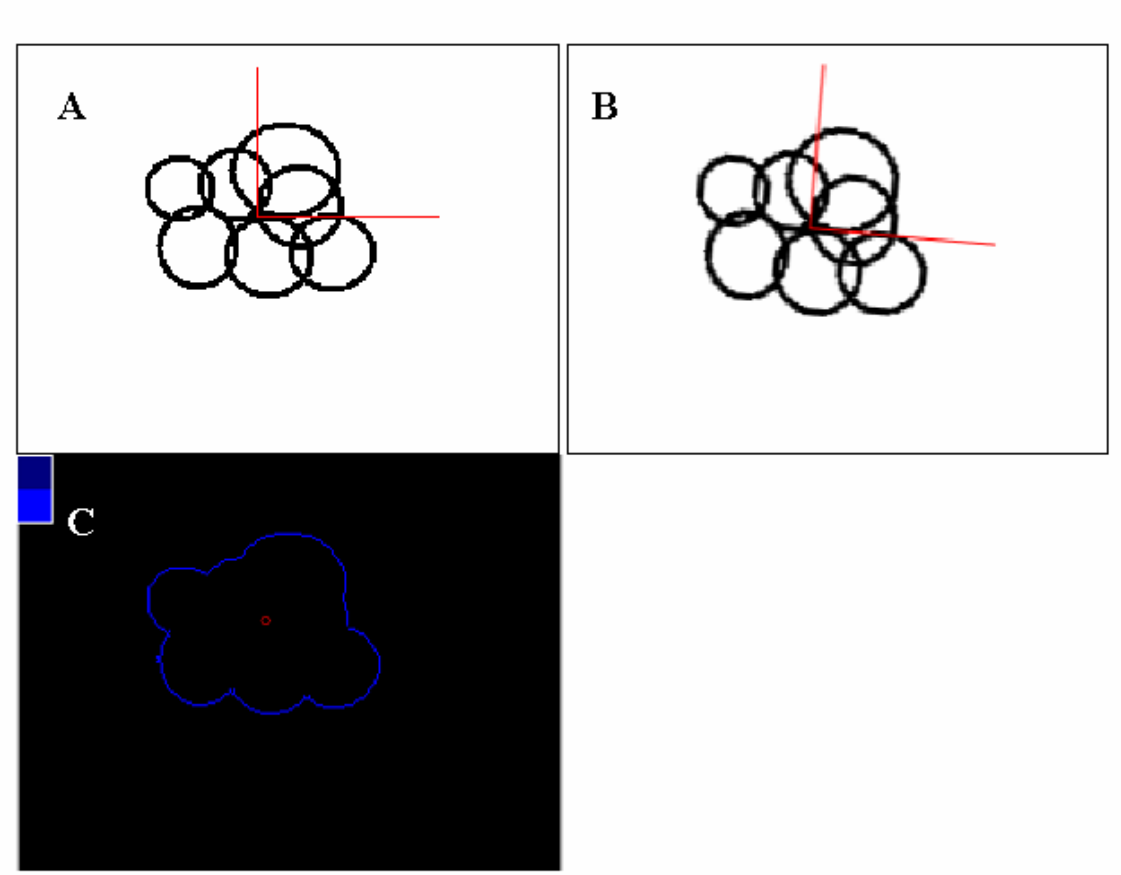

Figure 14. Test accuracy of correlation due to small rotation. (A) Original cell cluster. (B) Rotated original cluster clock-wise by 5°. The red coordinate lines indicate the direction of cluster. (C) Superimposed two clusters in A and B after correlation, with the center of the small red circle representing the reference point and the color bar representing the colors used for two clusters, respectively.

2.6.6 Validation results and discussions

2.6.6.1 Summary of validation results

The normalization procedure before correlation eliminates the effects of different lighting conditions and exposure times caused image grayscale variation. The algorithm of background noise removal is efficient even with manually processing involved. With the cost of a few minutes of threshold value setting, the measurement error due to edge blur can be controlled within one pixel. From the validation results, we can conclude that the cross-correlation method can compensate the lighting condition and exposure time differences during the duration of one experiment, and compensate the possible deformation of alginate film and the measurement error due to manually locating cell clusters. This method can provide perfect match for clusters over a certain time period of development.

2.6.6.2 Reference point selection

Since the directional growth is of most interest in this thesis, radial angle is applied to quantify the growth direction. Thus a reference point or the original of a polar coordinate needs to be set. For a three-dimensional (3D) object, the shifting of mass center will reflect its growth. Images of the object taken through a fluorescence microscope are its projection in 2D horizontal x-y plane. The center of mass obtained from the 2D image is the center of mass of the projected area of cells on x-y plane which is not the physical center of mass.

The appearance of the object through a microscope depends on the thickness of the sample. The thickness of the sample layer in microscope causes blurring to the objects (Dieterlen et al. 2002; Lockett and Herman 1994; Meinhart et al. 2000). The blurring originates from the 3D nature of the sample. Only flat objects on a focal plane can be thoroughly in focus. The further the objects are from the focal plane, the more blurred is their appearance. The general size of Norway spruce meristematic cells is around 20 to 30 μm, and the thickness of the focal plane for 10× and 15× lens with numerical aperture of 0.25 is around 10 μm. Since these two sizes are close, it is impossible to take images by segmenting the cell cluster at different depth. Thus, in this thesis, only 2D images are used to evaluate the growth of cells under different test conditions.

Although the center of mass of a 2D projection image is not the physical center of mass of one cell cluster, it reflects the shape of the projected cell contour. By tracing the contour changes, one can get the qualitative idea of how the cluster grows and develops in the 2D plane. Thus the center of mass of the projected 2D image of one cell cluster at the beginning of one experiment was selected as the reference point, or the origin of the polar coordinate, to evaluate the cells growth over time.

2.6.6.3 Division of angles when quantifying directions

To evaluate the direction of growth and not miss any new cells, the minimum division of angle was determined as shown in Figure 15. Cell cluster is around 200 μm in length (with the black circle represent the possible edge location of one cluster) with meristematic cells of diameter of 20 μm (which is represented as the red circle). The

minimum angle division not to miss the peak and valley of the new cell will be $\beta/2$. The triangle as sketched on the right of Figure 15 is used to determine the angle division, which is 5.8°.

Figure 16A shows such a cell cluster with the new cell on the edge labeled with red color, Figures 16B –D show the matched contours and measurements of the growth due to this new cell with white bars, using divisions of 36, 72 and 90, respectively, and Figure 16E shows the radial length of the growing cluster with division of 36, 72 and 90, respectively. There are two white bars in Figure 16B with 32 divisions that miss the peak of the new cell. There are three white bars showing the growth in Figure 16C with 72 divisions. These bars cover the peak and the valley of the cell along the edge. So do the white bars in Figure 16D with 90 divisions. Radial length line with 36 divisions differs to the radial length lines with 72 and 90 divisions, and the lines with 72 and 90 divisions match each other well. The more the divisions, the more computation time is needed. Based on the above discussion, division of 72 provides enough accuracy of catching the growth trend of a new cell with reasonable computation time, and a 5° is used in this thesis to get an even distribution of angles along each direction.

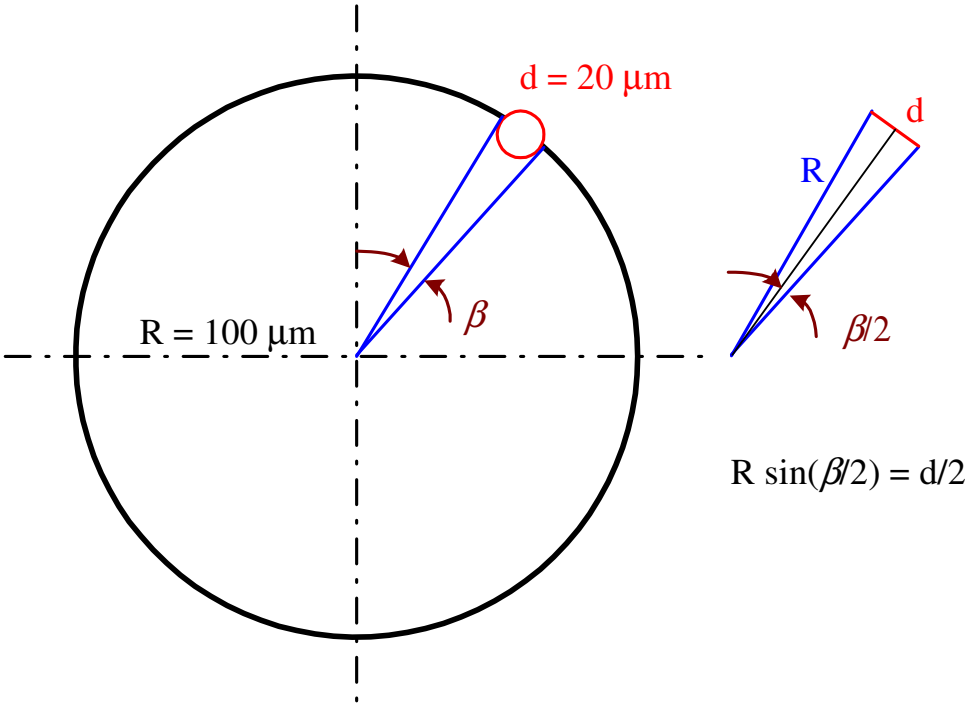

Figure 15. Sketch used to determine the angle division for radial growth evaluation. The black circle with radius R = 100 µm represents the possible edge location of one cluster, the red circle represents the new cell with diameter d = 20 µm, and $\beta/2$ is the angle representing the minimum angle division.

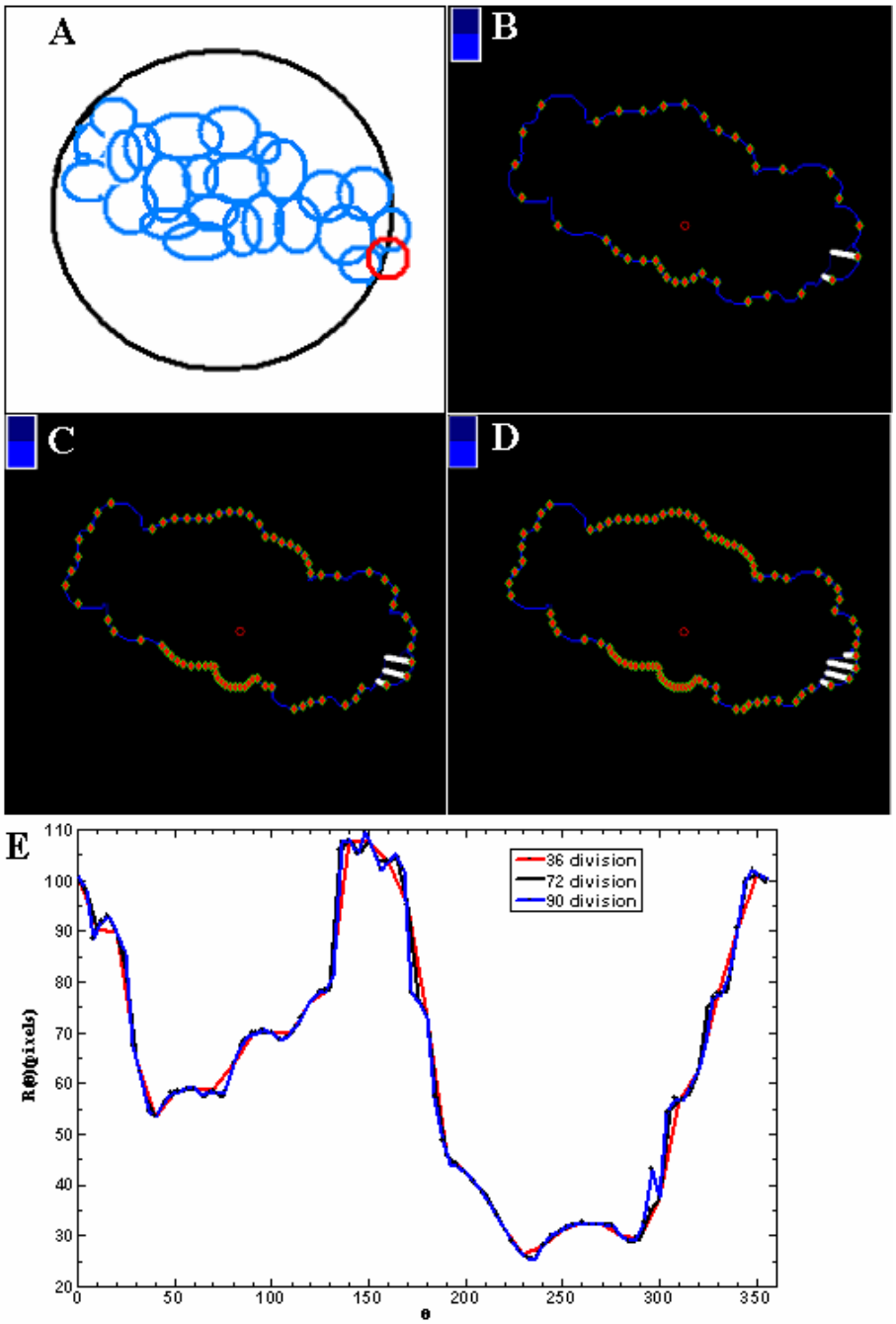

Figure 16. Evaluation of angle division. (A) One cell cluster with length of 200 µm, the black circle is of diameter of 200 µm and the red circle represents the new cell in the size of 20 µm. (B) Measurement of new cell growth with 36 divisions, white bars represent the growth along certain directions. (C) Measurement of growth with 72 divisions. (D) Measurement of 90 divisions. (E) Radial length of the growing cluster with division of 36, 72 and 90.

2.7 Signal transduction experiments

2.7.1 Integrin-like protein detection experiments

To verify if there are integrin-like proteins as stress signal molecules in Norway spruce somatic cells that could cross react with antibody against human integrin, and determine their distribution, immunofluorescence study was performed (Lü et al 2007). Suspension cultured cells passed 500 μm nylon mesh and the cells larger than 500 μm left on the mesh were collect for study. The detail procedure is as follows:

(1) The cells were treated with enzyme solution, containing 0.25% (w/v) Driselase (Sigma Aldrich), 0.25% (w/v) Macerozyme (Sigma Aldrich) and 1% (w/v) Cellulase (Sigma Aldrich) at room temperature, for 15 minutes on the 20 rpm rotary table in the dark to loose the cell wall and expose the membrane for further antibody treatment. The enzyme treatment dissolve cell walls in different extend and breaks down cell clusters to smaller size. Some cells with cell wall partially removed present as individual cell and a shape close to sphere; cells with cell wall completely removed present as protoplasts which are in spherical shape. In order to get cells in various states, such as intact cells, damaged cells, cells with cell wall partially removed, cells with membrane partially peeled from cell walls, and protoplasts with cell wall completely removed, larger fraction of cell clusters (> 500 μm) was used here.

(2) The cells were then washed with medium three times to remove the enzyme solution. During each wash, cells were put into Petri plates and shaken on the rotary table at 20 rpm for 5 minutes. Liquid was then removed with 1000 μl

pipettor. After wash, cells were divided in Petri plates and ready for further treatments.

(3) Six plates were marked as control. Three of them experienced no further treatment and ready to be observed under the microscope. The other three of these plates were incubated with secondary antibody followed the same procedure as in step 6 and 7.

(4) The cells in rest plates were incubated in phosphate-buffered saline (PBS) containing 10% (w/v) bovine serum albumin (BSA) in dark on the rotary table at 20 rpm for 10 minutes. Cells were washed with PBS as step (2) after incubation for three times.

(5) The primary rabbit antibody against human integrin β1 (M-106 from Santa Cruz Biotechnology Inc.) at a dilution of 1:400 was added to the Petri plates with cells. The plates were then incubated at 37 °C overnight (for total of 17 hours) then washed three times with PBS after the incubation.

(6) Tetramethylrhodamine isothiocyanate (TRITC)-conjugated anti-rabbit immunoglobulins (Sigma Aldrich) was added to the Petri plates at a dilution of 1:500. The plates were then incubated at 37 °C for 4 hours.

(7) After the incubation, cells were washed with PBS for four times and left in Petri plate for observation. The fluorescence microscope was equipped with a TRITC filter (with excitation: 535/50 nm and emission: 610/75 nm from

Chroma) capable of detecting the fluorescent signal from the secondary TRITC-conjugated antibody.

2.7.2 Reactive oxygen species detection experiments

Another cellular level signaling molecule studied in this thesis is hydrogen peroxide, H_2O_2, which is one of the reactive oxygen species (ROS) along with superoxide $O_2^{\bullet -}$ and hydroxyl radical OH-. Past studies show that ROS is a natural byproduct of the normal metabolism of oxygen and has important roles in cell signaling. Production of ROS has been studied as a parameter of shear stress effect on the plant cells (Gao et al 2007; Gens et al 1996; Swatzell et al 1999). In this section, the production of H_2O_2 in the stressed cells was tested using dihydrorhodamine 123 (DHR123). The accumulation of H_2O_2 can be detected by the stain of DHR123 by showing fluorescent signals of high intensity.

Suspension cultured cells at proliferation stage from cell line #3 were used as testing material. The detail procedure is following:

(1) Cells were first filtered through a 200 μm nylon mesh to get rid of the old culture medium, or the H_2O_2 in the medium; cells were rinsed on the mesh with fresh medium 5 times; washed cells were placed in Petri plates with fresh medium.

(2) One plate with cells was labeled as control and without any further treatment; a second Petri plate with cells was shaken vigorously at a frequency of 180 rpm for 2 minutes and then 20 μM dihydrorhodamine 123 (DHR123, Sigma

Aldrich) was added in this plate to stain the cells for 5 minutes; cells in a third Petri plate were stressed by fast pippeting the cells up and releasing them continuously at a frequency of 60 repetitions per minute for 2 minutes and then 20 μM DHR123 was added in this plate to stain the cells for 5 minutes.

(3) Stained cells in both last two plates were filtered and washed with fresh medium for 3 times; washed cells were put into two new Petri plates with a few drops of fresh medium for fluorescent signal detection. The microscope was equipped with I3 filter from Leica, with excitation of 450-490 nm and suppression long pass of 515 nm, to detect the signal.

2.7.3 Cell wall pore size experiments

To find the molecular response of cells to shear stress, the permeability of the cell walls of the cell clusters as a result of shear stress was tested. Signaling molecules need to pass the cell wall and reach the cell membrane in order to have an effect, and it has been argued that size exclusion at this level controls development (Jarvis 2009). In order to design experiments to further explore the physiological functions of cell wall and the uptake of molecules like proteins by intact plant cell, it is necessary to consider the pore size of plant cells.

Based on the phenomena of either plasmolysis or cytorrhysis, one can have the idea of how big the solutes size comparing with the pore size of the cell wall. Carpita et al. (1979) devised a solute exclusion method to determine the pore size of cell walls of living cells, by observing the plasmolysis and cytorrhysis of plant cells after immersing cells in a solute of certain size with a phase-contrast microscope. Based on their idea, a

procedure was designed to test pore size of the cell wall of Norway spruce somatic embryo cells.

2.7.3.1 Solute concentration concerns

In order to eliminate the effect from osmotic pressure, all the solutions will be in a concentration that keeps the osmotic pressure of each solution the same. Osmotic pressure is an important factor affecting cells. Plant cells in a hypotonic solution will swell and increase their volume, while the cell walls restrict the expansion and this results a turgor pressure on the cell wall from within, and turgor pressure allows plants stand upright in nature. Plant cells in hypertonic solution lose water and this will cause plasmolysis. The hypertonic solution may or may not have a higher osmotic pressure than the cell interior as the hypotonic solution since the rate of water entry/leave will depend upon the permeability of the cell wall. Testing the permeability of cell wall is the priority goal in the following designed experiments; the factor of osmotic pressure has to be considered to isolate the effect of cell wall pore size.

In the protoplast experiments of Norway spruce somatic embryos, 0.44 M of mannitol as an osmoticum was used. This helps the forming protoplasts keep their shape and not burst. For plasmolysing somatic embryos before transformation with particle bombardment, 0.25 M myoinositol was applied. Plasmolysis occurs under this condition. These two values can serve as guides for the osmotic pressure of cells in isotonic solution. The osmotic pressure, Π, in [atm] unit of a dilute solution can be approximated using the Morse equation (Amiji & Sandmann 2003)

$$\Pi = i_{os} m R_{gas} T \qquad (7)$$

where i_{os} is the dimensionless van't Hoff factor; m is the molarity of solution with unit of [mol·L^{-1}]; R_{gas}=0.08206 [L·atm·mol^{-1}·K^{-1}] is the gas constant; T is the thermodynamic (absolute) temperature in [K]. The van't Hoff factor is the ratio between the actual concentration of particles produced when the substance is dissolved, and the concentration of a substance as calculated from its mass. For most non-electrolytes dissolved in water, the van't Hoff factor is essentially 1. For most ionic compounds dissolved in water, the van't Hoff factor is equal to the number of discrete ions in a formula unit of the substance. This equation gives the pressure on one side of the membrane. The total pressure on the membrane is given by the difference between the pressures on the two sides. Based on the above equation, it is obvious that the osmotic pressure is proportion to molarity for non-electrolyte, thus molarity can serve as an easy indicator.

To get the mass concentration (C_N) in [g· L^{-1}] of one solute, the Morse equation can be rearranged as following formula:

$$C_N = M_W m = M_W \Pi/(i_{os} R_{gas} T) \quad (8)$$

Where M_W is the molecular weight of a solute in [g·mol^{-1}]. The mass used for 10 ml of solution for each solute will be 0.01 C_N grams. Table 3 listed the molecular weight along with mass concentration of each solute under different osmotic pressures/molarities of solutions.

Table 3. Solutes molecular weight and size, and mass used in 10 ml of different solutes based on molarity of 0.25 and 0.44, respectively.

Solute	Molecular weight [g/mol]	Molecular diameter [A]	Mass used for 10 ml solution of 0.25M [g]	Mass used for 10 ml solution of 0.44M [g]
Mannitol	182	8	0.46	0.80
Sucrose	342	10	0.86	1.50
Stachyose	666	14	1.67	2.93
Polyethylene glycol (PEG)				
PEG 400	380-420	22	1.00	1.76
PEG 600	570-630	29	1.50	2.64
PEG 1000	950-1050	35	2.50	4.40
PEG 1540	1305-1595	38	3.63	6.38
PEG 4000	3015-3685	45	8.38	14.74
PEG 6000	5000-7000	52	15.00	26.40

2.7.3.2 Experimental procedures

Norway spruce somatic embryo cell clusters in the proliferation stage are cultured on solid medium in 10 mm Petri plates in the dark. The solid medium has the same components as liquid ½ LP medium and is solidified with agar (0.35% w/v). Cell clusters from cell line 06:22:02 and 06:21:00 were picked for the pore size solute exclusion experiments due to their ease of dispersion. The response of cell clusters to one macromolecule with concentration of either 0.25 M or 0.44 M was observed. The experiment was repeated for total three times on one solute. Following is the procedure for preparing stressed cells.

(1) A very thin layer of cells (approximate 200 mg) were carefully taken out of the clumps of cells and put into a 6 mm Petri plate for control study as cells experienced no stress.

(2) For the stressed group of cells, about 1/3 of one clump of cells (approximate 200 mg) was taken out of the solid cultured plate and put into a 6 mm Petri plate filled with 2 ml of liquid culture medium. The cells were then liquid cultured in the plate on the rotary table at 100 rpm and covered in the dark.

(3) Cells were sampled from the liquid culture plate after 4 hours and overnight for 22 hours. Nine solutes (from Sigma-Aldrich) of different molecular diameters from literature (Carpita et al 1979), Mannitol, Sucrose, Stachyose, Polyethylene glycol (PEG) 400, 600, 1000, 1540, 4000 and 6000 as listed in Table 3 were dissolved with nanopure water to make solutions to test the pore size.

The experiment started with the solute preparation based on two concentrations as listed in Table 3. Following is the procedure for sample observation.

(1) Cells were put onto a glass slide with forceps. Two drops of liquid culture medium were dripped upon to disperse the cells quickly for control cells, this step was skipped for stressed cells. Cells were covered and affixed with a cover slip. The glass slide was then put on the stage of the microscope.

(2) One of the solutions was dripped drop wise on the right side of the slip. A piece of paper towel was positioned on the left side of the slip to absorb the

liquid between the glass slide and cover slip such that the test solution was drawn from right to left across the cells affixed between. The time between the drop contacting the slide and the cell clusters showing plasmolysis and cytorrhysis were recorded. The above cells testing procedure was repeated for the rest solutions.

After introduction of experimental setups, methods and procedures for each experiment, the results from controlled shear stress experiments and signal transduction experiments will be presented and discussed in next chapter.

CHAPTER 3

EXPERIMENTAL RESULTS AND DISCUSSION

This chapter presents the results and discussions for steady shear stress and signal transduction experiments. In order to make comparison of cell cluster growth and development, the results of cell cluster growth under control are presented first in Section 3.1, followed by the results of steady shear stress experiments and comparison between them in terms of cluster growth and formation of suspensor cells. Section 3.2 describes the results of signal transduction experiments that include integrin-like protein and reactive oxygen species detections and the pore size monitoring experiments with solute-exclusive method.

3.1 Cell cluster development

3.1.1 Cell cluster development in control group

To compare the difference between cell clusters experiencing shear stress and those in stationary culture, a second film was made at the same time as the film experiencing steady shear stress inside of the FCS2 chamber, following the same procedure. This second film served as control for the shear stress experiments.

The control film with immobilized cells was kept stationary in a Petri plate, with liquid medium partially immersed the film and immobilized cell clusters on top of the film exposed to air. The film was stored in the dark (by covering with aluminum foil) at 25 °C except when being imaged once a day. The amount of liquid medium was kept small to provide enough nutrients to the immobilized cells and prevent the film from floating around in the medium, which makes tracking the cells very difficult. The repeated tests on the control group show that the small amount of liquid medium (around 2 ml) is sufficient to supply the cells with nutrients over the two-week period.

The development of cell clusters over the 14 days of experimental period was recorded and processed. One representative cell cluster development in the control group is shown in Figure 17. The images present the status of the cluster on day 1 (A), day 5 (B), day 6 (C) and day 7 (D) of the experiment. The cell cluster started as a small aggregate and continued to divide and grow. Suspensor cells developed on this cell cluster at day 5 of the experiment and formed a polarized structure as indicated by the red arrows in Figures 17B-D. For all the experimental cases, the cell clusters in the control group which developed suspensor cells formed suspensor cells at day 5 to day 9 of an experiment. The suspensor cells formed unidirectionally on cell cluster and all the clusters with developed suspensor cells show polarized structure. The clusters which did not develop suspensor cells continued to divide and grow as an aggregate (as shown in Figure 18 on next sub section). The quantificational analysis will be presented in the quantification section.

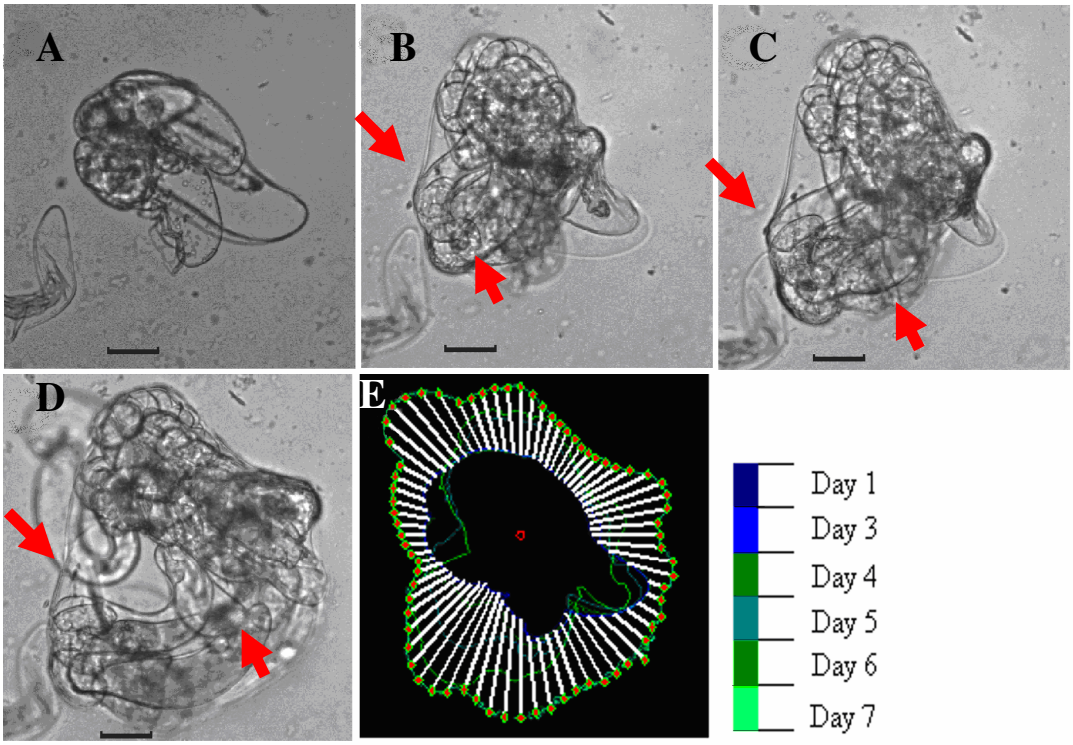

Figure 17. A cell cluster in the control group under stationary condition. (A) 1 day after the experiment was started; (B) 5 days; (C) 6 days; (D) 7 days. The red arrows indicate the location of suspensor cells. Scale bar = 50 µm. (E) Estimation of development and growth of the cell cluster by superimposing the cell contours from the 7 days of duration of the experiment by the step-wise method outlined in Figure 7. The different colors on the color bar represent the different day of experiment.

3.1.2 Cell cluster development under steady shear stress

The steady shear stresses that are exerted on the cell clusters immobilized on alginate films were generated by the peristaltic pump (Harvard) running at pre-set flow rates (0.3, 0.5, 1, 3 and 5 ml/min) as described in Chapter 2. To eliminate the pressure pulsation during operation of the pump, a pressure damper was added into the flow loop before the culture medium entered the FCS2. The flow rate was kept constant over the

full duration of the experiment—fourteen days. Each experiment at a given flow rate was carried out for three times to get triple set of data.

The embryo cells immobilized on the top of an alginate film are exposed to shear stresses generated by fluid flowing through the chamber. Flow rates of 0.3, 0.5, 1.0, 3.0 and 5.0 ml/min were used in the steady flow experiments, resulting in shear rates of 9, 14, 29, 86 and 140s^{-1}, respectively. These shear rates correspond to wall shear stresses of 0.009, 0.014, 0.029, 0.086 and 0.140 N/m^2, as shown in Table 2. The development of cell clusters under shear rates of 9, 14, 29, 86 and 140 s^{-1} over the 14 days of experimental period was recorded and processed. These cell clusters' morphological changes are further quantified in the later sub section. Experiments were also carried out at shear rates of 3 and 290 s^{-1}, corresponding to flow rates of 0.1 and 10 ml/min and wall shear stresses of 0.003 and 0.29 N/m^2, respectively. However, no cell clusters survived for more than two days under these two tested conditions. These results are therefore excluded from further analysis except the discussion of possible cause. The lower shear rates of 3, 9, 14 and 29 s^{-1} are in the range resembling the shear rates in a suspension culture flask. The higher shear rates of 86, 140 and 290 s^{-1} tested in this thesis are in the range of shear rates under which plant cells are claimed to be stress sensitive (Sun & Linden 1999).

Figures 18 to 20 show the representative cell cluster growth under shear rates of 140, 86 and 29 s^{-1}, respectively. As shown in Figure 18, the cell clusters under the shear rate of 140 s^{-1} started as a small aggregate at day 1 (A) and continued to divide and grow through day 3 (B), day 8 (C) and day 13 (D) of the 14-day period of experiment. But the cluster did not develop suspensor cells in this experiment during the two-week period of

experiment. This happens to all the cell clusters which were exposed to the shear rate of 140 s^{-1}. At shear rate of 86 and 29 s^{-1}, some of the clusters did form suspensor cells in a unidirectional manner, as shown in Figures 19 and 20, respectively. Most of the clusters which developed suspensor cells have suspensor cells formed at day 5 to day 9 of the experiment (as shown in Figures 19B and 20C). This is similar to the suspensor cell development on the clusters in the control group. At even lower shear rates of 14 and 9 s^{-1} not all clusters developed suspensor cells either. The clusters which developed suspensor cells grow in the similar pattern as those shown in Figures 19 and 20. The clusters which did not develop suspensor cells grow in the similar pattern as shown in Figure 18. The quantificational analysis about cluster growth will be discussed in quantification section below.

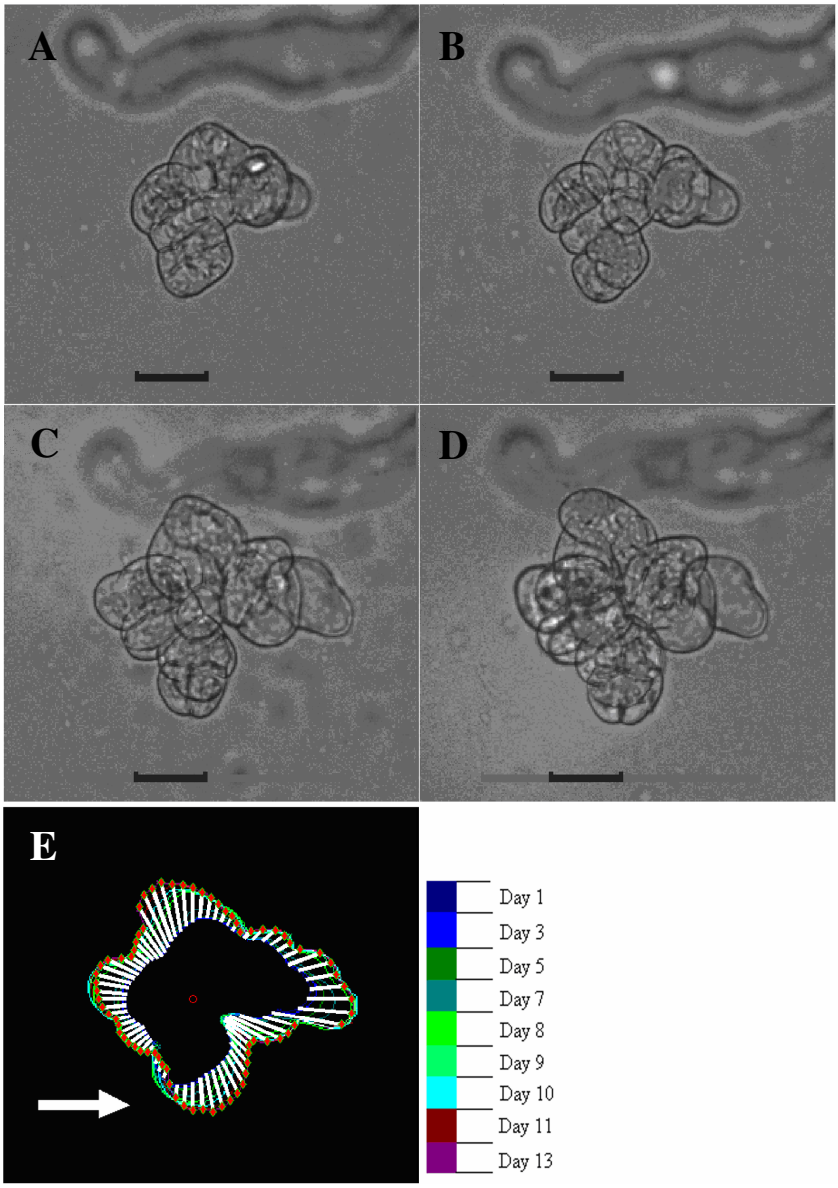

Figure 18. A cell cluster in the flow cell experiment subjected to steady stress at a shear rate of 140 s^{-1}. (A) 1 day after the experiment was started; (B) 3 days; (C) 8 days and (D) 13 days at the end of the experiment. Scale bar = 50 µm. (E) Estimation of development and growth of the cell cluster by superimposing the cell contours from the 13 days of duration of the experiment by the step-wise method outlined in Figure 7. The center of the red circle represents the origin of the radial coordinate, and the white bars represent the values of the growth vectors and the red end dots on the white bars indicate the positions of the cell cluster edge at the end of the experiment. The white arrow indicates the flow direction from left to right. The different colors on the color bar represent the different day of experiment.

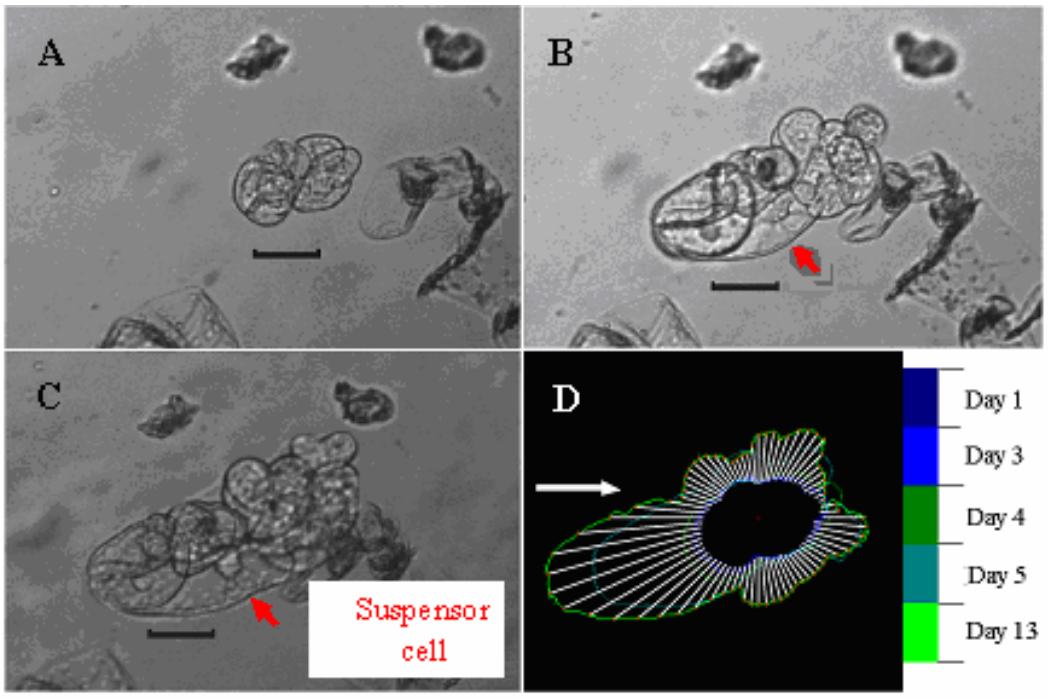

Figure 19. A cell cluster in the flow cell experiment subjected to steady stress at a shear rate of 86 s^{-1}. (A) 1 day after the experiment was started; (B) 5 days; (C) 13 days close to the end of the experiment with few suspensor cells forming. Scale bar = 50 µm. (D) Estimation of development and growth of the cell cluster by superimposing the cell contours from the 13 days of duration of the experiment by the step-wise method outlined in Figure 7. The center of the red circle represents the origin of the radial coordinate, and the white bars represent the values of the growth vectors and the red end dots on the white bars indicate the positions of the cell cluster edge at the end of the experiment. The white arrow indicates the flow direction from left to right. The different colors on the color bar represent the different day of experiment.

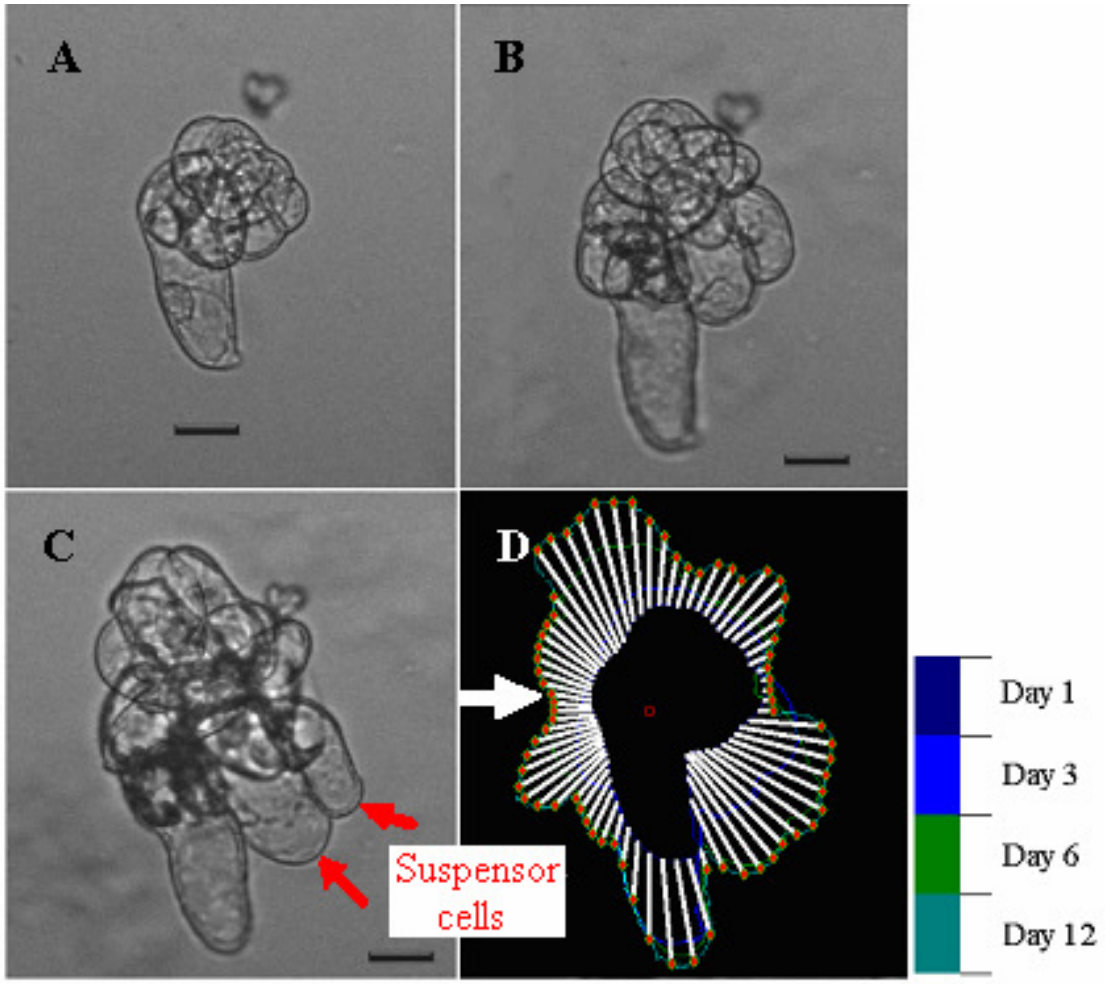

Figure 20. A cell cluster in the flow cell experiment subjected to steady stress at a shear rate of 29 s^{-1}. (A) 1 day after the experiment was started; (B) 3 days; (C) 6 days with few suspensor cells forming. Scale bar = 50 μm. (D) Estimation of development and growth of the cell cluster by superimposing the cell contours from the 12 days of duration of the experiment by the step-wise method outlined in Figure 7. The center of the red circle represents the origin of the radial coordinate, and the white bars represent the values of the growth vectors and the red end dots on the white bars indicate the positions of the cell cluster edge at the end of the experiment. The white arrow indicates the flow direction from left to right. The different colors on the color bar represent the different day of experiment.

3.1.3 Suspensor cell development

The clusters of somatic embryo cells subjected to shear and stationary cultured as control were imaged every 24 hours after the start of the experiment. Three repeated experiments under each shear rate were conducted and images of recorded clusters were analyzed. Shear stress effect is qualitatively measured by the growth of meristematic cells and monitoring the formation of suspensor cells. Suspensor cell development is a prerequisite for cell cluster showing polarized structure. The formation of suspensor cell is examined first before the growth of meristematic cells. The formation of suspensor cells under different test conditions is categorized in Table 4 as (a) no suspensor cells; (b) a few, randomly positioned; (c) many, randomly positioned; (d) a few, unidirectional; and (e) many, unidirectional. For the final evaluation of stress effects on the morphology of embryo cell clusters that is the growth of meristematic and suspensor cells, image analysis is used to evaluate the morphological changes by analyzing the collected images from the experiments using the in-house code.

As shown in Table 4, cell clusters develop suspensor cells in a polarized manner both under control and steady shear stressed groups except at the highest shear rate of 140 s^{-1}. Cell clusters exposed to shear rate of 140 s^{-1} did not form suspensor cells. Under other shear rate conditions, cell clusters exposed to shear rate of 86 s^{-1} have the lowest suspensor cell formation rate of 13.2% (5/38); cell clusters exposed to shear rate of 29 s^{-1} show the maximum suspensor cell formation rate of 47.1% (16/34) among the fluid shear cases; cell clusters exposed to shear rate of 14 and 9 s^{-1} have suspensor cell formation rate of 38.5% (10/26) and 27.3% (3/11), respectively. However, cell clusters in the control

group have the highest suspensor cell formation rate of 60.5% (23/38) among all the test conditions.

Table 4. Number of cell clusters with/without suspensor cells formation during 14 days of experiments under different test conditions (N: number of observations over all cell clusters).

Test condition as shear rate In s^{-1}	N	No suspensor cells	A few randomly positioned suspensor cells	Many randomly positioned suspensor cells	A few unidirectional positioned suspensor cells	Many unidirectional positioned suspensor cells
0 (control)	38	15	0	0	0	23
9	11	8	0	0	3	0
14	26	16	0	0	2	8
29	34	18	0	0	2	14
86	38	33	0	0	1	4
140	37	37	0	0	0	0

In order to quantitatively describe the suspensor cell formation under different test conditions, Table 5 and two polar diagrams (Figures 21 and 22) are made to represent the number and location of suspensor cells formed on cell clusters. In Table 5, only suspensor cells formed in horizontal (x) and vertical (y) directions within ±15° range are observed. These directions are either parallel (+x and –x) or perpendicular (+y and –y) to the flow direction (+x) in the x-y plane. In Figures 21 and 22, the clusters formed suspensor cells are all presented on the x-y plane. The dots on Figures 21 and 22

represent the number and direction of clusters formed suspensor cells in a 30° angle range.

Suspensor cells in control group are formed in a relatively random manner. As shown in Table 5, suspensor cells formed along ±x direction and ±y direction are close, with 17.4% formation rate along both +x and -x directions and 13.0% formation rate along both +y and -y directions. The even distributed dots along each 30° angle range as can be observed in Figure 21 also suggest the random distribution of suspensor cell formation, although all the clusters with suspensor cells showed polarized structure with meristematic cells as "head" region and suspensor cells as "tail" region. There is not a preferable direction of suspensor cell forming under control. The observation of all the clusters in the control group indicates that the direction at which the suspensor cells grow is random when cell clusters are not exposed to shear stress. This can be explained as the seeding orientation of cell clusters during immobilization is random. The development of suspensor cells in the control agrees with that when cell clusters are cultured on solid medium, with liquid culture medium of the same components and being solidified with agar. Past experience with somatic cell clusters has shown that somatic cell clusters form polarized structure with suspensor cells at the late stage of proliferation, after transferring the cell clusters onto solid medium (as shown in Figures 3A and 4A)(Egertsdotter & von Arnold 1998). For the control group, cell clusters were immobilized that are similar to cell clusters cultured on solid medium except the culture medium is in liquid phase and not solidified with alginate. Agar and alginate are both used as solidifying agent for liquid medium and proved to support cell cluster growth.

Cell clusters that formed suspensor cells under different shear stresses are further observed in term of forming directions, as shown in Figure 22. The directions along which the suspensor cell formed are mostly in either perpendicular (±y) or parallel (±x) to flow direction within ±15° range (as further observed in Table 5). Most of the suspensor cells grow in the horizontal (±x) direction, with over 80% formation rate along horizontal direction compared with about 20% formation rate along vertical direction. The number of suspensor cells formed on cell clusters under different shear rates along horizontal direction is significantly more than that formed in control, based on t-test with confidence level of 99%. The suspensor cells formed on cell clusters under different shear rates along vertical direction, however, are not significantly different from that in the control.

Table 5. Directions of suspensor cells formation under different test conditions, control, shear rates of 9, 14, 29, 86 and 140 s^{-1}, respectively. Positive horizontal direction is the flow direction which is the x axis in Cartesian coordinate and positive vertical direction is the y axis direction under different shear rate tests. ("+" is the +x/+y direction, "-" is the -x/-y direction.)

Test condition as shear rate (s^{-1})	Percentage of clusters formed suspensor cells (%)	Number of suspensor cells formed in horizontal (x) direction (±15°)			Number of suspensor cells formed in vertical (y) directions (±15°)		
		+	-	Percentage among all clusters formed suspensor cells (%)	+	-	Percentage among all clusters formed suspensor cells (%)
0(control)	60.5	2	2	17.4	2	1	13.0
9	27.3	2	1	100.0	0	0	0.0
14	38.5	5	3	80.0	0	2	20.0
29	47.1	8	6	87.5	1	1	12.5
86	13.2	2	2	80.0	1	0	20.0
140	0	0	0	0.0	0	0	0.0

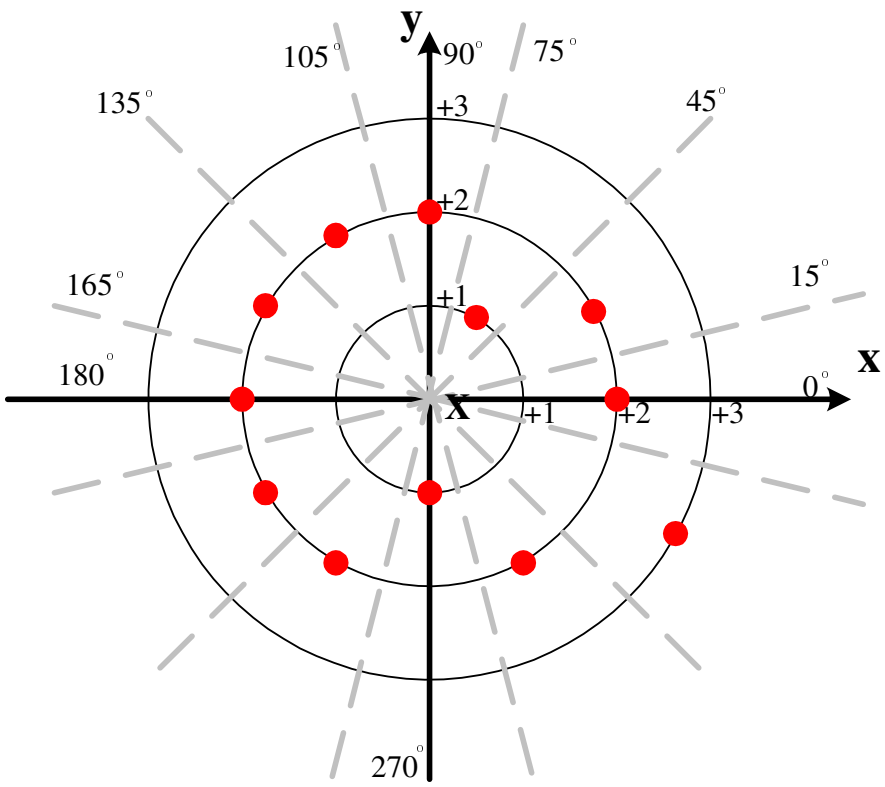

Figure 21. Polar diagram of suspensor cells forming direction in the control experiments after 14 days of growth. The red dots represent the number of cell clusters forming suspensor cells in each of a 30° angle range; the first 30° angle range starts with -15° to 15°, followed by 15° to 45°, 45° to 75°, and so on; there are total of 12 ranges.

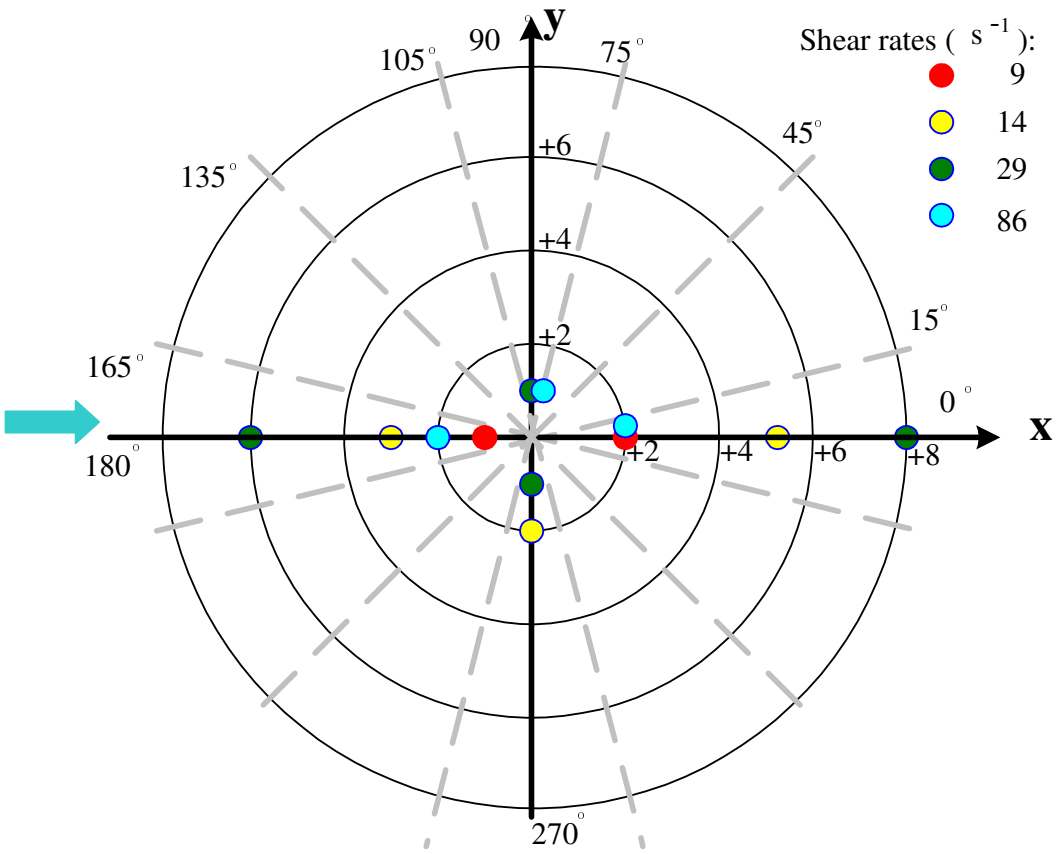

Figure 22. Polar diagram of suspensor cells forming direction in the shear stressed experiments after 14 days of growth. The dots represent the number of cell clusters forming suspensor cells in each of a 30° angle range; the first 30° angle range starts with -15° to 15°, followed by 15° to 45°, 45° to 75°, and so on; there are total of 12 ranges. The red dots are for shear rate of 9 s^{-1}, yellow for 14 s^{-1}, green for 29 s^{-1} and light blue for 86 s^{-1}. The blue arrow indicates the flow direction.

3.1.4 Quantification of cell cluster development

The general geometric outline of one cell cluster did not change significantly within 24 hours under any experimental conditions. The imaged patterns of the same somatic embryo cluster from two consecutive days were matched for image analysis. The growth of one cell cluster is quantified by the changes in its radial sizes measured in 72 directions, based on the validation results of minimum division angle of 5° to catch one single newly divided cell. The mean radial growth rate of a cell cluster was measured along each of the 72 directions.

The mean growth rates $\overline{\Delta R}$ were evaluated along different θ directions under different test conditions. Figure 23 shows the mean growth rates for meristematic cells, excluding the clusters that developed suspensor cells in the stressed groups and the suspensor cells in the control group. Since over 60% of cell clusters in the control group developed suspensor cells, all the meristematic cell clusters are counted for statistical analysis. The sub figures in Figure 23 are mean growth rates of meristematic cells under stationary culture (A), shear rate of 9 (B), 14 (C), 29 (D), 86 (E) and 140 s^{-1} (F), respectively. Figure 24 shows the mean growth rates for all the observed clusters, including the suspensor cell growth. The sub figures in Figure 24 are results under stationary culture (A), shear rate of 9 (B), 14 (C), 29 (D), 86 (E) and 140 s^{-1} (F), respectively. The error bars in both Figures 23 and 24 represent the standard deviation. The growth rates of meristematic cells (Figure 23) have relatively smaller variations along each direction compared with the growth rates of all the clusters including those developed suspensor cells (Figure 24). This is due mainly to the polarized structure of

these suspensor cells. The standard deviation in Figure 24, which is based on the data of all cell clusters including those formed suspensor cells, varies more along different direction than in Figure 23. Figure 24F shows the mean growth rates for meristematic cells at the shear rate of 140 s^{-1} since no cell cluster developed suspensor cell under this condition. As shown in the figure, the data has much less variation in the standard deviation along different directions than that in Figure 24E, which shows the results at the shear rate of 86 s^{-1}. This difference is attributed to the fact that no suspensor cells formed under shear rate of 140 s^{-1} (F) while about 13.2% of cell clusters formed suspensor cells under shear rate of 86 s^{-1}(E). Suspensor cells are larger than meristematic cells and in a vacuole shape, which contribute to larger mean growth rates than the ones of meristematic cells only, as further observed in Table 6.

Table 6 presents the mean growth rates based on the average of growth rates along 72 directions of both meristematic cells and all observed cell clusters, respectively. The meristematic cell cluster growth rate excludes the clusters that developed suspensor cells in the stressed groups and the suspensor cells in the control group. The growth rate of cell clusters with suspensor cells covers data from all the observed clusters including those developed suspensor cells and the meristematic cell clusters. The growth rates of meristematic cells along different directions are checked with significant test based on one-sided confidence level of 95% t-test. The mean growth rates of meristematic cells that were exposed to shear flows are lower than that of the control group (7.4 μm/day as shown in Table 6). Under shear rates of 9, 14 and 29 and 86 s^{-1}, some cell clusters form suspensor cells and the suspensor cell grow in a polarized fashion. The mean growth rates of cell clusters for these cases including suspensor cells are in the range of 7.3 to 7.7

μm/day which are also lower than the growth rate of 8.4 μm/day in the control group. The experiments under each test condition show consistent results among repetitions as the mean growth rates obtained in the three experiments at each shear rate vary within 10% range except experiment 2 under shear rate of 29 s^{-1} which has a bigger variation of 19%.

The student t-test about the growth rate of cell clusters between under stress and in the control shows significant difference. The significance occurs in both the growth rate of meristematic cell cluster and that of all cell clusters including suspensor cells. The growth rates of meristematic cell clusters under different shear stresses are significantly slower than that in the control, based on t-test with confidence level of 99%. The growth rates of all cell clusters including suspensor cells under different shear stresses are also significantly slower than that in the control, based on t-test with confidence level of 99%. These results suggest that cell clusters grow significantly slower in the stressed group than in the control.

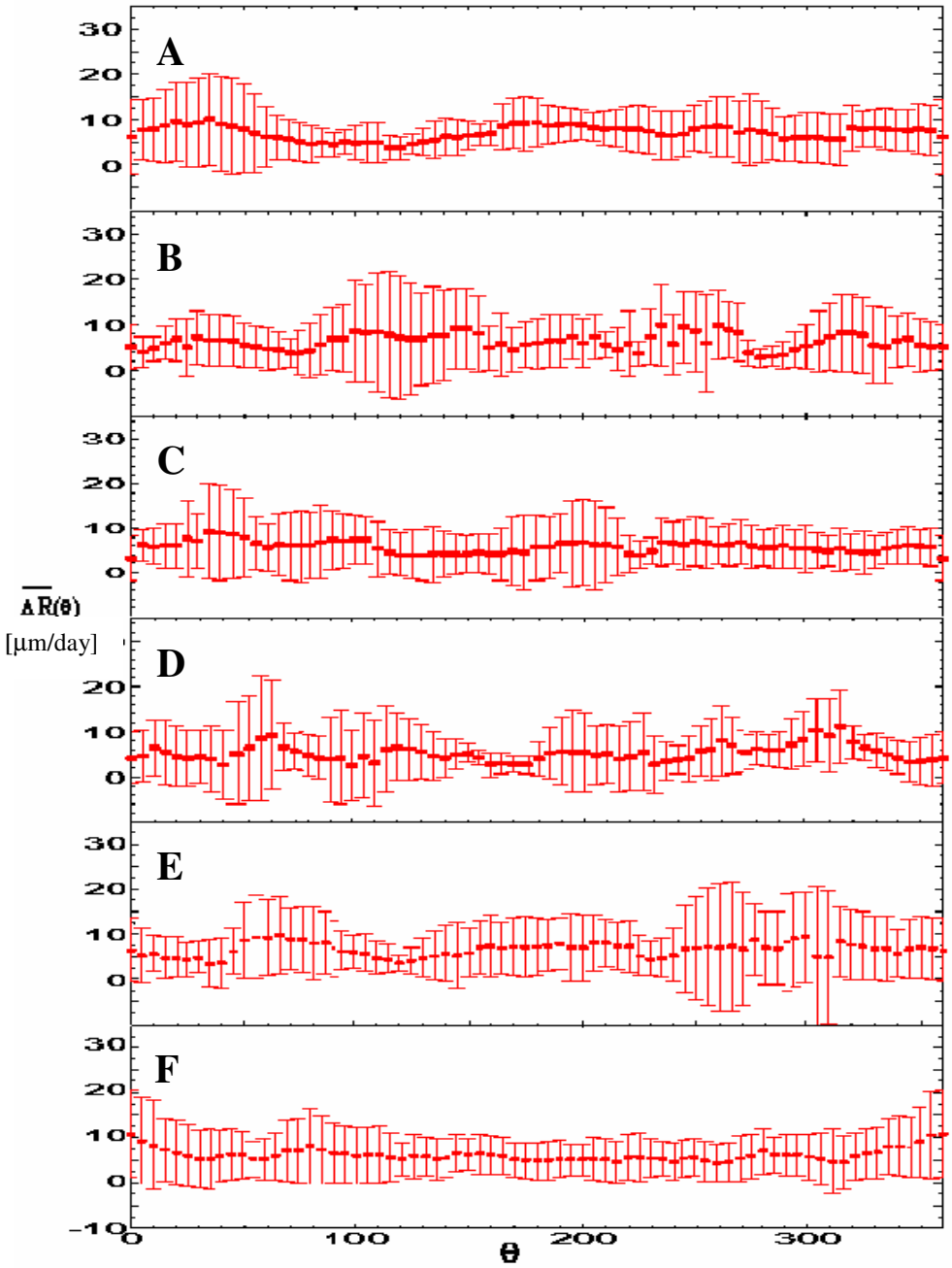

Figure 23. Meristematic cells mean growth rates $\overline{\Delta R}$ (µm/day) in θ (°) directions under different test conditions after 14 days of growth. The suspensor cells on the clusters in the control group are disregarded and the clusters developed suspensor cells in the stressed groups are also disregarded from the radial growth measurements. The radial growth for each direction was combined from the three experimental repetitions and the error bars represents the standard deviation. (A) Stationary culture condition. (B) Shear rate of 9 s^{-1}, (C) 14 s^{-1}, (D) 29 s^{-1}, (E) 86 s^{-1} and (F) 140 s^{-1}.

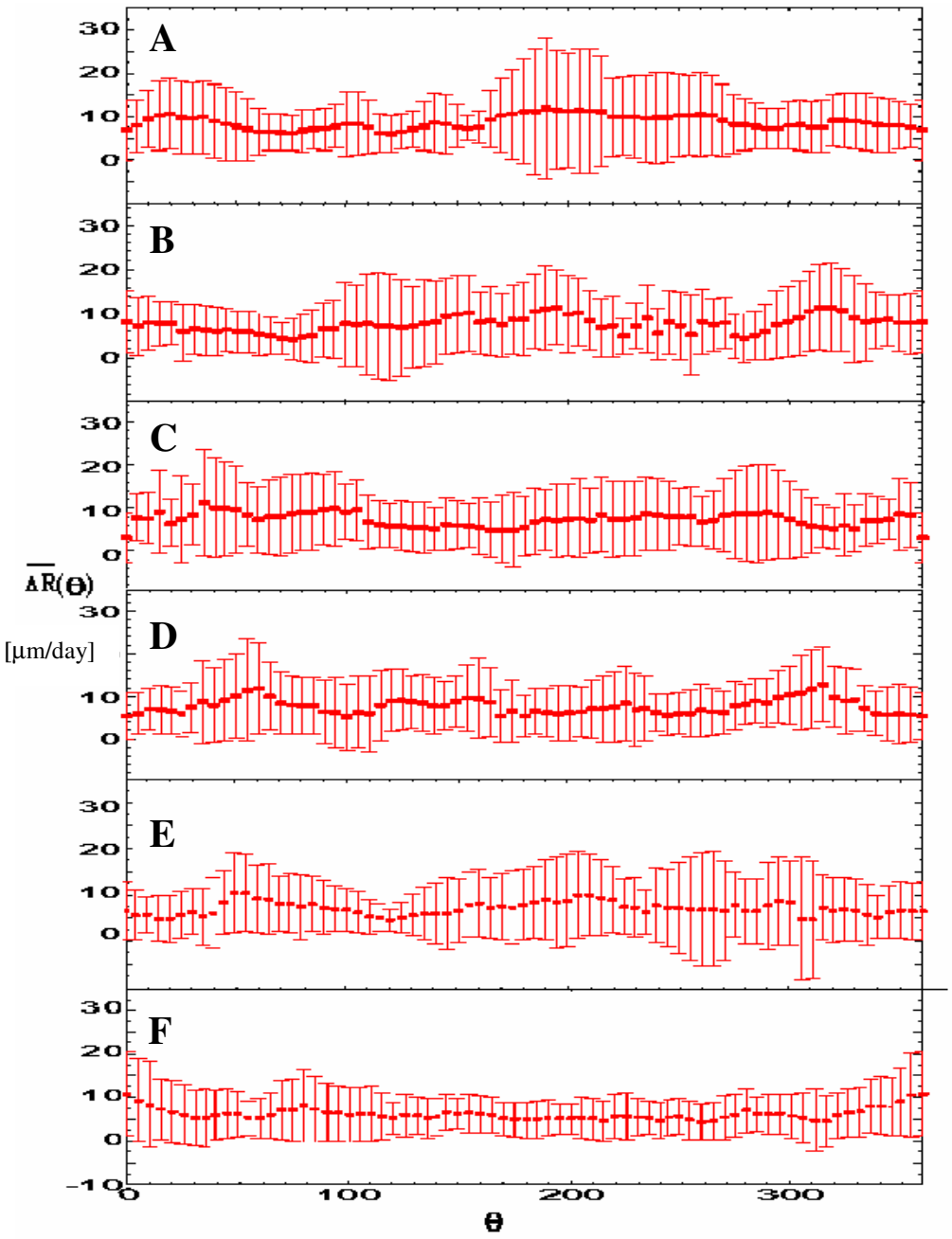

Figure 24. Cells mean growth rates $\overline{\Delta R}$ (µm/day) in θ (°) directions under different test conditions after 14 days of growth. The radial growth for each direction was combined from the three experimental repetitions and the error bars represents the standard deviation. (A) Stationary culture condition. (B) Shear rate of 9 s^{-1}, (C) 14 s^{-1}, (D) 29 s^{-1}, (E) 86 s^{-1} and (F) 140 s^{-1}.

It appears that there may be preference in growth of meristematic cell clusters in the flow direction (*i.e.*, $\theta = 0$) at shear rate of $140s^{-1}$ (Sun et al 2010). This observation is based on the statistical analysis showing 95% confidence for maximum growth in $\theta = 0$ direction for all three experimental repetitions. No other direction has maximum growth in all experimental repetitions at 95% confidence. There are also no significant correlation between the radial growth direction of the meristematic cell clusters and the direction of flow for any of the other test conditions, based on the results of one-sided statistical significance t-test analysis with confidence level of 95% (Table 6).

The highest growth rate of merisimatic cells under stress is obtained at the shear rate of 86 s^{-1}. This is also the highest shear rate under which suspensor cells form on the meristematic cells. These data suggest that there is a shear rate threshold between 86 and 140 s^{-1}, above which the cell clusters can no longer form suspensor cells; there is also a suitable growth condition for meristematic cells between shear rates of 86 and 140 s^{-1} (growth rate of 6.90 μm/day under the shear rate of 86 s^{-1} and 5.80 μm/day under shear rate of 140 s^{-1}), under which meristematic cells grow faster than under other shear rates.

Few clusters survived the experiments under the shear rate of 9 s^{-1}. This is mainly due to the difficulties in supplying and removing gaseous components from the system at low shear rates (Sajc et al 2000). For the controlled stationary culture, the alginate film partially immersed in liquid medium and the top surface exposed to air. Culture medium used in control Petri plate is only around 2 ml. However, the medium used in stress experiments is about 50 times of that in control. Considering the small amount of liquid medium used during two weeks experiment in the control group, nutrients are not concerned to cause lower cell cluster survival rate since cell clusters in the control group

grow and develop appropriately. For the same reason, the diffusion of mass transfer for nutrients at low shear rates does not make big difference compared with the control either. Another issue for cells grow properly is gas components, oxygen and carbon dioxide (Preil 1991). In the control group, cells exposed to air and the gas components exchange is free. The cells exposed to low shear rates, however, are confined in a relatively closed chamber without free exchange of gas components. The slow diffusion of gas components thus leads to low survival rate of cell clusters. Of the conditions tested, the experiments at the shear rate of 9 s^{-1} give the lowest survival rate. In Table 6, data shown for the shear rate of 9 s^{-1} is the combination of three individual experiments under the same condition. Due to the lowest survival rate, data collected from this test condition is not statistically reliable and listed for information purpose only.

The suspensor cell formation rates along horizontal and vertical directions are tested with statistical significance t-test with confidence level of 99%. The result shows that suspensor cells formed in horizontal direction under different shear stresses are significantly more than that formed in control; while the rates of suspensor cell formation in vertical direction under different shear stresses are not significant different to that formed in control.

Table 6.Average growth rate $\overline{\Delta R}$ of meristematic cell clusters with and without suspensor cell formation under various experimental conditions with shear rates of 0 (stationary culture condition), 9, 14, 29, 86 and 140 s^{-1}. Significant growth directions are the results based on one-sided confidence level of 95 % t-test for the different test conditions (N: number of total observed clusters; Exp.: experiment).

Test condition as shear rate in s^{-1}	Exp.	Meristematic cell clusters only			with suspensor cells	
		N	Mean growth rate (µm/day)	Significant fast growth direction (°)	N	Mean growth rate (µm/day)
0 (control)	1	14	6.8	N/A	14	8.7
	2	11	7.7	N/A	11	8.5
	3	13	7.9	N/A	13	8
	Average	38	**7.40**	N/A	38	**8.40**
9	Average	8	**6.27**	N/A	11	**7.59**
14	1	6	6.11	N/A	9	8.3
	2	5	5.42	N/A	9	6.9
	3	5	5.89	N/A	8	6.68
	Average	16	**5.73**	N/A	26	**7.32**
29	1	8	4.9	N/A	10	7.21
	2	6	6.35	N/A	12	8.09
	3	4	5.8	N/A	12	8.16
	Average	18	**5.33**	N/A	34	**7.68**
86	1	12	6.8	N/A	15	7.1
	2	10	7	N/A	11	7.5
	3	11	7.1	N/A	12	7.5
	Average	33	**6.90**	N/A	38	**7.30**
140	1	11	5.9	0, 350, 355	N/A	N/A
	2	14	6	0, 115, 120	N/A	N/A
	3	12	5.6	0, 120, 125, 130, 135, 205, 210, 250, 255, 260	N/A	N/A
	Average	37	**5.80**	0, 355	N/A	N/A

3.2 Cellular response of cell clusters under shear stress

After the study of the effect of shear stresses of 0.009, 0.014, 0.029, 0.089 and 0.14 N/m^2 on the development of early stage conifer somatic embryos, the cellular level experiments of somatic cell clusters under shear stress were further carried out to study cellular level responses. These include integrin-like protein detection, ROS detection and monitoring of the pore size of meristematic cell wall and uptake of marcomolecule before and after the cell clusters were exposed to shear stress.

Evidence from previous research using monoclonal and polyclonal antibodies to localize β1 integrin-like proteins in plants suggests that integrin-like proteins may be present in plants as well, and these proteins may function in signal transduction (Gao et al. 2007; Lü et al. 2007; Sun et al. 2000; Sun and Sun 2001; Swatzell et al. 1999).

3.2.1 Integrin-like protein detection

Immunofluorescence study was performed to verify whether integrin-like proteins involved in signal transduction as a response to shear stress in the Norway spruce somatic cells that could crossreact with antibody against human integrin. The stained cells were treated with enzyme solution first then stained with primary antibody, a rabbit polyclonal antibody against human integrin β1 (Santa Cruz Biotech.), and followed by the stain of secondary antibody, TRITC-conjugated anti-rabbit immunoglobulin (Sigma Aldrich), for fluorescent signal display. In order to compare the signal intensity from the primary antibody stain, cell clusters without antibody treatments were recorded as control 1 and cell clusters stained with only secondary antibody were recorded as control 2. Both

controls and stained cell clusters were observed using the microscope equipped with a TRITC filter and a 40x lens at an exposure time of 2 seconds.

Figure 25 shows the images of cell clusters in the control 1 group. Both fluorescent and bright field images are shown here. These cell clusters were treated with enzyme solution to make plasma membranes exposed to culture medium, which is also the treatment for clusters before antibody stain. Clusters of different size respond to the treatment at different degree. The bigger the cluster is, the harder the cell walls are to get loose and plasma membranes are to expose to culture medium. Clusters with intact cell walls show no fluorescent signal (Figure 25A); protoplasts with cell wall completely removed show no fluorescent signal either; however, cells with cell wall partially removed and damaged cells show dim fluorescent signals (Figures 25C and E).

Figure 26 shows the images of cell clusters in the control 2 group. Cell clusters experienced enzyme treatment and stained with secondary antibody only. This control 2 serves as a negative primary antibody stain group to compare with the cell clusters treated with both primary and secondary antibodies. As shown in Figure 26, cell clusters with intact cell walls show no fluorescent signal (Figure 26A); protoplasts with cell wall completely removed show no fluorescent signal either (Figures 26A and C); however, cells with plasma membrane partially peeled from cell wall and damaged cells show dim fluorescent signals (Figures 26A and E). These results are consistent with the ones in control 1 group where no antibody stain involved.

Stained cell clusters were treated with both primary and secondary antibody stains. The clusters were then washed on a rotary table. These cell clusters exposed to

the processing are “stressed” and differ from the naturally grown or cultured cells. Figure 27 shows cell clusters that were stained with antibodies. Cell clusters were incubated with a rabbit polyclonal antibody against human integrin β1 and then with TRITC-conjugated anti-rabbit immunoglobulin. As shown in the figure, cells with their cell wall partially removed show strong fluorescence along the membrane and nuclei (Figure 27A). Cells with membrane partially peeled from the cell wall show strong fluorescence along the separation position (Figure 27C). Protoplasts without cell wall show no fluorescent signal (Figure 27E), and damaged cells show strong fluorescence (Figures 27C and E).

Protoplasts are cells with cell wall completely removed thus connection between membrane and cell wall is destroyed. Protoplasts did not show fluorescence on both the control group and the antibody treated group. The membranes of cells with cell wall partially removed are exposed to culture medium; and cells having membrane partially separated from the cell wall and the damaged cells do not have intact cell structure. All these cells are stressed and show strong fluorescence in the antibody treated group. This suggests the integrin-like proteins in Norway spruce somatic cells locate mainly in the Hechtian stands (Domozych et al 2003), which is a complex anchoring structure linking the plasma membrane to the cell wall at specific sites.

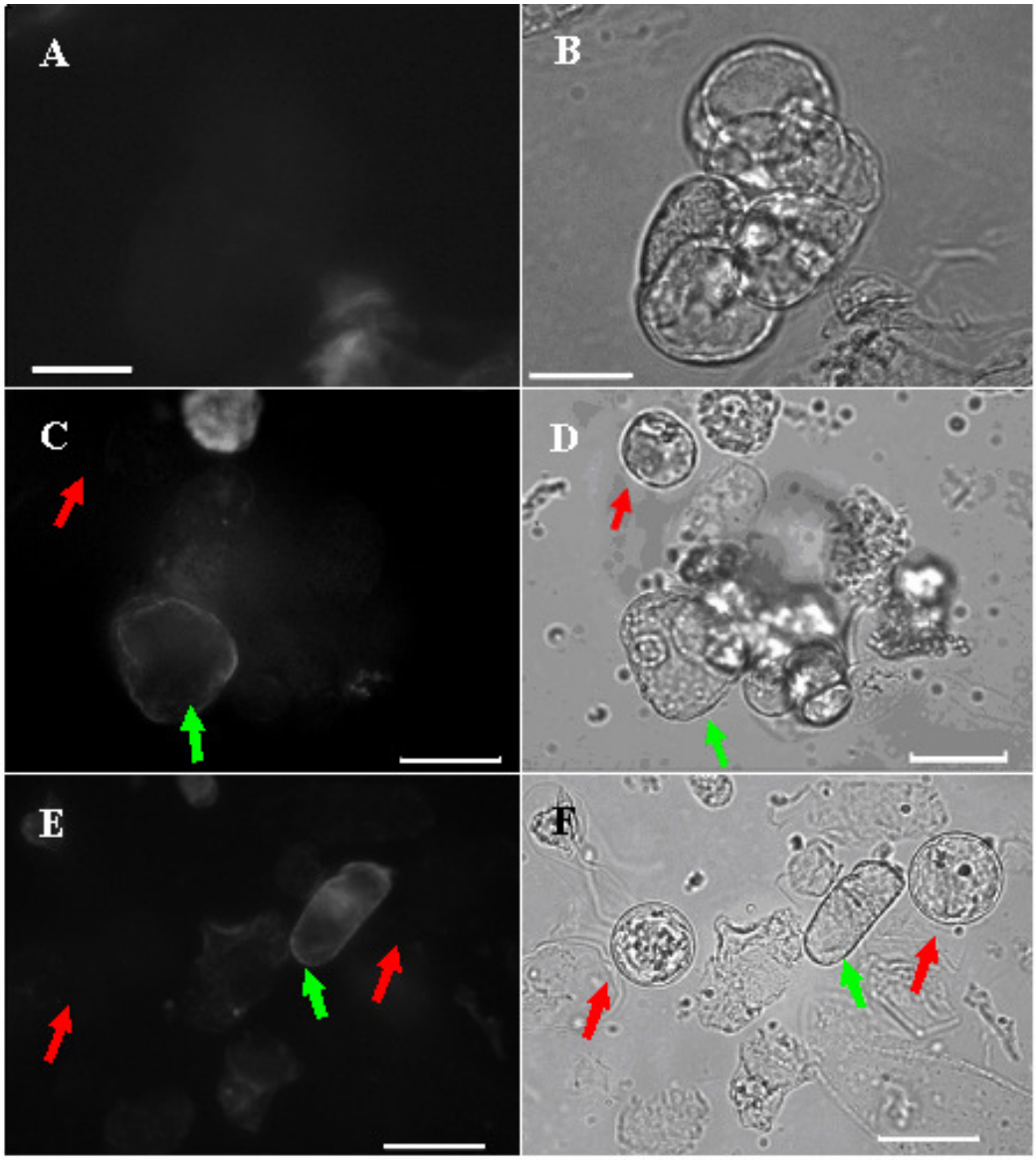

Figure 25. Immunofluorescence localization of integrin-like proteins in Norway spruce somatic cell clusters without antibody treatments as control 1. The clusters experienced enzyme treatment for 10 minutes to make plasma membrane exposed to culture medium at different level. The images on the left are fluorescent images, and the images on the right are the relative bright field ones. (A & B) Cells with cell wall intact show no fluorescent signal. (C & D) and (E & F) Protoplasts without cell wall show no fluorescent signal as indicating by red arrows pointing to right; damaged cells and cells with cell wall partially removed show dim fluorescent signal as indicating by green arrows pointing left. Scale bar = 50 µm.

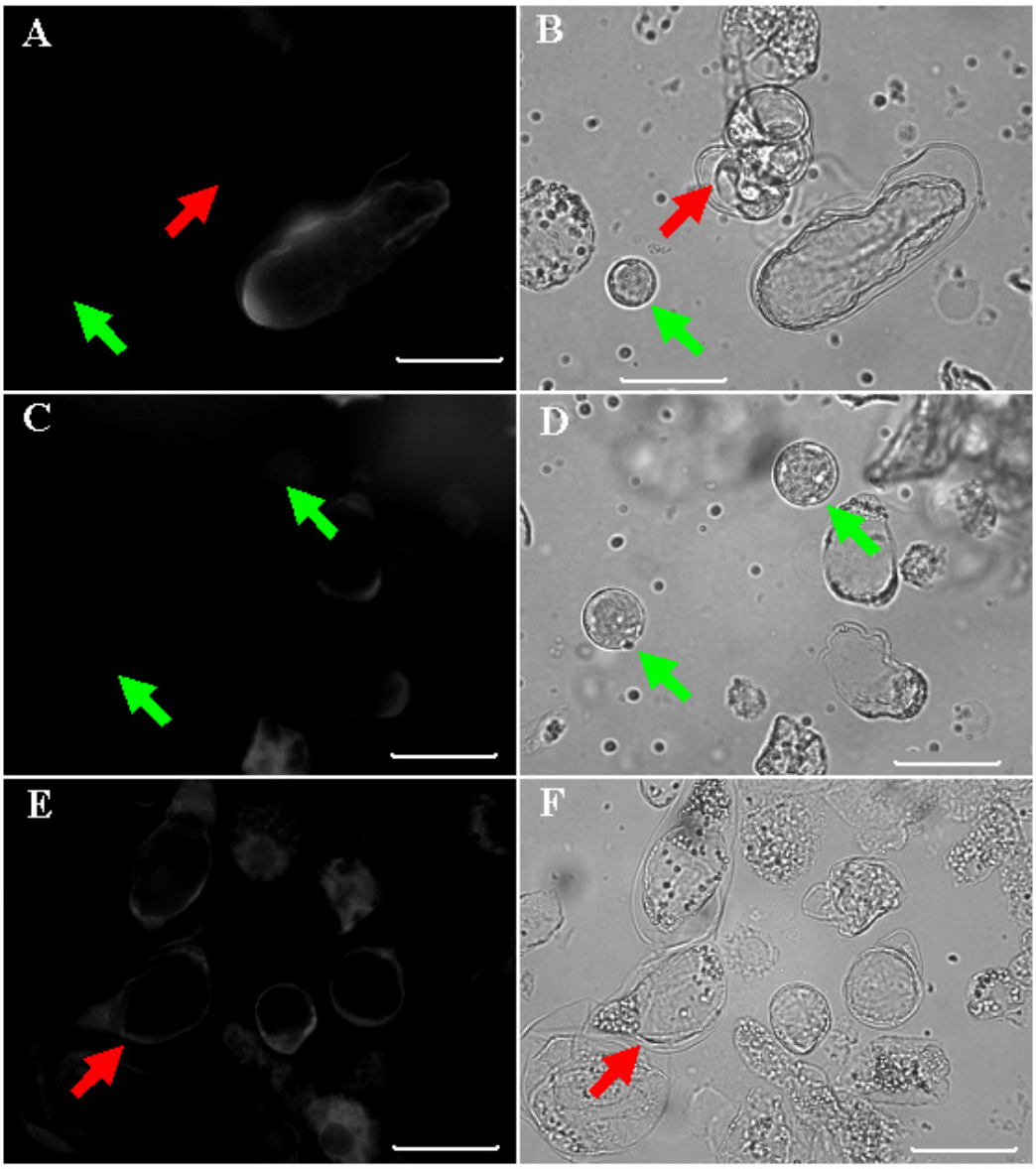

Figure 26. Immunofluorescence localization of integrin-like proteins in Norway spruce somatic cell clusters with only secondary antibody treatments as control 2. The clusters experienced enzyme treatment for 10 minutes to make plasma membrane exposed to culture medium at different level. After washing, cells were further stained with secondary antibody and incubated at 37 °C for 4 hours in dark. The images on the left are fluorescent images, and the images on the right are the relative bright field ones. (A & B) Cells with cell wall intact show no fluorescent signal as indicated by red arrows pointing to right. Green arrow pointing to left indicates a protoplast without cell wall showing no fluorescent signal. (C & D) Protoplasts without cell wall show no fluorescent signal as indicating by green arrows pointing to left. (E & F) Cells with plasma membrane partially peeled from cell wall show dim fluorescent signal as indicating by red arrows pointing to right. Scale bar = 50 μm.

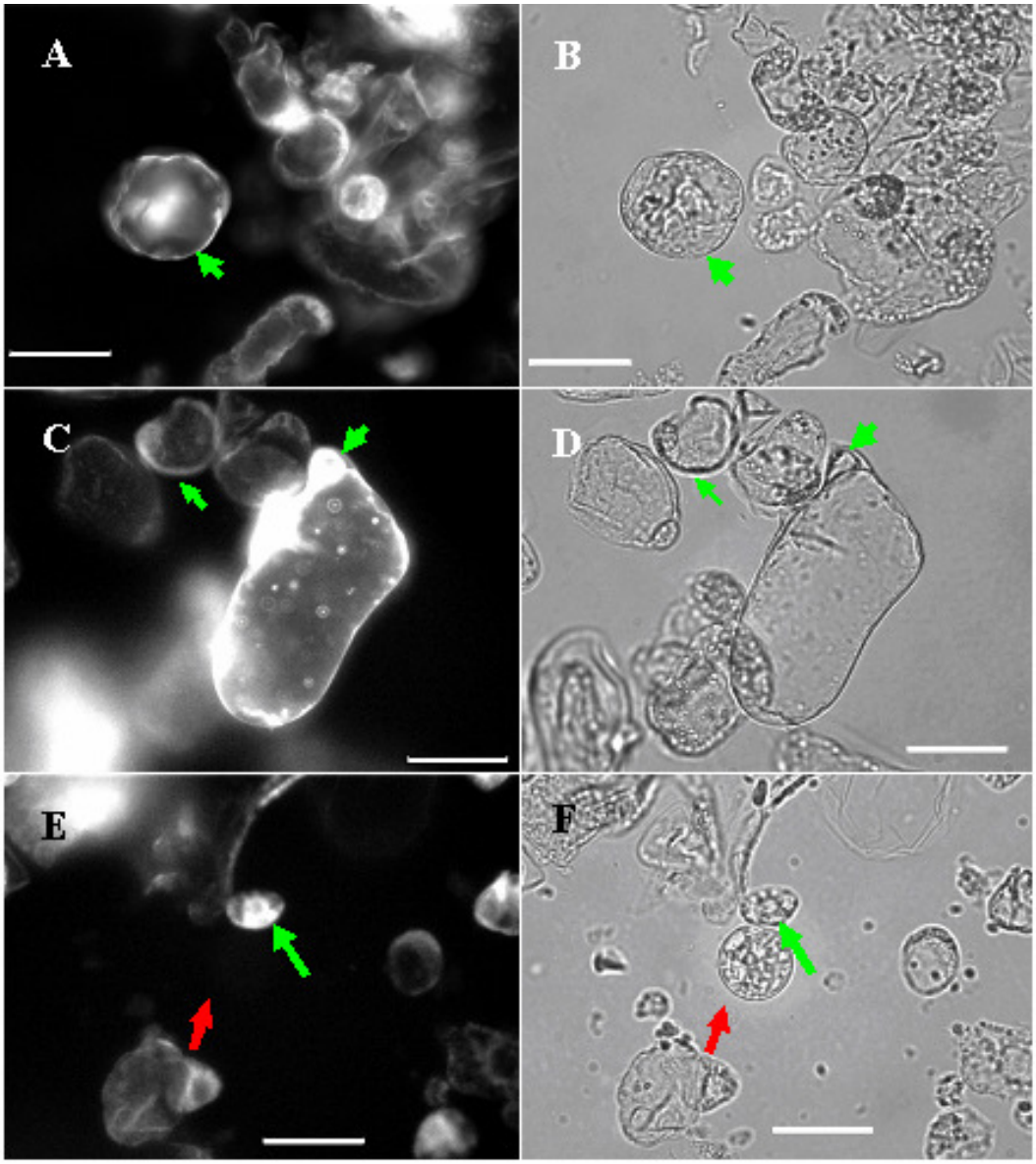

Figure 27. Immunofluorescence localization of integrin-like proteins in Norway spruce somatic cells. Cells are incubated with a rabbit polyclonal antibody against human integrin β1 for 17 hours and then with TRITC-conjugated anti-rabbit immunoglobulin for 4 hours at 37 °C in the dark. Images on the left are showing fluorescent signal and images on the right are the relative bright field images, corresponding to the left. (A-B) Cells with cell walls partially removed show strong fluorescence along the membrane and nuclei as indicating with green arrows pointing left. (C-D) Cell with plasmolysis shows strong fluorescence along the position where membrane separating from the cell wall, as indicating with green arrows pointing left. (E-F) Protoplasts without cell wall show no fluorescent signal as indicating by red arrows pointing to right, and damaged cells showing strong fluorescence as indicating by green arrows pointing left. Scale bar = 50 μm.

3.2.2 Reactive oxygen species detection

Another cellular level signaling molecule studied in this thesis is hydrogen peroxide, H_2O_2, which is one of the reactive oxygen species (ROS) along with superoxide ($O_2^{\bullet -}$) and hydroxyl radical (OH-). Several ROS are continuously produced in plants as byproducts of aerobic metabolism and some are highly toxic and rapidly detoxified by various cellular enzymatic and nonenzymatic mechanisms (Bartosz 2009; Kotchoni & Gachomo 2006; Pandhair & Sekhon 2006). In other circumstances plants appear to purposefully generate ROS as signaling molecules to control various processes including pathogen defense, programmed cell death, and stomatal behavior (Apel & Hirt 2004; Davies et al 2006; Kotchoni & Gachomo 2006). Production of ROS has also been studied as a parameter of shear stress effect on the plant cells (Gao et al 2007; Gens et al 1996; Swatzell et al 1999). In this section, the production of ROS in the stressed cells were tested using dihydrorhodamine 123 (DHR123).

Cells were observed under the microscope equipped with I3 filter cube which has a band-pass excitation filter of 450-490 nm and a long pass filter with a cut-off wavelength of 510 nm for the DHR123 fluorescence detection. Both fluorescent and bright field images were taken for each test group. Figure 28 shows the comparison of cell clusters before and after shear stress. Two kind of stressing methods are used to stress the cell clusters. One is pipetting cell clusters through 1000 μl pipette tube at a frequency of 60 repetitions per minute for two minutes. The stress is generated by the suction and discharge motion through the tube. Pipette handling is a normal procedure occurred during cell cluster culture and tests. Past study of human embryos has shown

stress effect of this procedure to the cells (Xie et al 2007). Another way is through vigorous shaking of cell clusters at a frequency of 180 rpm for two minutes, which is an extreme condition as liquid culture on a rotary table. Figure 28A indicates that there is only dim autofluorescence showing up on the already stressed cell clusters during suspension culture in the controlled group. The stressed cell clusters in suspension culture lose the shiny look of healthy cells and show dark color under microscope. As the counter part of the control, the vigorously stressed cell clusters by two different ways show strong fluorescent signals (Figure 28C and E). H_2O_2 is detected in most of the stressed cells by showing bright fluorescence contours which is the result from the stain of DHR123. Comparison of cells in Figure 28C and 28E shows that the more stressed the cells are, the stronger the fluorescence from ROS is as indicated by the arrows. The dim signal from the control suggests that the suspension cultured cell clusters are accustomed to the stress from the culture medium after suspension is well established, which generally takes weeks to months in Norway spruce somatic cell clusters.

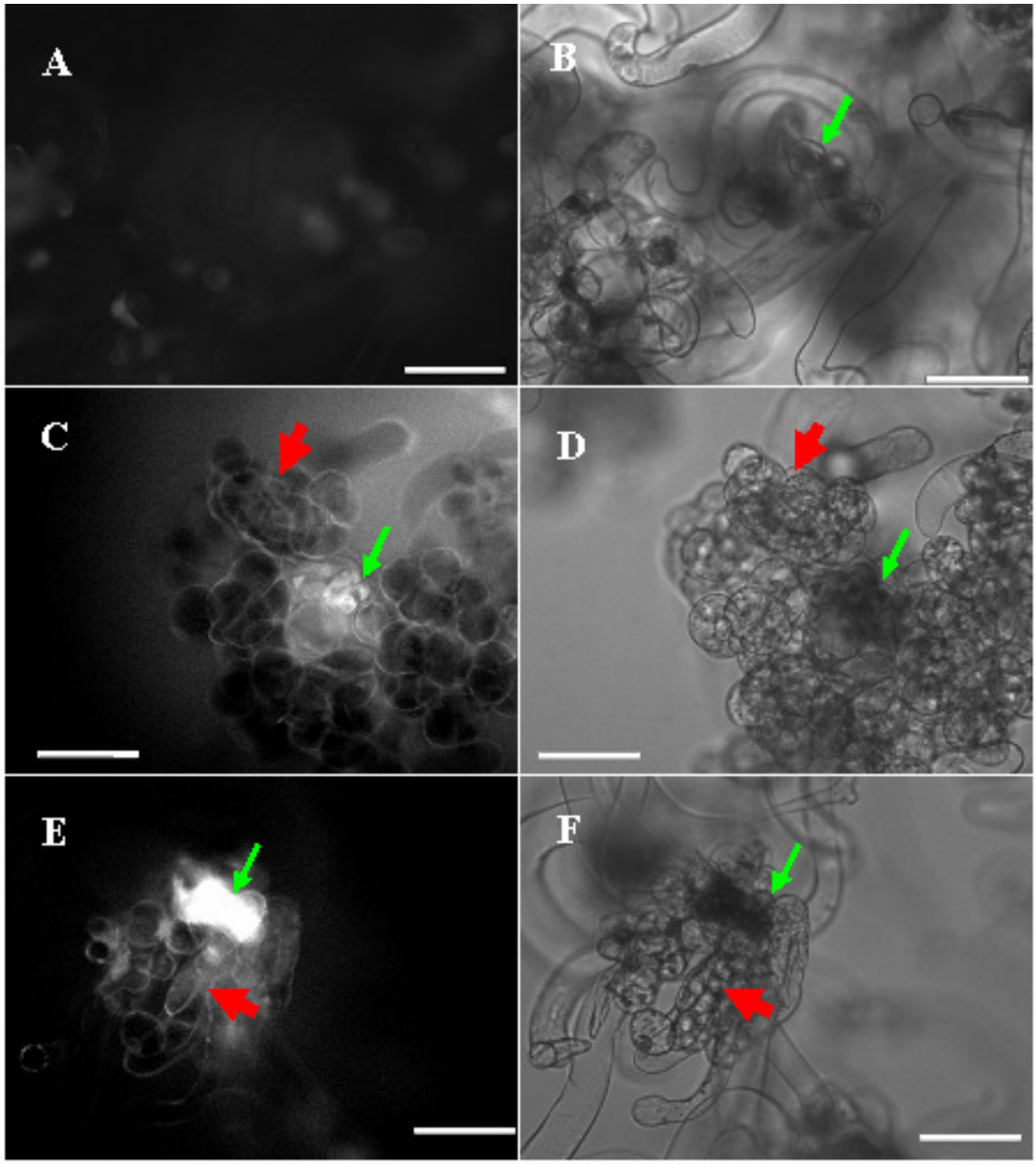

Figure 28. Reactive oxygen species detection in suspension cultured Norway spruce somatic cells (cell line #3). Cell clusters were stained with dihydrorhodamine 123. Images on the left are showing fluorescent signal. Images on the right are the corresponding bright field images, respectively. (A-B) Normal suspension cells as control showing dim autofluorescence. (C-D) Stressed cells by vigorously shaking (180 rpm) for 2 minutes showing strong fluorescence after stain especially the most stressed cells as indicated by narrow green arrows. Live stressed cells show bright contour as indicated by broad red arrows. (E-F) Stressed cells by pippeting vigoursly (60 repetitions per minute) for 2 minutes showing strong fluorescence after stain especially the most stressed cells as indicated by narrow green arrows. Live stressed cells show bright contour as indicated by broad red arrows. Scale bar = 50 µm.

3.2.3 Pore size of cell wall and response to macromolecule

Osmotic stress is an important factor during plant embryo development (von Aderkas & Bonga 2000). The osmotic pressure of loblolly pine (*Pinus taeda*) seeds changes as the zygotic embryo inside the ovule develops (Pullman & Johnson 2009). The high molecule weight molecules added to the culture medium of somatic embryos induce osmotic stress in the cells by depletion of intracellular water and stimulate the embryos to further develop to maturation. It has been argued that size exclusion at this level controls development (Jarvis 2009). Based on the phenomena of either plasmolysis or cytorrhysis, one can have the idea of the size of the pore in the cell wall compared with the solutes size.

The past pore size tests with solute exclusion technique are based on the plasmolysis and cytorrhysis responses of cells to macromolecules of known sizes. In this thesis, not only the cellular response of plasmolysis/cytorrhysis was observed, but also the uptake time of macromolecules in cells under different conditions was noted. By combining the cellular responses with the examination of the uptake time of different macromolecules in stressed cells and control cells, the effect of shear stress will be detected. The hypothesis of the pore size experiments here is that there is a difference in macromolecular uptake induced by shear stress.

Since it is unclear if other signal cascades may be activated during the solute-exclusion experiments, the observations were recorded by the timing of events which is when the plasmolysis or cytorrhysis occurs after continuously dripping one solution to the cell clusters. Two cell lines, 06:22:02 and 06:21:00, were tested for solute exclusion

experiments. The cell clusters were imaged with the microscope with a 15× magnification and representative example images of plasmolysis and cytorrhysis of Norway spruce somatic cell clusters are shown in Figure 29. Figure 29B shows the plasmolysis that occurs as the volume of the cell in control group decreases, water is lost from the cell (A) and plasma membrane is partially peeled from the cell wall, after continuously dripping 0.4M macromolecule mannitol solution for 10 minutes. In this case, the cell cluster still keeps its shape. Figure 29D shows the cytorrhysis that occurs as the volume of the cell cluster in the control decreases dramatically and cell walls collapse right after dripping 0.4M PEG 4000 (C).

The stresses experienced by the cell clusters in the Petri plate on the rotary shaker simulate the shear stress in a suspension culture flask. The stressed sample after 4 hours of liquid suspension culture show no significant difference to the control sample, for both 0.25M and 0.44 M solutions. However, stressed cell clusters sampled after 22 hours are obviously different from the control. The detail comparison of cell clusters under stress to the control in responses to different solutes is listed in Table 7, for two cell lines. The two concentrations of macromolecule solutions, 0.25 M and 0.44 M, are based on the previously published data for high osmotic solutions that are compatible with somatic embryos of Norway spruce (Clapham et al 2000; Egertsdotter & Von Arnold 1993). Responses tested with 0.25 M solutes are similar to the ones with 0.44M solutes but are generally slower. The longest response of cell clusters to 0.25M Mannitol is 45 minutes. Only responses to 0.44M solutes are listed below in Table 7.

The experiments with each solute for one testing material are carried out for total three times. For each experiment, there is at least one cell cluster recorded. The error

listed in Table 7 is the standard deviation from different observations. Response from cell clusters stressed for 22 hours is significantly faster than control cells in response to all the solutes in both cell lines; cytorrhysis occurs in the solutes of smaller molecules in stressed cells comparing with the control. For example, meristematic cells in cell clusters from cell line 06:22:02 show cytorrhysis with molecules of 2.9 nm (PEG600) after getting stressed and molecules of 3.8 nm (PEG1540) in the control; meristematic cells in cell clusters fromn cell line 06:21:00 show cytorrhysis with molecules of 3.5 nm (PEG1000) after getting stressed and molecules of 3.8 nm (PEG1540) in the control. Cell clusters from cell line 06:21:00 response generally slower than that of cell line 06:22:02. The above responses are for meristematic cells. The suspensor cells generally respond (around 2 to 5 seconds) faster than meristematic cells as showing plasmolysis or cytorrhysis which also proves that meristematic cells are more stress tolerant than suspensor cells as revealed in shear stress experiments. The difference of response time between meristematic cells and suspensor cells falls in the range of standard deviation from different observations.

These results show the pore size of meristematic cells of somatic embryos in Norway spruce to be between 2.2 to 3.5 nm and different cell lines may have slight variance. Stressed cells respond to marcomolecules significantly faster than that in control. Shear stress exposure does not induce a detectable change in pore size (Table 7).

Table 7. Response of Norway spruce somatic cells from two cell lines to various 0.44M solutes as showing plasmolysis and cytorrhysis. Stressed cells are stressed in liquid medium for 22 hours and the control cells are taken directly from clumps cultured on solid medium. The uptake of each macromolecule for one tested plant material is conducted three times. The standard deviation is listed after each mean response time. (D_m: molecular diameter; PL: plasmolysis; CR: cytorrhysis)

Solute	D_m [nm]	Cell line 06:22:02		Cell line 06:21:00	
		Time of response showing after solution dripping [minute & second]		Time of response showing after solution dripping [minute & second]	
		Control	Stressed	Control	Stressed
Mannitol	0.8	10'±2'11", PL	2'5"±23", PL	20'±1'5", PL	10'6"±50", PL
Sucrose	1.0	30'20"±2'31", PL	6'8"±49", PL	30'20"±1'30", PL	7'5"±52", PL
Stachyose	1.4	29'50"±1'15", PL	58"±5", PL	30'23"±2'26", PL	3'5"±12", PL
PEG 400	2.2	5'6"±55", PL with CR; 30'10"±1'43", PL	1'53"±21", PL with CR	5'2"±17", PL with CR; 30'15"±2'11", PL	2'3"±11", PL with CR
PEG 600	2.9	10'9"±1'16", PL	2'3"±8", CR	24'40"±1'31", PL	1'58"±13", PL; 10'21"±1'3", CR
PEG 1000	3.5	Instant, CR; 10'20"±1'40", PL	1'4"±15", CR	Instant, CR; 10'3"±53", PL	1'53"±21", CR
PEG 1540	3.8	Instant, CR	Instant, CR	Instant, CR	Instant, CR
PEG 4000	4.5	Instant, CR	Instant, CR	Instant, CR	Instant, CR
PEG 6000	5.2	Instant, CR	Instant, CR	Instant, CR	Instant, CR

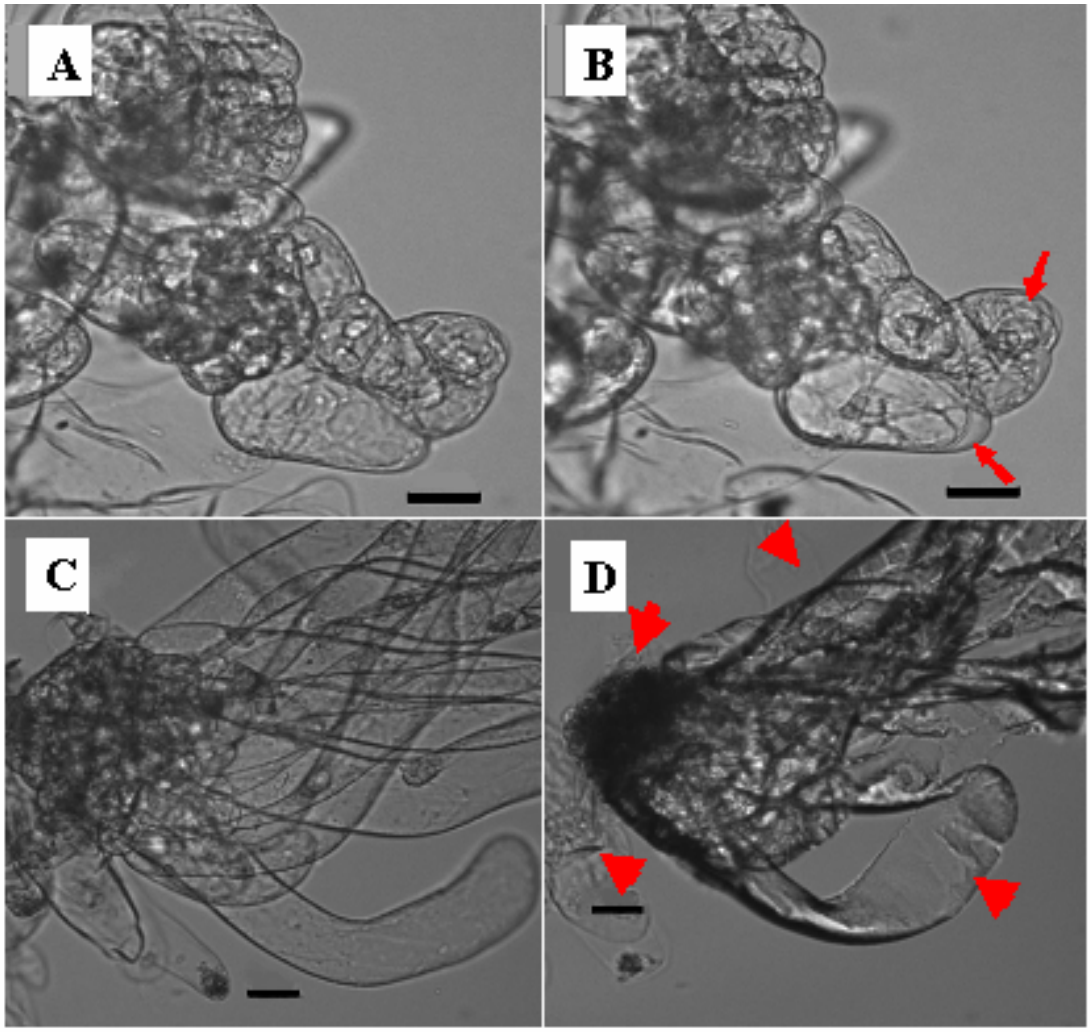

Figure 29. Representative examples of observation of plasmolysis and cytorrhysis of Norway spruce somatic cells in response to solutes of various molecular diameters. Images on the left show the clusters before dripping a solute; images on the right show the response of the cluster on left after dripping the solute. (A) Cells in control group before continuously dripping 0.4M Mannitol solution; (B) Cells show plasmolysis as labeled by arrows after dripping 0.4M Mannitol solution for 10 minutes. The narrow red arrows indicate the positions where plasmolysis happens. (C) Cell cluster in control group before continuously dripping 0.4M PEG 4000 solution; (D) Cell cluster show instant cytorrhysis after dripping PEG 4000. The broad red arrow heads indicate the positions where cytorrhsis happens. Scale bar = 50 μm.

3.3 Discussion

The inhibition on the growth of somatic embryos exposed to shear stresses suggests that shear stress negatively affects the development of somatic embryos under liquid culture conditions. Similar results have been observed on California poppy (*Eschscholzia californica*) using a helical ribbon impeller bioreactor (Archambault et al 1994). The experimental work done by Moorhouse et al. (1996) also reported that shear stress affects the development of gymnosperm somatic embryos for Sitka spruce (*Picea sitchensis*) using a Braun Biostat BF2 system which resulted in similar performance of the bioreactor culture to a suspension culture in Erlenmeyer flasks. The authors indicated that no mature embryos could be obtained, which suggests that the somatic embryos can not reach the developmental stage permissive to maturation stimuli.

Agitation in the culture flask/bioreactor causes shear flow around cell clusters. A rough estimation of shear rates inside of a shaking flask is carried out based on the rotation speed of shaker table (100 rpm), rotation radius (15 mm) and radius of culture Erlenmeyer flasks (45 mm). It is determined that the shear rate at the flask wall is in the range of 5 to 50 s^{-1}. The three tested lower shear rates, 9, 14 and 29 s^{-1}, fall right into this range. It should be noted, however, the cell clusters inside a shaking flask experience shear that is more random in nature than that in the current study wherein immobilized cells are exposed to constant and unidirectional shear flow. The randomness of shear experienced may make cells to lose their polarization when developing suspensor cells. The meristematic cells rarely form suspensor cells in liquid culture or form suspensor cells randomly around meristematic cells during proliferation stage (as shown in Figures 3B and 4B) (Egertsdotter & von Arnold 1998). The clusters under shear rates of 9, 14, 29

and 86 s^{-1} form suspensor cells in a unidirectional manner, with most of the suspensor formed along horizontal direction either parallel or against flow direction (as shown in Figure 20). The suspensor cells formed along horizontal direction, however, are significantly more than those formed along vertical direction. The clusters in the control group with cells randomly seeded on the film form suspensor cells also in a unidirectional manner, however, the direction suspensor cells formed is random and even distributed in all directions (as shown in Figure 19). Based on these comparisons, it suggests that the unidirectional flow or shear rate helps the unidirectional growth and alignment of suspensor cells.

The results are in agreement with the previous findings suggesting that plant cells are most sensitive to hydrodynamic shear stress in the range of shear rate from 30 to 300 s^{-1} (Sun & Linden 1999). No suspensor cells form at shear rate of 140 s^{-1} and suspensor cells form under lower shear rates of 86, 29, 14 and 9 s^{-1}. Meristematic cells, however, grow under all these shear rates with lower growth rates compared with stationary control. While at shear rate of 280 s^{-1}, cell clusters do not survive for more than 3 days. The meristematic cells in the cell clusters are more stress tolerant than the suspensor cells since meristematic cells grow and develop under the five shear rates, 9, 14, 29, 86 and 140 s^{-1} while suspensor cells only develop under shear rate of 86 s^{-1} and lower. It is also known that meristematic cells are more tolerant than other cell types to other type of stresses, such as cold stress during cryopreservation (Wang et al 2009). The suspensor cells associated with somatic embryos resembles undifferentiated cells in cell cultures, notably by a large vacuole and less cytoplasm, rendering the cells less density.

Past studies show that drastic changes in the cellular environment like nutrient and hormone supply (as *in vitro* culture conditions) can generate significant stress effects (Costa & Shaw 2006; Pullman & Johnson 2009). The response to stress conditions depends on the level of the stress and the physiology state of the cells. While lower level of stress enhances metabolism and induce adaptation mechanisms (Lichtenthaler 1998), if the stress level exceeds cellular tolerance, the cells die. For example, the highest shear rate of 280 s^{-1} was tested in this thesis in the same flow cell followed the same procedure, the cell clusters only survived two to three days under this condition. Shear rate of 280 s^{-1} exceeds the stress tolerance of somatic cell clusters of Norway spruce. The adaptations of cells exposed to lower level of stresses include the reprogramming of gene expression, as well as changes in the physiology and metabolism of the cells (Roitsch 1999; Takeda et al. 1998; Zhong et al. 1994). Recently, more and more researches are focused on the cellular and molecular responses of plant cells to shear stress. To elucidate the mechanisms that regulate shear stress response in cellular and molecular level, complementing experimental approaches are required.

Integrin-like proteins carry and transfer signals (e.g., stress induced by osmotic pressure) between cell walls and the intercellular structures. Therefore integrins connect the extracellular matrix (ECM) to the plasma membrane and/or cytoskeleton as suggested by other researchers (Lü et al. 2007; Swatzell et al. 1999; Wang et al. 1993). When cell wall is completely removed, the connections between cell wall and plasma membrane are destroyed and integrin-like proteins are lost which results in no fluorescence on protoplasts. In this thesis, the immunofluorescent experimental results suggest that the integrin-like proteins mainly locate on the Hechtian stands which link the plasma

membrane and the cell wall at specific sites. Lynch and coworkers suggested that a β1-integrin-like protein was present in amyloplasts of *Nicotiana* root cells (in both tissue culture cells and whole root), but not on the plasma membrane (Lynch et al 1998). However in *Arabidopsis* cells, β1-integrin-like proteins were found on the plasma membrane fractions (Canut et al 1998; Swatzell et al 1999). These findings suggest that integrin-like proteins may function differently in different species.

Another cellular level signaling molecule studied in this thesis is hydrogen peroxide, H_2O_2, which is one of the reactive oxygen species (ROS) along with superoxide ($O_2^{\bullet -}$) and hydroxyl radical (OH-). Past studies show that ROS as a natural byproduct of the normal metabolism of oxygen has important roles in cell signaling. Studies with Arabidopsis (Arabidopsis thaliana) and rice (Oryza sativa) have shown that ROS are associated with aging, cellular and molecular alteration in animal and plant cells, and are essential to induce disease resistance and mediate resistance to multiple stresses in plant (for a review, Kotchoni & Gachomo 2006). Production of ROS has been studied as a parameter of shear stress effect on the plant cells (Gao et al. 2007; Gens et al. 1996; Swatzell et al. 1999).

Since the pose size in plant cell wall affects the transportation of marcomolecules, in order to find if pore size is affected by shear stress, size exclusion experiments are conducted. The experiment results show that the pore size of Norway spruce meristematic cells in somatic embryos is between 2.2 to 3.5 nm. The meristematic cells respond to shear stress by a faster response to plasmolyzing compounds in the culture medium. There are no measurable effects on the pore size of the cells exposed to shear

stress. The high molecule weight molecules added to the culture medium of somatic embryos induce osmotic stress in the cells by depletion of intracellular water. The fast response of stressed cells to the plasmolyzing compounds indicates that shear stress may affect the maturation response of somatic embryos in liquid culture medium. Shear stress expedites the response of cells to the plasmolyzing agents added as a desiccation treatment. The treatment is used to induce the maturation, thus the conversion of PEMs into mature somatic embryos.

Cell-wall pore size can determine the movement of many large molecules such as proteins, nucleic acids, and toxins across the cell walls. Past studies show that when a foreign organism trying to invade plant cells, the limited pore size of the cell wall restricts access for enzymes produced by pathogens which tend to degrade the cell wall (Deising et al. 2000; Hardham 2001; Jones et al. 1972). Study on wheat cell walls suggests that the predominated pore size of 3 to 6 nm in diameter is bellow the size limit that allows free penetration of the wall by degrading enzymes (Chesson et al 1997).

Several researches found pH changes in culture media connecting to signal cascade mechanisms and coupling to developmental phenomena (Felle 1989). For example, pH increase inside of echinoderm eggs, slime molds and mammalian cells acts as a cell division signal (Oberdorf et al 1989); cytosolic pH alkalinization was found in guard cells as a measure of abscisic acid (ABA) regulation (Pei & Kuchitsu 2005); and mechanical stimulation of plants cells triggers an apoplastic alkalinization and cytoplasmic acidification as well as apoplastic reactive oxygen species (ROS) production (Monshausen et al 2009). Monshausen et al. (2009) also suggested that the transient changes in pH and extracellular ROS are signals involved in modulating cell wall

characteristics to counteract mechanical stress. Further studies of acid and pH value in the digestion of plant leaves by animals and algae by marine fish have shown impact on the pore size of plant cell walls (Ramirez et al. 2000; Zemke-White et al. 2000). At low pH value, acid helps increase the pore size and digestive enzymes are allowed to enter the cells. Cold acclimation of suspension cultured cells of grapes (*Vitis spp*.) and apple (*Malus domestica*) also showed that there is a decrease of the limiting cell wall pore size from 3.5 to 2.2 nm in grape cells and from 2.9 to 2.2 nm in apple cells (Rajashekar & Lafta 1996).

It is well-known that the continuous proliferation of embryogentic culture needs auxin and cytokinin (Dong & Dunstan 1994) and the further development and maturation of individual somatic embryos requires abscisic acid (ABA) that is a plant hormone involved in many plant developmental processes (Dunstan et al 1998), there is little knowledge about the molecular mechanisms by which plant embryos activate specific gene sets shortly after fertilization (Kawashima et al 2009). For angiosperm embryos, G564 was found in scarlet runner bean (Weterings et al 2001) and further used to identify the *cis*-regulatory sequences in the suspensor transcription in tobacco embryo (Kawashima et al 2009). There are increasing evidence showing that two particular modes of signaling via auxin and cell wall components play important roles in plant cell polarity in *Arabidopsis* cells (Souter & Lindsey 2000). The complexity of signal transduction and the cross talk between signals make the identification of mechanism more difficult. It is uncertain if all the signal pathways are conserved between gymnosperm and angiosperm species, which warranties further study.

CHAPTER 4

CONCLUSIONS AND CONTRIBUTIONS

Norway spruce somatic cell clusters at proliferation stage are exposed to shear stresses of 0.009, 0.014, 0.029, 0.086 and 0.140 N/m^2 (with respect to shear rates of 9, 14, 29, 86, 140 s^{-1}). The development of meristematic cell clusters is evaluated by radial growth and suspensor cell formation with image analysis based on normalized cross-correlation method. The results are checked with statistical significance t-test with confidence level of 95 and/or 99%. To the author's knowledge, this is the first study that monitors the shear stress effects on somatic embryo development by following the development of individual embryos in a flow cell. In conclusion, this study shows that

(a) the growth of meristematic cell clusters (PEMs) are negatively affected by shear stresses. The mean growth rates of meristematic cell clusters under different shear stresses are significantly slower than that under stationary control based on t-test with confidence level of 99%;

(b) there is no significant correlation between the radial growth direction of meristematic cell clusters and the direction of flow; there might be a preference in growth of meristematic cell clusters in the flow direction (i.e., $\theta = 0$) at shear rate of 140 s^{-1} based on the statistical analysis showing 95% confidence for maximum growth in this direction for all three experimental repetitions;

(c) there is a critical shear stress above which no suspensor cells are developed in somatic embryo cell clusters of Norway spruce, and present experiments showed that this critical shear stress is between 0.086 and 0.14 N/m^2 (with respect to shear rates of 86 and 140 s^{-1}, respectively);

(d) meristematic cells in the cell clusters are more stress tolerant than the suspensor cells. Meristematic cells grow and develop under all the tested conditions and suspensor cells are only formed at lower shear stresses;

(e) the unidirectional flow or shear rate helps the unidirectional growth and alignment of suspensor cells. The suspensor cells that formed on cell clusters under shear rates of 9, 14, 29 and 86 s^{-1} are unidirectional and in polarized structure, and are significantly more along horizontal directions than that along vertical direction, based on t-test with confidence level of 99% ;

(f) cellular responses of reactive oxygen species (ROS) are detected in the stressed Norway spruce somatic cell clusters. The immunofluorescent experiments tested the formation of H_2O_2 in the stressed cell clusters. The high intensity of H_2O_2 fluorescent signals show that ROS are generated as cell clusters are exposed to shear stresses.

(g) integrin-like proteins are detected in stressed Norway spruce somatic cells; possible locations of integrin-like proteins in somatic cells of Norway spruce are the Hechtian strands which connect the plasma membrane and the cell wall at some specific sites;

(h) pore size on the cell walls of meristematic cells of Norway spruce somatic cell clusters is around 2.2 to 3.5 nm. Suspensor cells' uptake of macromolecules is faster than meristematic cells. This also supports the conclusion of meristematic cells are more stress tolerant than suspensor cells. The stressed cell clusters have a significantly faster response to macromolecules compared to cell clusters in the control although no detectable pore size changes after cell clusters exposed to shear stress;

(i) the immobilization method developed in this thesis provides a platform to have cell clusters affixed on the top of alginate film and exposed to defined shear stresses. This makes the study of shear stress effect on the cell cluster development possible;

(j) the image analysis method based on normalized cross-correlation in the present study provides a direct and quantitative evaluation of cell cluster growth and allows for detailed analysis of cellular response to applied stresses. The accuracy of correlation among images of different time periods of one cell cluster is within one pixel.

The studies reported in this thesis contribute to the knowledge of how shear stress introduced by liquid medium affects the growth and development of Norway spruce immature somatic embryos in liquid culture, establish the correlation between shear stresses and somatic embryo development.

CHAPTER 5

FUTURE DIRECTIONS

There are several suggestions for the future study and continuous work after the conclusions in chapter 4. A long-term goal of this study is to identify the specific marker genes that are triggered by shear stress. Identification of gene markers that are activated when plant cells are exposed to shear stress will shed light on a better understanding of the mechanism of plant cells response to shear stress through the signal transduction pathway.

Further test of the capability of immature somatic embryo developing into maturation under different shear stresses will be appreciated in terms of design of new culture protocol and bioreactors. The critical shear stress between 0.086 and 0.14 N/m^2 is a threshold for suspensor cells to develop on meristematic cell clusters. In practical, how to design a bioreactor that provides shear stress lower than this critical value will be of great interest in order to apply the gained knowledge from this study.

The uptake into animal cells (for example, proteins like low density lipoprotein, transferring and insulin) is well characterized for a number of different animal cell systems (see reviews by Goldstein et al 1985; Sythe & Warren 1991). In contrast, uptake in plants is not well understood (Brownlee 2002; Coleman et al 1988; Deising et al 2000; Foyer et al 1994; see reviews by Low & Chandra 1994; Lynch et al 1998; Malinowski & Filipecki 2002; Schwartz et al 1995). One major difficulty in studying uptake into plant cells is the existence of the plant cell wall, which limits the types of marker molecules

that can be used to probe the plasma membrane. Furthermore, specific plant ligands have been difficult to identify thus precluding detailed studies of receptors and their role in the process. Protoplasts that lack a cell wall can, however, be labeled with a variety of electron dense probes such as cationized ferritin and colloidal gold, which normally do not penetrate the intact cell wall or do so only very slowly (Fowke et al 1995).

REFERENCES

Adrian RJ. 1991. Particle-imaging techniques for experimental fluid-mechanics. *Ann Rev Fluid Mech* 23:261-304

Adrian RJ. 2004. Twenty years of particle image velocimetry. *12th International Symposium on Applications of Laser Techniques to Fluid Mechanics, Lisbon, July 12-15, 2004*

Allen RD. 1995. Dissection of oxidative stress tolerance using transgenic plants. *Plant Physiology* 107:1049-1054

Amiji MM, Sandmann BJ. 2003. *Applied physical pharmacy*. New York: McGraw-Hill

Ang-Lee MK, Moss J, Yuan CS. 2001. Herbal medicines and perioperative care. *Jama-Journal of the American Medical Association* 286:208-216

Aoyagi H, Sakamoto Y, Asada M, Tanaka H. 1998. Indole alkaloids production by Catharanthus roseus protoplasts with artificial cell walls containing of guluronic acid rich alginate gel. *Journal of Fermentation and Bioengineering* 85:306-311

Aoyagi H, Yokoi H, Tanaka H. 1992. Measurement of fresh and dry densitites of suspended plant cells and estimation of their water content. *Journal of Fermentation and Bioengineering* 73:490-496

Apel K, Hirt H. 2004. Reactive oxygen species: Metabolism, oxidative stress, and signal transduction. *Annual Review of Plant Biology* 55:373-399

Archambault J, Williams RD, Lavoie L, Pepin MF, Chavarie C. 1994. Production of somatic embryos in a helical ribbon impeller bioreactor. *Biotechnology and Bioengineering* 44:930-943

Attele AS, Wu JA, Yuan CS. 1999. Ginseng pharmacology - Multiple constituents and multiple actions. *Biochemical Pharmacology* 58:1685-1693

Barry-Etienne D, Bertrand B, Vasquez N, Etienne H. 2002. Comparison of Somatic Embryogenesis-derived Coffee (Coffea arabica L.) Plantlets Regenerated in vitro or ex vitro: Morphological, Mineral and Water Characteristics. *Ann Bot* 90:77-85

Bartosz G. 2009. Reactive oxygen species: Destroyers or messengers? *Biochemical Pharmacology* 77:1303-1315

Birnbaum S, Mosbach K. 1991. Perspectives on immobilized proteins. *Current Opinion in Biotechnology* 2:44-51

Bozhkov PV, Filonova LH, von Arnold S. 2002. A key developmental switch during Norway spruce somatic embryogenesis is induced by withdrawal of growth regulators and is associated with cell death and extracellular acidification. *Biotechnology and Bioengineering* 77:658-667

Bringezu S, Schutz H, O'Brien M, Kauppi L, Howarth RW, McNeely J. 2009. Towards sustainable production and use of resources: assessing biofules. United Nations Environment Programme. Online: http://www.unep.fr/scp/rpanel/pdf/Assessing_Biofuels_Full_Report.pdf

Brodelius P, Rosevear A. 1985. Plant-cell culture - keeping control. *Trends in Biotechnology* 3:195

Brownlee C. 2002. Role of the extracellular matrix in cell-cell signalling: paracrine paradigms. *Current Opinion in Plant Biology* 5:396-401

Canut H, Carrasco A, Galaud JP, Cassan C, Bouyssou H, et al. 1998. High affinity RGD-binding sites at the plasma membrane of Arabidopsis thaliana links the cell wall. *Plant Journal* 16:63-71

Carpita N, Sabularse D, Montezinos D, Delmer DP. 1979. Determination of the pore-size of cell-walls of living plant cells. *Science* 205:1144-1147

Cazzulino D, Pedersen H, Chin CK, Venkat K, Styer C. 1987. Characterization of plant somatic embryo development using Fourier shape analysis. *Annals of the New York Academy of Sciences* 506:190-195

Cervantes MIS, Lacombe J, Muzzio FJ, Alvarez MM. 2006. Novel bioreactor design for the culture of suspended mammalian cells. Part 1: Mixing characterization. *Chemical Engineering Science* 61:8075-8084

Che P, Love T, Frame B, Wang K, Carriquiry A, Howell S. 2006. Gene Expression Patterns During Somatic Embryo Development and Germination in Maize Hi II Callus Cultures. *Plant Molecular Biology* 62:1-14

Chen SY, Huang SY. 2000. Shear stress effects on cell growth and L-DOPA production by suspension culture of Stizolobium hassjoo cells in an agitated bioreactor. *Bioprocess Engineering* 22:5-12

Cheng JS, Yuan YJ. 2009. Release of proteins: Insights into oxidative response of Taxus cuspidata cells induced by shear stress. *Journal of Molecular Catalysis B-Enzymatic* 58:84-92

Cheng M, Wu J, Li Y, Nie YM, Chen HQ. 2008. Activation of MAPK participates in low shear stress-induced IL-8 gene expression in endothelial cells. *Clinical Biomechanics* 23:S96-S103

Chesson A, Gardner PT, Wood TJ. 1997. Cell wall porosity and available surface area of wheat straw and wheat grain fractions. *Journal of the Science of Food and Agriculture* 75:289-295

Chi CM, Zhang C, Staba EJ, Cooke TJ. 1996. An advanced image analysis system for evaluation of somatic embryo development *Biotechnology and Bioengineering* 50:65-72

Chi CM, Vits H, Staba EJ, Cooke TJ, Hu WS. 1994. Morphological kinetics and distribution in somatic embryo cultures. *Biotechnology and Bioengineering* 44:368-378

Clapham D, Elfstrand M, Sabala I, Von Arnold S, Demel P, Koop H-U. 2000. Gene Transfer by Particle Bombardment to Embryogenic Cultures of Picea abies and the Production of Transgenic Plantlets. *Scandinavian Journal of Forest Research* 15:151-160

Coleman J, Evans D, Hawes C. 1988. Plant coated vesicles. *Plant, Cell and Environment* 11:669-684

Costa S, Shaw P. 2006. Chromatin organization and cell fate switch respond to positional information in Arabidopsis. *Nature* 439:493-496

Cunningham KS, Gotlieb AI. 2005. The role of shear stress in the pathogenesis of atherosclerosis. *Laboratory Investigation* 85:9-23

Curtin ME. 1983. Harvesting profitable products from plant-tissue culture. *Bio-Technology* 1:649-659

Curtis WR, Wang P, Humphrey A. 1995. Role of calcium and differentiation in enhanced sesquiterpene elicitation from calcium alginate-immobilized plant tissue. *Enzyme and Microbial Technology* 17:554-557

Dat J, Vandenabeele S, Vranova E, Van Montagu M, Inze D, Van Breusegem F. 2000. Dual action of the active oxygen species during plant stress responses. *Cellular and Molecular Life Sciences* 57:779-795

Davenport RJ, Curtis TP, Goodfellow M, Stainsby FM, Bingley M. 2000. Quantitative use of fluorescent in situ hybridization to examine relationships between mycolic acid-containing actinomycetes and foaming in activated sludge plants. *Applied and Environmental Microbiology* 66:1158-1166

Davies DR, Bindschedler LV, Strickland TS, Bolwell GP. 2006. Production of reactive oxygen species in Arabidopsis thaliana cell suspension cultures in response to an elicitor from Fusarium oxysporum: implications for basal resistance. *Journal of Experimental Botany* 57:1817-1827

Debnath SC. 2007. A two-step procedure for in vitro multiplication of cloudberry (Rubus chamaemorus L.) shoots using bioreactor. *Plant Cell Tissue and Organ Culture* 88:185-191

Debnath SC. 2009. Characteristics of strawberry plants propagated by *in vitro* bioreactor culture and *ex vitro* propagation method. *Engineering in Life Sciences* 9:239-246

Deising HB, Werner S, Wernitz M. 2000. The role of fungal appressoria in plant infection. *Microbes and Infection* 2:1631-1641

Domozych DS, Roberts R, Danyow C, Flitter R, Smith B, Providence K. 2003. Plasmolysis, hechtian strand formation, and localized membrane-wall adhesions

in the desmid, Closterium acerosum (Chlorophyta). *Journal of Phycology* 39:1194-1206

Dong JZ, Dunstan DI. 1994. Growth parameters, protein and DNA synthesis of an embryogenic suspension culture of white spruce (*Picea glauca*). *Journal of Plant Physiology* 144:201-208

Dunlop EH, Namdev PK, Rosenberg MZ. 1994. Effect of fluid shear forces on plant cell suspensions. *Chemical Engineering Science* 49:2263-2276

Dunstan DI, Dong JZ, Carrier DJ, Abrams SR. 1998. Events following ABA treatment of spruce somatic embryos. *In Vitro Cellular & Developmental Biology-Plant* 34:159-168

Eeva M, Ojala T, Tammela P, Galambosi B, Vuorela H, et al. 2003. Propagation of Angelica archangelica plants in an air-sparged bioreactor from a novel embryogenic cell line, and their production of coumarins. *Biologia Plantarum* 46:343-347

Egertsdotter E-MU. 1996. *Regulation of embryo development in Norway spruce (Picea abies)*. Dissertation. Swedish University. Research Notes 52. Dissertation. ISBN 91-576- 5124-8; ISSN 0348- 565X, Uppsala, Sweden

Egertsdotter U. 1999. Somatic Embryogenesis in Picea Suspension Cultures. In *Methods in Molecular Biology*, ed. RD Hall, pp. 51-60. Totowa, NJ: Humana Press

Egertsdotter U, Mo LH, von Arnold S. 1993. Extracellular proteins in embryogenic suspension cultures of Norway spruce (*Picea abies*). *Physiologia Plantarum* 88:315-321

Egertsdotter U, von Arnold S. 1992. Classification of embryogenic cell lines of Picea abies as regards protoplast isolation and culture. *Journal of Plant Physiology* 141:222-229

Egertsdotter U, von Arnold S. 1995. Importance of arabinogalactan proteins for the development of somatic embryos of Norway spruce (Picea abies). *Physiologia Plantarum* 93:334-345

Egertsdotter U, von Arnold S. 1998. Development of somatic embryos in Norway spruce. *J. Exp. Bot.* 49:155-162

Ewing RM, Ben Kahla A, Poirot O, Lopez F, Audic S, Claverie JM. 1999. Large-scale statistical analyses of rice ESTs reveal correlated patterns of gene expression. *Genome Research* 9:950-959

Felle H. 1989. pH as a second messenger in plants. In *Second messengers in plant growth and development*, ed. WF Boss, DJ Moore, pp. 145-166. New York: AR Liss Inc.

Filonova LH, Bozhkov PV, von Arnold S. 2000. Developmental pathway of somatic embryogenesis in Picea abies as revealed by time-lapse tracking. *Journal of Experimental Botany* 51:249-264

Fisher AB, Chien S, Barakat AI, Nerem RM. 2001. Endothelial cellular response to altered shear stress. *American Journal of Physiology-Lung Cellular and Molecular Physiology* 281:L529-L533

Fleischer A, Titel C, Ehwald R. 1998. The boron requirement and cell wall properties of growing and stationary suspension-cultured Chenopodium album L. cells. *Plant Physiology* 117:1401-1410

Foreman J, Demidchik V, Bothwell JHF, Mylona P, Miedema H, et al. 2003. Reactive oxygen species produced by NADPH oxidase regulate plant cell growth. *Nature* 422:442-446

Fowke LC, Attree SM, Binarova P, Galway ME, Wang H. 1995. Conifer somatic embryogenesis for studies of plant cell biology. *In Vitro Cellular & Developmental Biology-Plant* 31:1-7

Foyer CH, Descourvieres P, Kunert KJ. 1994. Protection against oxygen radicals: An important defense mechanism studied in transgenic plants. *Plant Cell and Environment* 17:507-523

Fugh-Berman A. 2000. Herb-drug interactions. *Lancet* 355:134-138

Fujii N, Yamashita Y, Arima Y, Nagashima M, Nakano H. 1992. Induction of topoisomerase II mediated DNA cleavage by the plant naphthoquinones plumbagin and shikonin. *Antimicrobial Agents and Chemotherapy* 36:2589-2594

Gao H, Gong YW, Yuan YJ. 2007. RGD-dependent mechanotransduction of suspension cultured Taxus cell in response to shear stress. *Biotechnology Progress* 23:673-679

Gens JS, Reuzeau C, Doolittle KW, McNally JG, Pickard BG. 1996. Covisualization by computational optical-sectioning microscopy of integrin and associated proteins at the cell membrane of living onion protoplasts. *Protoplasma* 194:215-230

Gloe T, Sohn HY, Meininger GA, Pohl U. 2002. Shear stress-induced release of basic fibroblast growth factor from endothelial cells is mediated by matrix interaction via integrin alpha(V)beta(3). *Journal of Biological Chemistry* 277:23453-23458

Golds TJ, Babczinsky J, Rauscher G, Koop HU. 1992. Computer-controlled tracking of single cell development in Nicotiana tabacum L and Hordeum vulgare L protoplasts embedded in agarose alginate films. *Journal of Plant Physiology* 140:582-587

Goldstein J, Brown M, Anderson R, Russell D, Schneider W. 1985. Receptor-mediated endocytosis: concepts emerging from the LDL receptor system. *Ann Rev Cell Biol.* 1:1-39

Gontier E, Sangwan BS, Barbotin JN. 1994. Effects of calcium, alginate, and calcium-alginate immobilization on growth and tropane alkaloid levels of a stable suspension cell line of Datura inoxia Mill. *Plant. Cell. Rep* 13:533-536

Gorbatenko O, Hakman I. 2001. Desiccation-tolerant somatic embryos of norway spruce (Picea abies) can be produced in liquid cultures and regenerated into plantlets. *International Journal of Plant Sciences* 162:1211-1218

Gupta PK, Timmis R. 2005. Mass propagation of conifer trees in liquid cultures-progress towards commercialization. *Plant Cell Tissue and Organ Culture* 81:339-346

Hakman I, von Arnold S. 1985. Plantlet regeneration through somatic embryogenesis in Picea abies (Norway spruce). *Journal of Plant Physiology* 121:149-158

Hall JL, Flowers TJ, Robert RM. 1981. *Plant-Cell Structure and Metabolism*. Longman, London

Han RB, Yuan YJ. 2004. Oxidative burst in suspension culture of Taxus cuspidata induced by a laminar shear stress in short-term. *Biotechnology Progress* 20:507-513

Harry IS, Thorpe TA, eds. 1999. *Clonal Propagation of Woody Species*, Vols. 111: Plant Cell Culture Protocols. Totowa, NJ: Humana Press. 149-57 pp.

Hematy K, Sado PE, Van Tuinen A, Rochange S, Desnos T, et al. 2007. A receptor-like kinase mediates the response of Arabidopsis cells to the inhibition of cellulose synthesis. *Current Biology* 17:922-931

Herbst RS, Giaccone G, Schiller JH, Natale RB, Miller V. 2004. Gefitinib in combination with paclitaxel and carboplatin in advanced non-small-cell lung cancer: A phase III trial - INTACT 2. *Journal of Clinical Oncology* 22:785-794

Högberg K-A. 2003. *Possibilities and limitations of vegetative propagation in breeding and mass propagation of Norway spruce*. Thesis. Acta Universitatis agriculturae Sueciae, Silvestria

Holden MA, Hall RD, Lindsey K, Yeoman MM. 1987. Capsaicin biosynthesis in cell cultures of Capsicum frutescens. In *Plant and Animal Cells: Process Posibilites*, ed. C Webb, F Mavituna, pp. 45-61: Ellis Horwood Limited

Hooker BS, Lee JM, An G. 1989. Response of plant tissue culture to a high shear environment. *Enzyme and Microbial Technology* 11:484-490

Hynes RO. 2002. Integrins: Bidirectional, allosteric signaling machines. *Cell* 110:673-687

Ibaraki Y, Kenji K. 2001. Application of image analysis to plant cell suspension cultures. *Computers and Electronics in Agriculture* 30:193-203

Ingram B, Mavituna F. 2000. Effect of bioreactor configuration on the growth and maturation of Picea sitchensis somatic embryo cultures. *Plant Cell Tissue and Organ Culture* 61:87-96

Inouye H, Ueda S, Inoue K, Matsumura H. 1979. Quinones and related compounds in higher-plants. 8. Biosynthesis of shikonin in callus-cultures of lithospermum-erythrorhizon. *Phytochemistry* 18:1301-1308

Jarvis MC. 2009. Plant cell walls: supramolecular assembly, signalling and stress. *Structural Chemistry* 20:245-253

Jeffers P, Kerins S, Baker CJ, Kieran PM. 2007. Generation of Reactive Oxygen and Antioxidant Species by Hydrodynamically Stressed Suspensions of *Morinda citrifolia*. *Biotechnol Prog.* 23:138-145

Jo UA, Murthy HN, Hahn EJ, Paek KY. 2008. Micropropagation of Alocasia amazonica using semisolid and liquid cultures. *In Vitro Cellular & Developmental Biology-Plant* 44:26-32

Kargi F, Rosenberg MZ. 1987. Plant cell bioreactors: present status and future trends. *Biotechnology Progress* 3:1-8

Kawashima T, Wang XJ, Henry KF, Bi YP, Weterings K, Goldberg RB. 2009. Identification of cis-regulatory sequences that activate transcription in the suspensor of plant embryos. *Proceedings of the National Academy of Sciences of the United States of America* 106:3627-3632

Kieran PM, MacLoughlin PF, Malone DM. 1997. Plant cell suspension cultures: some engineering considerations. *Journal of Biotechnology* 59:39-52

Kieran PM, Malone DM, MacLoughlin PF. 2000. *Effects of hydrodynamic and interfacial forces on plant cell suspension systems*: Springer Berlin / Heidelberg. 139-177 pp.

Kieran PM, Odonnell HJ, Malone DM, Macloughlin PF. 1995. Fluid shear effects on suspension cultures of Morinda citrifolia. *Biotechnology and Bioengineering* 45:415-425

Kotchoni SO, Gachomo EW. 2006. The reactive oxygen species network pathways: an essential prerequisite for perception of pathogen attack and the acquired disease resistance in plants. *Journal of Biosciences* 31:389-404

Krishna H, Singh SK. 2007. Biotechnological advances in mango (Mangifera indica L.) and their future implication in crop improvement -- A review. *Biotechnology Advances* 25:223-243

Kristensen E, Parsons TE, Hallgrimsson B, Boyd SK. 2008. A Novel 3-D Image-Based Morphological Method for Phenotypic Analysis. *Ieee Transactions on Biomedical Engineering* 55:2826-2831

Kurata H, Furusaki S. 1993. Immobilized *Coffea arabica* cell culture using a bubble-column reactor with controlled light intensity. *Biotechnology and Bioengineering* 42:494-502

Lakshmanan P, Geijskes R, Wang L, Elliott A, Grof C, et al. 2006. Developmental and hormonal regulation of direct shoot organogenesis and somatic embryogenesis in sugarcane (Saccharum spp. interspecific hybrids) leaf culture. *Plant Cell Reports* 25:1007-1015

Lehmussola A, Ruusuvuori P, Selinummi J, Huttunen H, Yli-Harja O. 2007. Computational framework for simulating fluorescence microscope images with cell populations. *Ieee Transactions on Medical Imaging* 26:1010-1016

Lehmussola A, Ruusuvuori P, Selinummi J, Rajala T, Yli-Harja O. 2008. Synthetic images of high-throughput microscopy for validation of image analysis methods. *Proceedings of the Ieee* 96:1348-1360

Li YSJ, Haga JH, Chien S. 2005. Molecular basis of the effects of shear stress on vascular endothelial cells. *Journal of Biomechanics* 38:1949-1971

Lichtenthaler HK. 1998. The stress concept in plants: An introduction. In *Stress of Life - from Molecules to Man*, ed. P Csermely, pp. 187-198

Lindsey K, Yeoman MM, Black GM, Mavituna F. 1983. A novel method for the immobilization and culture of plant-cells. *Febs Letters* 155:143-149

Lindsey K, Yeoman MM. 1984. The synthetic potential of immobilized cells of Capsicum-frutescens mill cv annuum. *Planta* 162:495-501

Lockett SJ, Herman B. 1994. Automatic detection of clustered, fluorescent stained nuclei by digital image-based cytometry. *Cytometry* 17:1-12

Low P, Chandra S. 1994. Endocytosis in plants. *Annual Review of Plant Physiology and Plant Molecular Biology* 45:609-631

Lü B, Chen F, Gong ZH, Xie H, Zhang JH, Liang JS. 2007. Intracellular localization of integrin-like protein and its roles in osmotic stress-induced abscisic acid biosynthesis in Zea mays. *Protoplasma* 232:35-43

Luo BH, Springer TA. 2006. Integrin structures and conformational signaling. *Current Opinion in Cell Biology* 18:579-586

Lynch TM, Lintilhac PM. 1997. Mechanical signals in plant development: A new method for single cell studies. *Developmental Biology* 181:246-256

Lynch TM, Lintilhac PM, Domozych D. 1998. Mechanotransduction molecules in the plant gravisensory response: amyloplast/statolith membranes contain a beta(1) integrin-like protein. *Protoplasma* 201:92-100

MacLoughlin PF, Malone DM, Murtagh JT, Kieran PM. 1998. The effects of turbulent jet flows on plant cell suspension cultures. *Biotechnology and Bioengineering* 58:595-604

Malinowski R, Filipecki M. 2002. The role of cell wall in plant embryogenesis. *Cellular & Molecular Biology Letters* 7:1137-1151

Mavituna F, Park JM, Wilkinson AK, Williams PD. 1987. Characteristics of immobilised plant cell reactors. In *Plant and Animal Cells: Process Posibilites*, ed. C Webb, F Mavituna, pp. 92-115: Ellis Horwood

McDonald R, Fieuw S, Patrick JW. 1996. Sugar uptake by the dermal transfer cells of developing cotyledons of Vicia faba L - Mechanism of energy coupling. *Planta* 198:502-509

McGuire WP, Hoskins WJ, Brady MF, Kucera PR, Partridge EE, et al. 1996. Cyclophosphamide and cisplatin compared with paclitaxel and cisplatin in patients with stage III and stage IV ovarian cancer. *New England Journal of Medicine* 334:1-6

Mehrotra S, Goel MK, Kukreja AK, Mishra BN. 2007. Efficiency of liquid culture systems over conventional micropropagation: A progress towards commercialization. *African Journal of Biotechnology* 6:1484-1492

Meinhart CD, Wereley ST, Gray MHB. 2000. Volume illumination for two-dimensional particle image velocimetry. *Meas. Sci. Technol.* 11:809–814

Meinhart CD, Zhang HS. 2000. The flow structure inside a microfabricated inkjet printhead. *Journal of Microelectromechanical Systems* 9:67-75

Menke C, Renault N, Mueller-Roeber B. 2000. StGCPRP, a potato gene strongly expressed in stomatal guard cells, defines a novel type of repetitive proline-rich proteins. *Plant Physiology* 122:677-686

Merkle SA, Dean JFD. 2000. Forest tree biotechnology. *Current Opinion in Biotechnology* 11:298-302

Metallo CM, Vodyanik MA, Pablo JJd, Slukvin II, Palecek SP. 2008. The response of human embryonic stem cell-derived endothelial cells to shear stress. *Biotechnology and Bioengineering* 100:830-837

Mo LH, Egertsdotter U, VonArnold S. 1996. Secretion of specific extracellular proteins by somatic embryos of Picea abies is dependent on embryo morphology. *Annals of Botany* 77:143-152

Monshausen GB, Bibikova TN, Weisenseel MH, Gilroy S. 2009. Ca^{2+} Regulates Reactive Oxygen Species Production and pH during Mechanosensing in Arabidopsis Roots. *Plant Cell* 21:2341-2356

Moore DS, McCabe GP. 1999. *Introduction to the practice of statistics*: New York : W.H. Freeman

Moorhouse SD, Wilson G, Hennerty MJ, Selby C, tSaoir SMA. 1996. A plant cell bioreactor with medium-perfusion for control of somatic embryogenesis in liquid cell suspensions. *Plant Growth Regulation* 20:53-56

Morcillo F, Gagneur C, Adam H, Richaud F, Singh R, et al. 2006. Somaclonal variation in micropropagated oil palm. Characterization of two novel genes with enhanced

expression in epigenetically abnormal cell lines and in response to auxin. *Tree Physiology* 26:585-594

Morris P, Fowler MW. 1981. A new method for the production of fine plant cell suspension cultures. *Plant cell, tissue and organ culture.* 1:15-24

Mygatt E. 2006. World's Forests Continue to Shrink. In *Eco-Economy Indicators: Forest Cover*, ed. Earth Policy Institute

Neill S, Desikan R, Hancock J. 2002. Hydrogen peroxide signalling. *Current Opinion in Plant Biology* 5:388-395

Nerem RM, Alexander RW, Chappell DC, Medford RM, Varner SE, Taylor WR. 1998. The study of the influence of flow on vascular endothelial biology. *American Journal of the Medical Sciences* 316:169-175

Nyberg GB, Balcarcel RR, Follstad BD, Stephanopoulos G, Wang DIC. 1999. Metabolism of peptide amino acids by Chinese hamster ovary cells grown in a complex medium. *Biotechnology and Bioengineering* 62:324-335

Oberdorf J, Vilarrojas C, Epel D. 1989. The localization of PI and PIP kinase activities in the sea-urchin egg and their modulation following fertilization. *Developmental Biology* 131:236-242

Ono K, Xu HJ, Park C, McKay P, Aidun C, Yoda M. 2001. Forming jet surface velocity profile measurements with high speed digital imaging. *Tappi Journal* 84:60

Paek KY, Hahn EJ, Son SH. 2001. Application of bioreactors for large-scale micropropagation systems of plants. *In Vitro Cellular & Developmental Biology-Plant* 37:149-157

Pandhair V, Sekhon BS. 2006. Reactive oxygen species and antioxidants in plants: An overview. *Journal of Plant Biochemistry and Biotechnology* 15:71-78

Papageorgiou VP, Assimopoulou AN, Couladouros EA, Hepworth D, Nicolaou KC. 1999. The chemistry and biology of alkannin, shikonin, and related naphthazarin natural products. *Angewandte Chemie-International Edition* 38:270-301

Parker JR. 1997. *Algorithms for image processing and computer vision*: New York : Wiley Computer Pub. 23-29 pp.

Pati PK, Sharma M, Ahuja PS. 2005. Extra thin alginate film: an efficient technique for protoplast culture. *Protoplasma* 226:217

Paul R, Apel J, Klaus S, Schugner F, Schwindke P, Reul H. 2003. Shear stress related blood damage in laminar Couette flow. *Artificial Organs* 27:517-529

Pei ZM, Kuchitsu K. 2005. Early ABA signaling events in guard cells. *Journal of Plant Growth Regulation* 24:296-307

Pendzich J, Motykiewicz G, Michalska J, Wang LY, Kostowska A, Chorazy M. 1997. Sister chromatid exchanges and high-frequency cells in men environmentally and occupationally exposed to ambient air pollutants: an intergroup comparison with respect to seasonal changes and smoking habit. *Mutation Research-Fundamental and Molecular Mechanisms of Mutagenesis* 381:163-170

Pepperkok R, Ellenberg J. 2006. Innovation - High-throughput fluorescence microscopy for systems biology. *Nature Reviews Molecular Cell Biology* 7:690-696

Petřek J, Baloun J, Vlašínová H, Havel L, Adam V, et al. 2007. Image analysis and activity of intracellular esterases as new analytical tools for determination of growth and viability of embryonic cultures of spruce (Picea sp.) treated with cadmium. *Chemické listy* 101:569 -577

Petřek J, Víteček J, Vlašínová H, Kizek R, Kramer K, et al. 2005. Application of computer imaging, stripping voltammetry and mass spectrometry to study the effect of lead (Pb-EDTA) on the growth and viability of early somatic embryos of Norway spruce (Picea abies /L./ Karst.). *Analytical and Bioanalytical Chemistry* 383:576-586

Petrosyan A. 2009. Vision System for Disabled People Using Pattern Matching Algorithm. In *CSIT 2009-Seventh International Conference on Computer Science and Information Technologies. 28 September - 2 October, 2009*. Yerevan, Armenia

Pinto G, Loureiro J, Lopes T, Santos C. 2004. Analysis of the genetic stability of Eucalyptus globulus Labill. somatic embryos by flow cytometry. *TAG Theoretical and Applied Genetics* 109:580-587

Preil W. 1991. Application of bioreactors in plant propagation. In *Micropropgation: Technology and application*, ed. P Debergh, R Zimmerman, pp. 425-455: Kluwer Acad. Publ. Dordrecht, The Netherlands

Prenosil JE, Pedersen H. 1983. Immobilized plant-cell reactors. *Enzyme and Microbial Technology* 5:323-331

Prentice HL, Ehrenfels BN, Sisk WP. 2007. Improving performance of mammalian cells in fed-batch processes through "bioreactor evolution". *Biotechnology Progress* 23:458-464

Pullman GS, Gupta PK, Timmis R, Carpenter C, Kreitinger M, Welty E. 2005a. Improved Norway spruce somatic embryo development through the use of abscisic acid combined with activated carbon. *Plant Cell Reports* 24:271-279

Pullman GS, Johnson S. 2009. Osmotic measurements in whole megagametophytes and embryos of loblolly pine (Pinus taeda) during seed development. *Tree Physiol* 29:819-827

Pullman GS, Johnson S, Van Tassel S, Zhang Y. 2005b. Somatic embryogenesis in loblolly pine (*Pinus taeda*) and Douglas fir (*Pseudotsuga menziesii*): improving culture initiation and growth with MES pH buffer, biotin, and folic acid. *Plant Cell Tissue and Organ Culture* 80:91-103

Rajashekar CB, Lafta A. 1996. Cell-wall changes and cell tension in response to cold acclimation and exogenous abscisic acid in leaves and cell cultures. *Plant Physiology* 111:605-612

Rathore K, Sunilkumar G, Campbell LM. 2006. Cotton (Gossypium hirsutum L.). *Methods in molecular biology (Clifton, N.J.)* 343:267-279

Reid RC, Alonso JM. 1995. Specificity of monosynaptic connections from thalamus to visual cortex. *Nature* 378:281-284

Reneman RS, Arts T, Hoeks APG. 2006. Wall shear stress - an important determinant of endothelial cell function and structure - in the arterial system in vivo. *Journal of Vascular Research* 43:251-269

Rout GR, Mohapatra A, Jain SM. 2006. Tissue culture of ornamental pot plant: A critical review on present scenario and future prospects. *Biotechnology Advances* 24:531-560

Rout GR, Samantaray S, Das P. 2000. In vitro manipulation and propagation of medicinal plants. *Biotechnology Advances* 18:91-120

Rowinsky EK, Donehower RC. 1995. Drug therapy: paclitaxel (taxol). *New England Journal of Medicine* 332:1004-1014

Sajc L, Grubisic D, Vunjak-Novakovic G. 2000. Bioreactors for plant engineering: an outlook for further research. *Biochemical Engineering Journal* 4:89-99

Sajc L, Obradovic B, Vukovic D, Bugarski B, Grubisic D, Vunjak-Novakovic G. 1995a. Hydrodynamics and mass transfer in a four-phase external loop air lift bioreactor. *Biotechnol. Prog.* 11:420-428

Sajc L, Vunjak-Novakovic G, Grubisic D, Kovačević N, Vuković D, Bugarski B. 1995b. Production of anthraquinones by immobilized Frangula alnus Mill. plant cells in a four-phase air-lift bioreactor. *Applied Microbiology and Biotechnology* 43:416-423

Sandler A, Gray R, Perry MC, Brahmer J, Schiller JH, et al. 2006. Paclitaxel-carboplatin alone or with bevacizumab for non-small-cell lung cancer. *New England Journal of Medicine* 355:2542-2550

Sankawa U, Ebizuka Y, Miyazaki T, Isomura Y, Otsuka H, et al. 1977. Anti-tumor activity of shikonin and its derivatives. *Chemical & Pharmaceutical Bulletin* 25:2392-2395

Santiago JG, Wereley ST, Meinhart CD, Beebe DJ, Adrian RJ. 1998. A particle image velocimetry system for microfluidics. *Experiments in Fluids* 25:316

Schiavone FM, Cooke TJ. 1985. A geometric analysis of somatic embryo formation in carrot cell-cultures. *Canadian Journal of Botany-Revue Canadienne De Botanique* 63:1573-1578

Schindler M, Meiners S, Cheresh DA. 1989. RGD-dependent linkage between plant cell wall and plasma membrane: consequences for growth. *Journal of Cell Biology* 108:1955-1965

Schneider F. 1979. *Sugar Analysis-ICUMSA Methods*: International Commission for Uniform Methods of Sugar Analysis (ICUMSA)

Schwartz MA, Schaller MD, Ginsberg MH. 1995. Integrins: Emerging paradigms of signal transduction. *Annual Review of Cell and Developmental Biology* 11:549-599

Scragg AH, Fowler WM. 1985. Mass culture of plant cells. In *Cell Culture and Somatic Cell Genesis of Plants*, ed. I Vasil, pp. 103-128. London: Academic Press

Scragg AH, Morris P, Allan EJ, Bond P, Hegarty P, et al. 1987. The effect of scaled-up on plant-cell culture performance. In *Plant and Animal Cells: Process Posibilites*, ed. C Webb, F Mavituna, pp. 77-89: Ellis Horwood

Sequeira L. 1978. Lectins and their role in host-pathogen specificity. *Annual Review of Phytopathology* 16:453-481

Serra M, Brito C, Leite SB, Gorjup E, von Briesen H, et al. 2009. Stirred bioreactors for the expansion of adult pancreatic stem cells. *Annals of Anatomy-Anatomischer Anzeiger* 191:104-115

Sharma M, Rai SK, Purshottam DK, Jain M, Chakrabarty D, et al. 2009. In vitro clonal propagation of Clerodendrum serratum (Linn.) Moon (barangi): a rare and threatened medicinal plant. *Acta Physiologiae Plantarum* 31:379-383

Shi ZD, Yuan YJ, Wu JC, Shang GM. 2003. Biological responses of suspension cultures of Taxus chinensis var. mairei to shear stresses in the short term. *Applied Biochemistry and Biotechnology* 110:61-74

Shin S, Lee SW, Ku YL. 2004. Measurements of blood viscosity using a pressure-scanning slit viscometer. *Ksme International Journal* 18:1036-1041

Souter M, Lindsey K. 2000. Polarity and signalling in plant embryogenesis. *Journal of Experimental Botany* 51:971-983

Sowana DD, Williams DRG, Dunlop EH, Dally BB, O'Neill BK, Fletcher DF. 2001. Turbulent shear stress effects on plant cell suspension cultures. *Chemical Engineering Research & Design* 79:867-875

Spiteller G. 2003. The relationship between changes in the cell wall, lipid peroxidation, proliferation, senescence and cell death. *Physiologia Plantarum* 119:5-18

Stadler R, Lauterbach C, Sauer N. 2005. Cell-to-Cell Movement of Green Fluorescent Protein Reveals Post-Phloem Transport in the Outer Integument and Identifies Symplastic Domains in Arabidopsis Seeds and Embryos. *Plant Physiol.* 139:701-712

Starkuviene V, Pepperkok R. 2007. The potential of high-content high-throughput microscopy in drug discovery. *British Journal of Pharmacology* 152:62-71

Stathopoulos NA, Hellums JD. 1985. Shear-stress effects on human-embryonic kidney cells in vitro. *Biotechnology and Bioengineering* 27:1021-1026

Stolberg S, McCloskey KE. 2009. Can shear stress direct stem cell fate? *Biotechnology Progress* 25:10-19

Street HE. 1977. *Plant Tissue and Cell Culture*. Blackwell, London

Sun H, Aidun CK, Egertsdotter U. 2010. Effects from shear stress on morphology and growth of early stages of Norway spruce somatic embryos. *Biotechnology and Bioengineering* 105:588-599

Sun X, Linden JC. 1999. Shear stress effects on plant cell suspension cultures in a rotating wall vessel bioreactor. *Journal of Industrial Microbiology & Biotechnology* 22:44-47

Sun Y, Qian H, Xu XD, Han Y, Yen LF, Sun DY. 2000. Integrin-like proteins in the pollen tube: Detection, localization and function. *Plant and Cell Physiology* 41:1136-1142

Sun Y, Sun DY. 2001. Advance in intergrin-like proteins in plants. *Progress in Biochemistry and Biophysics* 28:283-286

Swatzell LJ, Edelmann RE, Makaroff CA, Kiss JZ. 1999. Integrin-Like Proteins are Localized to Plasma Membrane Fractions, not Plastids, in Arabidopsis. *Plant Cell Physiol.* 40:173-183

Sythe E, Warren G. 1991. The mechanism of receptor-mediated endocytosis. *European Journal of Biochemistry* 202:689-699

Takeda T, Kitagawa T, Takeuchi Y, Seki M, Furusaki S. 1998. Metabolic responses of plant cell culture to hydrodynamic stress. *Canadian Journal of Chemical Engineering* 76:267-275

Tanaka H. 1981. Technological problems in cultivation of plant-cells at high density. *Biotechnology and Bioengineering* 23:1203-1218

Tanaka K. 1985. Organization of geniculate inputs to visual cortical-cells in the cat. *Vision Research* 25:357-364

Tautorus T, Dunstan D. 1995. Scale-up of embryogenic plant suspension cultures in bioreactors. In *Somatic Embryogenesis in Woody Plants: History, Molecular and Biochemical Aspects and Applications*, ed. S Jain, P Gupta, R Newton, pp. 265-292: Kluwer Academic Publishers, Dordrecht

Thomas CR. 1992. Image analysis: putting filamentous microorganisms in the picture. *Trends in Biotechnology* 10:343-348

Thomas CR, Paul GC. 1996. Applications of image analysis in cell technology. *Current Opinion in Biotechnology* 7:35-45

Thorpe TA, Harry IS, Yeung EC. 2006. Clonal propagation of softwoods. *Methods in molecular biology (Clifton, N.J.)* 318:187-197

Thu B, Smidsrod O, Skjak-Brak G, eds. 1996. *Alginate gels-Some structure-function correlations relevant to their use as immobilization matrix for cells*: Elsevier Science B.V. 19-30 pp.

Turner SR. 2007. Cell walls: Monitoring integrity with The kinase. *Current Biology* 17:R541-R542

Vits H, Chi CM, Hu WS, Staba EJ, Cooke TJ. 1994. Characterizing patterns in plant somatic embryo cultures: its morphology and development. *AICHE Journal* 40:1728-1740

von Aderkas P, Bonga JM. 2000. Influencing micropropagation and somatic embryogenesis in mature trees by manipulation of phase change, stress and culture environment. *Tree Physiol* 20:921-928

von Arnold S. 1987. Improved efficiency of somatic embryogenesis in mature embryos of Picea abies (L.) Karst. *Journal of Plant Physiology* 128:233-244

von Arnold S, Bozhkov P, Clapham D, Dyachok J, Filonova L, et al. 2005. Propagation of Norway spruce via somatic embryogenesis. *Plant Cell Tissue and Organ Culture* 81:323-329

Von Arnold S, Clapham D. 2007. Plant Embryogenesis. Chapter: Spruce Embryogenesis. In *Methods in Molecular Biology, vol.427*, ed. MF Suárez, PV Bozhkov, pp. 31- 46: Springer Verlag, Humana Press

von Arnold S, Eriksson T. 1981. In vitro studies of adventitious shoot information in Pinus contorta. *Canadian Journal of Botany* 59:870-874

Wang QC, Panis B, Engelmann F, Lambardi M, Valkonen JPT. 2009. Cryotherapy of shoot tips: a technique for pathogen eradication to produce healthy planting materials and prepare healthy plant genetic resources for cryopreservation. *Annals of Applied Biology* 154:351-363

Weterings K, Apuya NR, Bi YP, Fischer RL, Harada JJ, Goldberg RB. 2001. Regional localization of suspensor mRNAs during early embryo development. *Plant Cell* 13:2409-2425

Xie Y, Wang F, Puscheck EE, Rappolee DA. 2007. Pipetting Causes Shear Stress and Elevation of Phosphorylated Stress-Activated Protein Kinase/Jun Kinase in Preimplantation Embryos. *Molecular Reproduction and Development* 74:1287-1294

Ye C, Bai L, Yan ZQ, Wang YH, Jiang ZL. 2008. Shear stress and vascular smooth muscle cells promote endothelial differentiation of endothelial progenitor cells via activation of Akt. *Clinical Biomechanics* 23:S118-S124

Yu HM, Zeng YJ, Hu JL, Li CX. 2002. Fluid shear stress induces the secretion of monocyte chemoattractant protein-1 in cultured human umbilical vein endothelial cells. *Clinical Hemorheology and Microcirculation* 26:199-207

Zhang C, Chi C, Staba E, Cooke T, Hu W. 1996. Application of image analysis to fed-batch cultures of somatic embryos *In vitro cellular & developmental biology. Plant* 32:190-198

Zhang X, Stettler M, Reif O, Kocourek A, DeJesus M, et al. 2008. Shaken helical track bioreactors: Providing oxygen to high-density cultures of mammalian cells at volumes up to 1000 L by surface aeration with air. *New Biotechnology* 25:68-75

Zhong C, Yuan YJ. 2009. Responses of Taxus cuspidata to hydrodynamics in bubble column bioreactors with different sparging nozzle sizes. *Biochemical Engineering Journal* 45:100-106

Zhong J-J, Fujiyama K, Seki T, Yoshida T. 1994. A quantitative analysis of shear effects on cell suspension and cell culture of perilla frutescens in bioreactors. *Biotechnology and Bioengineering* 44:649-654

Ziv M. 1991. Morphogenic patterns of plants micropropagated in liquid medium in shaken flasks or large-scale bioreactor cultures. *Israel journal of botany* 40:145-153

Ziv M, Kahany S, Lilienkipnis H. 1994. Scaled-up proliferation and regeneration of Nerine in liquid cultures. I. The induction and maintenance of proliferating meristematic cultures by paclobutrazol in bioreactors. *Plant Cell Tissue and Organ Culture* 39:109-115